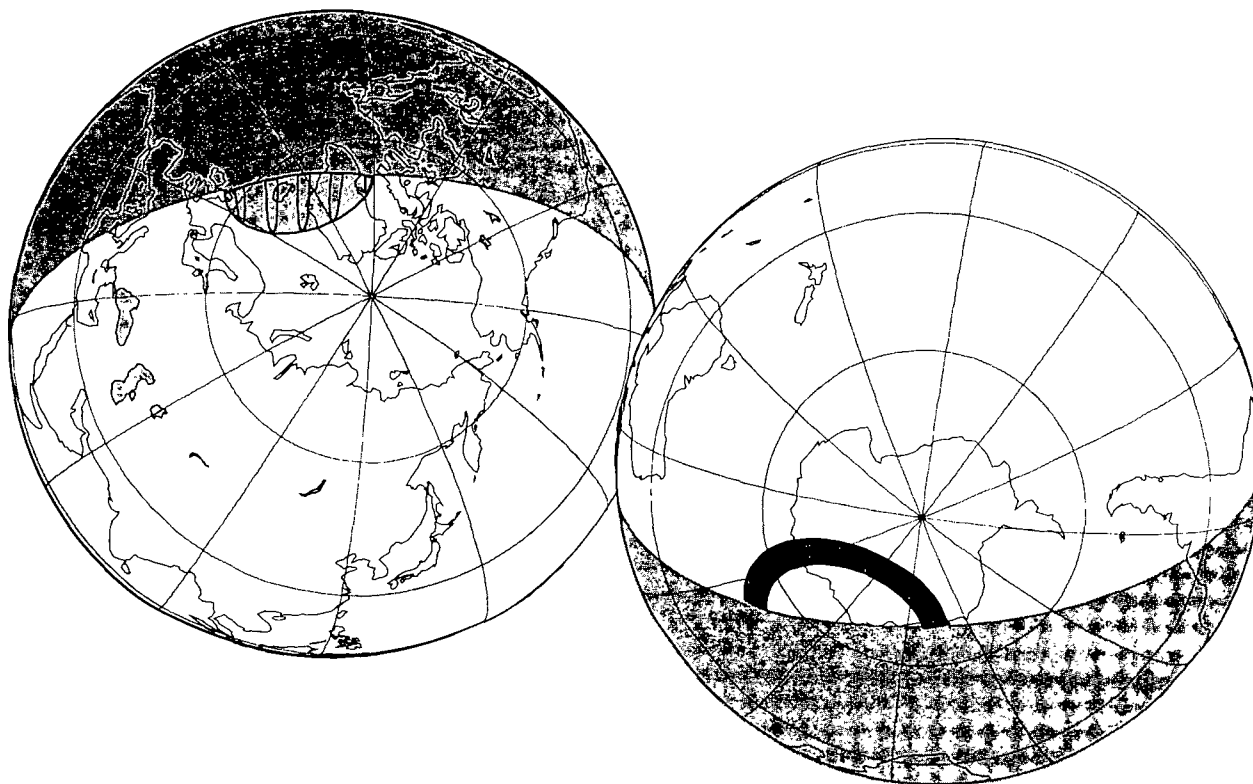


NASA/TP—2002—211618



Annular and Total Solar Eclipses of 2003

F. Espenak and J. Anderson



National Aeronautics and
Space Administration

Goddard Space Flight Center
Greenbelt, Maryland 20771

Available from:

NASA Center for Aerospace Information
7121 Standard Drive
Hanover, MD 21076-1320
Price Code: A17

National Technical Information Service
5285 Port Royal Road
Springfield, VA 22161
Price Code: A10

PREFACE

This work is the ninth in a series of NASA publications containing detailed predictions, maps and meteorological data for future central solar eclipses of interest. Published as part of NASA's Technical Publication (TP) series, the eclipse bulletins are prepared in cooperation with the Working Group on Eclipses of the International Astronomical Union and are provided as a public service to both the professional and lay communities, including educators and the media. In order to allow a reasonable lead time for planning purposes, eclipse bulletins are published 12 to 24 months before each event.

Single copies of the bulletins are available at no cost by sending a 9 x 12 inch self addressed stamped envelope with postage for 12 oz. (340 g.). Detailed instructions and an order form can be found at the back of this publication.

Unlike previous publications in this series each of which focused on a single event, the current bulletin covers predictions for two disparate solar eclipses. The annular eclipse of 2003 May 31 has a short broad path which stretches from northern Scotland to Iceland and central Greenland. Six months later, the total eclipse of 2003 November 23 sweeps across Antarctica. To include both of these very different eclipses into one publication, we've organized the bulletin into three sections:

Section 1.0 - Annular Solar Eclipse of 2003 May 31

Section 2.0 - Total Solar Eclipse of 2003 November 23

Section 3.0 - Eclipse Resources

The figures, tables and sub-sections in each of these divisions are labeled with decimal numerals to quickly identify which section they refer to (e.g., Figure 2.3 is part of Section 2.0). This organization will make it easier to navigate around the publication.

The 2003 bulletin uses the World Data Bank II (WDBII) mapping data base for the path figures. WDBII outline files were digitized from navigational charts to a scale of approximately 1:3,000,000. The data base is available through the *Global Relief Data CD-ROM* from the National Geophysical Data Center.

The geographic coordinates data base includes over 90,000 cities and locations. This permits the identification of many more cities within the umbral paths and their subsequent inclusion in the local circumstances tables. These same coordinates are plotted in the path figures and are labeled when the scale allows. The source of these coordinates is Rand McNally's *The New International Atlas*. A subset of these coordinates is available in a digital form which we've augmented with population data.

The bulletins have undergone a great deal of change since their inception in 1993. The expansion of the mapping and geographic coordinates data bases have significantly improved the coverage and level of detail demanded by eclipse planning. Some of these changes are the direct result of suggestions from our readers. We strongly encourage you to share your comments, suggestions and criticisms on how to improve the content and layout in subsequent editions. Although every effort is made to ensure that the bulletins are as accurate as possible, an error occasionally slips by. We would appreciate your assistance in reporting all errors, regardless of their magnitude.

We thank Dr. B. Ralph Chou for a comprehensive discussion on solar eclipse eye safety. Dr. Chou is Professor of Optometry at the University of Waterloo and he has over twenty-five years of eclipse observing experience. As a leading authority on the subject, Dr. Chou's contribution should help dispel much of the fear and misinformation about safe eclipse viewing.

Dr. Joe Gurman (GSFC/Solar Physics Branch) has made this and previous eclipse bulletins available over the Internet. They can be read or downloaded via the World Wide Web from Goddard's Solar Data Analysis Center eclipse information page: <http://umbra.nascom.nasa.gov/eclipse/>.

In 1996, Espenak launched the *NASA Eclipse Home Page*, a web site which provides general information on every solar and lunar eclipse occurring during the period 1951 through 2050. An online catalog also lists that date and characteristics of every solar and lunar eclipse from 2000 BC through AD 3000. The URL for the site is: <http://sunearth.gsfc.nasa.gov/eclipse/eclipse.html>.

In addition to the general information web site above, two special web sites have been set up:

2003 annular solar eclipse – <http://sunearth.gsfc.nasa.gov/eclipse/ASE2003/ASE2003html>

2003 total solar eclipse – <http://sunearth.gsfc.nasa.gov/eclipse/TSE2003/TSE2003html>

These sites include supplemental predictions, figures, tables and maps.

Since the eclipse bulletins are of a limited and finite size, they cannot include everything needed by every scientific investigation. Some investigators may require exact contact times which include lunar limb effects or for a specific observing site not listed in the bulletin. Other investigations may need customized predictions for an aerial rendezvous or from the path limits for grazing eclipse experiments. We would like to assist such investigations by offering to calculate additional predictions for any professionals or large groups of amateurs. Please contact Espenak with complete details and eclipse prediction requirements.

We would like to acknowledge the valued contributions of a number of individuals who were essential to the success of this publication. The format and content of the NASA eclipse bulletins has drawn heavily upon over 40 years of eclipse *Circulars* published by the U.S. Naval Observatory. We owe a debt of gratitude to past and present staff of that institution who have performed this service for so many years. The many publications and algorithms of Dr. Jean Meeus have served to inspire a life-long interest in eclipse prediction. Prof. Jay M. Pasachoff reviewed the manuscript and offered many helpful suggestions. Internet availability of the eclipse bulletins is due to the efforts of Dr. Joseph B. Gurman. The support of Environment Canada is acknowledged in the acquisition of the weather data.

Permission is freely granted to reproduce any portion of this publication, including data, figures, maps, tables and text. All uses and/or publication of this material should be accompanied by an appropriate acknowledgment (e.g., “Reprinted from *Annular and Total Solar Eclipses of 2002*, Espenak and Anderson, 2002”). We would appreciate receiving a copy of any publications where this material appears.

The names and spellings of countries, cities and other geopolitical regions are not authoritative, nor do they imply any official recognition in status. Corrections to names, geographic coordinates and elevations are actively solicited in order to update the data base for future eclipses. All calculations, diagrams and opinions are those of the authors and they assume full responsibility for their accuracy.

Fred Espenak
NASA/Goddard Space Flight Center
Planetary Systems Branch, Code 693
Greenbelt, MD 20771
USA

Jay Anderson
Environment Canada
123 Main Street, Suite 150
Winnipeg, MB,
CANADA R3C 4W2

email: espenak@gsfc.nasa.gov email:

FAX: (301) 286-0212

jander@cc.umanitoba.ca

FAX: (204) 983-0109

Current and Future NASA Solar Eclipse Bulletins

<u>NASA Eclipse Bulletin</u>	<u>RP #</u>	<u>Publication Date</u>
<i>Annular Solar Eclipse of 1994 May 10</i>	1301	<i>April 1993</i>
<i>Total Solar Eclipse of 1994 November 3</i>	1318	<i>October 1993</i>
<i>Total Solar Eclipse of 1995 October 24</i>	1344	<i>July 1994</i>
<i>Total Solar Eclipse of 1997 March 9</i>	1369	<i>July 1995</i>
<i>Total Solar Eclipse of 1998 February 26</i>	1383	<i>April 1996</i>
<i>Total Solar Eclipse of 1999 August 11</i>	1398	<i>March 1997</i>

NASA Eclipse Bulletin

TP #

Publication Date

Total Solar Eclipse of 2001 June 21

1999-209484

November 1999

Total Solar Eclipse of 2002 December 04

2001-209990

October 2001

Annular and Total Solar Eclipses of 2003

2002-211618

October 2002

----- future -----

Annular and Total Solar Eclipses of 2005

—

2003

Total Solar Eclipse of 2006 March 29

—

2004

CONTENTS

1.00 - ANNULAR SOLAR ECLIPSE OF 2003 MAY 31	1
1.01 - INTRODUCTION	1
1.02 - PATH OF ANNULARITY	1
1.03 - ORTHOGRAPHIC MAP OF THE MAY 31 ECLIPSE PATH	2
1.04 - STEREOGRAPHIC MAP OF THE MAY 31 ECLIPSE PATH	2
1.05 - DETAILED MAPS OF THE PATH OF ANNULARITY	3
1.06 - ELEMENTS, SHADOW CONTACTS AND MAY 31 ECLIPSE TABLES	3
1.07 - LOCAL CIRCUMSTANCES TABLES FOR MAY 31	5
1.08 - LUNAR LIMB PROFILE FOR MAY 31	6
1.09 - INTRODUCTION TO WEATHER PROSPECTS FOR MAY 31	7
1.10 - WEATHER PROSPECTS FOR GREENLAND	7
1.11 - WEATHER PROSPECTS FOR ICELAND	8
1.12 - WEATHER PROSPECTS FOR SCOTLAND	8
1.13 - WEATHER STRATEGIES	9
1.14 - WEATHER WEB SITES FOR THE MAY 31 ANNULAR ECLIPSE	9
FIGURES	
1.1 - ORTHOGRAPHIC MAP OF 2003 MAY 31 ANNULAR ECLIPSE	11
1.2 - STEREOGRAPHIC MAP OF 2003 MAY 31 ANNULAR ECLIPSE	12
1.3 - ECLIPSE PATH THROUGH EUROPE.....	13
1.4 - PATH OF ANNULARITY	14
1.5 - ANNULAR PATH THROUGH SCOTLAND AND FAEROE ISLANDS	15
1.6 - ANNULAR ECLIPSE PATH THROUGH ICELAND	16
1.7 - LUNAR LIMB PROFILE FOR 2003 MAY 31 AT 04:05 UT	17
TABLES	
1.1 - ELEMENTS OF ANNULAR ECLIPSE OF 2003 MAY 31	18
1.2 - SHADOW CONTACTS AND CIRCUMSTANCES OF ANNULAR ECLIPSE	19
1.3 - PATH OF ANTUMBRAL SHADOW OF ANNULAR ECLIPSE	20
1.4 - PHYSICAL EPHEMERIS OF ANTUMBRAL SHADOW OF ANNULAR ECLIPSE	21
1.5 - LOCAL CIRCUMSTANCES ON CENTRAL LINE OF ANNULAR ECLIPSE	21
1.6 - LOCAL CIRCUMSTANCES FOR SCOTLAND AND OUTLYING ISLANDS	22
1.7 - LOCAL CIRCUMSTANCES FOR ICELAND.....	23
1.8 - LOCAL CIRCUMSTANCES FOR FAEROE ISLANDS AND GREENLAND	24
1.9 - LOCAL CIRCUMSTANCES FOR ENGLAND, IRELAND AND WALES	24
1.10 - LOCAL CIRCUMSTANCES FOR EUROPE: ALBANIA - FRANCE	25
1.11 - LOCAL CIRCUMSTANCES FOR EUROPE: GERMANY - NORWAY	26
1.12 - LOCAL CIRCUMSTANCES FOR EUROPE: POLAND - YUGOSLAVIA	27
1.13 - LOCAL CIRCUMSTANCES FOR ASIA MINOR	28
1.14 - LOCAL CIRCUMSTANCES FOR ASIA	29
1.15 - LOCAL CIRCUMSTANCES FOR ALASKA & CANADA	29
1.16 - WEATHER STATISTICS FOR ANNULAR ECLIPSE	30
KEY TO TABLE 1.16	31
2.00 - TOTAL SOLAR ECLIPSE OF 2003 NOVEMBER 23	33
2.01 - INTRODUCTION	33
2.02 - PATH OF TOTALITY	33
2.03 - ORTHOGRAPHIC PROJECTION MAP OF THE ECLIPSE PATH	34
2.04 - STEREOGRAPHIC MAP OF THE NOVEMBER 23 ECLIPSE PATH	34
2.05 - DETAILED MAP OF THE PATH OF TOTALITY	35
2.06 - ELEMENTS, SHADOW CONTACTS AND ECLIPSE PATH TABLES	35
2.07 - LOCAL CIRCUMSTANCES TABLES FOR NOVEMBER 23	37
2.08 - LUNAR LIMB PROFILE FOR NOVEMBER 23	38

2.09 - SKY DURING TOTALITY	39
2.10 - INTRODUCTION TO WEATHER PROSPECTS FOR NOVEMBER 23	40
2.11 - WEATHER PATTERNS	40
2.12 - COAST OF QUEEN MARY LAND - MIRNY	41
2.13 - INTERIOR OF ANTARCTICA	42
2.14 - COAST OF QUEEN MAUD LAND - MAITRI, NEUMAYER, AND NOVOLAZAREVSKAJA	42
2.15 - SELECTING A SITE	43
2.16 - WEATHER WEB SITES FOR NOVEMBER 23 TOTAL ECLIPSE	43

FIGURES

2.1 - ORTHOGRAPHIC MAP OF 2003 NOVEMBER 23 TOTAL ECLIPSE	45
2.2 - STEREOGRAPHIC MAP OF 2003 NOVEMBER 23 TOTAL ECLIPSE	46
2.3 - ECLIPSE PATH THROUGH ANTARCTICA	47
2.4 - LUNAR LIMB PROFILE FOR 2003 NOVEMBER 23 AT 22:40 UT	48
2.5 - SKY DURING TOTALITY FOR 2003 NOVEMBER 23 AT 22:40 UT	49
2.6 - CLOUD STATISTICS FOR THREE STATIONS FOR NOVEMBER ECLIPSE	50

TABLES

2.1 - ELEMENTS OF TOTAL ECLIPSE OF 2003 NOVEMBER 23	51
2.2 - SHADOW CONTACTS AND CIRCUMSTANCES OF TOTAL ECLIPSE	52
2.3 - PATH OF UMBRAL SHADOW OF TOTAL ECLIPSE	53
2.4 - PHYSICAL EPHEMERIS OF UMBRAL SHADOW OF TOTAL ECLIPSE	54
2.5 - LOCAL CIRCUMSTANCES ON CENTRAL LINE OF TOTAL ECLIPSE	55
2.6 - LOCAL CIRCUMSTANCES FOR ANTARCTICA	56
2.7 - LOCAL CIRCUMSTANCES FOR ARGENTINA, CHILE AND FALKLAND ISLANDS	56
2.8 - LOCAL CIRCUMSTANCES FOR AUSTRALIA	57-58
2.9 - LOCAL CIRCUMSTANCES FOR NEW ZEALAND	58
2.10 - LOCAL CIRCUMSTANCES FOR INDONESIA	58
2.11 - ANTARCTIC STATION CLIMATOLOGY FOR TOTAL ECLIPSE	59

3.00 - ECLIPSE RESOURCES	61
3.01 - EYE SAFETY AND SOLAR ECLIPSES	61
3.02 - SOURCES FOR SOLAR FILTERS	63
3.03 - IAU SOLAR ECLIPSE EDUCATION COMMITTEE	64
3.04 - ECLIPSE PHOTOGRAPHY	64
3.05 - ECLIPSES AT COLD TEMPERATURES	66
3.06 - IAU WORKING GROUP ON ECLIPSES	67
3.07 - INTERNATIONAL SOLAR ECLIPSE CONFERENCE	68
3.08 - NASA ECLIPSE BULLETINS ON INTERNET	68
3.09 - FUTURE ECLIPSE PATHS ON INTERNET	68
3.10 - SPECIAL WEB SITES FOR 2003 SOLAR ECLIPSES	69
3.11 - PREDICTIONS FOR ECLIPSE EXPERIMENTS	69
3.12 - MEAN LUNAR RADIUS	69
3.13 - ALGORITHMS, EPHEMERIDES AND PARAMETERS	70

FIGURES

3.1 - SPECTRAL RESPONSE OF SOLAR FILTERS	71
--	----

TABLES

3.1 - 35MM FIELD OF VIEW	72
3.2 - SOLAR ECLIPSE EXPOSURE GUIDE	72

BIBLIOGRAPHY	73
REFERENCES	73
METEOROLOGY	73
EYE SAFETY	73
FURTHER READING	74
REQUEST FORM	75

1.00 ANNULAR SOLAR ECLIPSE OF 2003 MAY 31

1.01 INTRODUCTION

On Saturday, 2003 May 31, an annular eclipse of the Sun will be visible from a broad corridor that traverses the North Atlantic. The path of the Moon's antumbral shadow begins in northern Scotland, crosses Iceland and central Greenland, and ends at sunrise in Baffin Bay (Canada). A partial eclipse will be seen within the much broader path of the Moon's penumbral shadow, which includes most of Europe, the Middle East, central and northern Asia, and northwestern North America (Figures 1.1 and 1.2).

The trajectory of the Moon's shadow is quite unusual during this event. The shadow axis passes to the far north where it barely grazes Earth's surface. In fact, the northern edge of the antumbra actually misses Earth so that one path limit is defined by the day/night terminator rather than by the shadow's upper edge. As a result, the track of annularity has a peculiar "D" shape that is nearly 1200 kilometers wide. Since the eclipse occurs just three weeks prior to the northern summer solstice, Earth's northern axis is pointed sunwards by 22.8° . As seen from the Sun, the antumbral shadow actually passes between the North Pole and the terminator. As a consequence of this extraordinary geometry, the path of annularity runs from east to west rather than the more typical west to east.

The event transpires near the Moon's ascending node in Taurus five degrees north of Aldebaran. Since apogee occurs three days earlier (May 28 at 13 UT), the Moon's apparent diameter (29.6 arc-minutes) is still too small to completely cover the Sun (31.6 arc-minutes) resulting in an annular eclipse.

1.02 PATH OF ANNULARITY

The annular eclipse begins in northern Scotland about 100 kilometers north of Glasgow when the Moon's antumbral shadow first touches down on Earth at 03:45 UT (Figures 1.3 and 1.4). The antumbra quickly extends northward as it travels on a northwestern trajectory. In Scotland, the Northwest Highlands, Loch Ness, the Isle of Lewis (Outer Hebrides), Orkney Islands and Shetland Islands all lie in the annular track where maximum eclipse occurs at or shortly after sunrise (Figure 1.5). Several minutes later, the shadow's edge reaches the Faeroe Islands (03:51 UT) where annularity lasts 03 minutes 08 seconds with the Sun 4° above the northeastern horizon.

By 03:59 UT, the leading edge of the antumbra arrives along the southeastern coast of Iceland (Figure 1.6). Traveling with a ground velocity of 2 kilometers per second, the shadow sweeps across the entire North Atlantic nation in ten minutes. The shadow is so broad that the duration of the three and a half minute annular phase varies by less than 5 seconds across all of Iceland. The capital city of Reykjavik lies in the southwest corner of the country. Here, the Sun will stand 2° high during the 3 minute 36 second annular phase. Unfortunately, the low altitude spectacle may be hidden from city dwellers by mountains lying to the northeast.

The instant of greatest eclipse¹ occurs at 04:08:18 UT when the axis of the Moon's shadow passes closest to the center of Earth ($\gamma^2 = +0.996$). The length of annularity reaches its maximum duration of 3 minutes 37 seconds, the Sun's altitude is 3° , and the antumbra's velocity is 1.06 km/s. At that time, the shadow's axis is just 60 kilometers northwest of Iceland.

After traversing the Denmark Strait, the highly elliptical antumbra bisects Greenland where over a third of the enormous island lies within the track (Figure 1.4). Crossing the ill-named land mass, the path width rapidly shrinks as the grazing antumbra begins its return to space. From Umanak, the Sun stands 3° above the Arctic horizon during the 2 minute 24 second annular phase. Seven hundred kilometers to the south, Godthåb (Nuuk) lies completely outside the path and will not even witness a partial eclipse.

¹ The instant of greatest eclipse occurs when the distance between the Moon's shadow axis and Earth's geocenter reaches a minimum.

² Minimum distance of the Moon's shadow axis from Earth's center in units of equatorial Earth radii.

As it departs Greenland and crosses Baffin Bay, the shadow leaves Earth's surface at 04:31 UT. From start to finish, the antumbra sweeps over its entire path in a little under 47 minutes.

1.03 ORTHOGRAPHIC MAP OF THE MAY 31 ECLIPSE PATH

Figure 1.1 is an orthographic projection map of Earth [adapted from Espenak, 1987] showing the path of penumbral (partial) and antumbral (annular) eclipse. The daylight terminator is plotted for the instant of greatest eclipse with north at the top. The point of greatest eclipse is indicated with an asterisk-like symbol. The sub-solar point (Sun in zenith) at greatest eclipse is also shown.

The limits of the Moon's penumbral shadow define the region of visibility of the partial eclipse. This saddle shaped region often covers more than half of Earth's daylight hemisphere and consists of several distinct zones or limits. At the southern boundary lies the limit of the penumbra's path. Great loops at the western and eastern extremes of the penumbra's path identify the areas where the eclipse begins/ends at sunrise and sunset, respectively. Bisecting the 'eclipse begins/ends at sunrise and sunset' loops is the curve of maximum eclipse at sunrise (western loop) and sunset (eastern loop). The exterior tangency points **P1** and **P4** mark the coordinates where the penumbral shadow first contacts (partial eclipse begins) and last contacts (partial eclipse ends) Earth's surface. The path of the antumbral shadow travels east to west and is shaded dark gray.

A curve of maximum eclipse is the locus of all points where the eclipse is at maximum at a given time. They are plotted at each half hour Universal Time (UT), and generally run in a north-south direction. The outline of the antumbral shadow is plotted every ten minutes in UT. Curves of constant eclipse magnitude³ delineate the locus of all points where the magnitude at maximum eclipse is constant. These curves run exclusively between the curves of maximum eclipse at sunrise and sunset. Furthermore, they are quasi-parallel to the southern penumbral limit. This limit may be thought of as a curve of constant magnitude of 0%, while adjacent curves are for magnitudes of 20%, 40%, 60% and 80%.

At the top of Figure 1.1, the Universal Time of geocentric conjunction between the Moon and Sun is given followed by the instant of greatest eclipse. The eclipse magnitude is given for greatest eclipse. For central eclipses (both total and annular), it is equivalent to the geocentric ratio of diameters of the Moon and Sun. Γ is the minimum distance of the Moon's shadow axis from Earth's center in units of equatorial Earth radii. Finally, the Saros series number is given along with the eclipse's relative sequence in the series.

1.04 STEREOGRAPHIC MAP OF THE MAY 31 ECLIPSE PATH

The stereographic projection of Earth in Figure 1.2 depicts the path of penumbral and antumbral eclipse in greater detail. The map is oriented with the north up. International political borders are shown and circles of latitude and longitude are plotted at 20° increments. The region of penumbral or partial eclipse is identified by its southern limit, curves of eclipse begins or ends at sunrise and sunset, and curves of maximum eclipse at sunrise and sunset. Curves of constant eclipse magnitude are plotted for 20%, 40%, 60% and 80%, as are the limits of the path of annular eclipse. Also included are curves of greatest eclipse at every half hour Universal Time.

Figures 1.1 and 1.2 may be used to quickly determine the approximate time and magnitude of maximum eclipse at any location within the eclipse path.

³ Eclipse magnitude is defined as the fraction of the Sun's diameter occulted by the Moon. It is strictly a ratio of *diameters* and should not be confused with eclipse obscuration, which is a measure of the Sun's surface *area* occulted by the Moon. Eclipse magnitude may be expressed as either a percentage or a decimal fraction (e.g.: 50% or 0.50).

1.05 DETAILED MAPS OF THE PATH OF ANNULARITY

The path of annularity is plotted on a series of detailed maps appearing in Figures 1.3 through 1.6. The maps were chosen to isolate small regions along the path using coastline data from the World Data Bank II (WDBII). The WDBII outline files are digitized from navigational charts to a working scale of approximately 1:3 million.

The positions of larger cities and metropolitan areas are depicted as black dots. The size of each city is logarithmically proportional to its population using 1990 census data (Rand McNally, 1991). City data selected from a geographic data base of over 90,000 cities are plotted to give as many locations as possible in the path of annularity. Local circumstances have been calculated for many of these positions and can be found in Tables 1.6 through 1.15.

Although no corrections have been made for center of figure or lunar limb profile, they have little or no effect at this scale. Atmospheric refraction⁴ has not been included because it depends on the atmospheric temperature-pressure profile, which cannot be predicted in advance. These maps are also available on the web at <http://sunearth.gsfc.nasa.gov/eclipse/ASE2003/ASE2003.html>.

1.06 ELEMENTS, SHADOW CONTACTS AND MAY 31 ECLIPSE TABLES

The geocentric ephemeris for the Sun and Moon, various parameters, constants, and the Besselian elements (polynomial form) are given in Table 1.1. The eclipse elements and predictions were derived from the DE200 and LE200 ephemerides (solar and lunar, respectively) developed jointly by the Jet Propulsion Laboratory and the U.S. Naval Observatory for use in the *Astronomical Almanac* for 1984 and thereafter. Unless otherwise stated, all predictions are based on center of mass positions for the Moon and Sun with no corrections made for center of figure, lunar limb profile or atmospheric refraction. The predictions depart from normal IAU convention through the use of a smaller constant for the mean lunar radius k for all antumbral contacts (see: LUNAR LIMB PROFILE). Times are expressed in either Terrestrial Dynamical Time (TDT) or in Universal Time (UT), where the best value of ΔT ⁵ available at the time of preparation is used.

From the polynomial form of the Besselian elements, any element can be evaluated for any time t_1 (in decimal hours) via the equation:

$$a = a_0 + a_1 * t + a_2 * t^2 + a_3 * t^3 \quad (\text{or } a = \sum [a_n * t^n], n = 0 \text{ to } 3)$$

where: $a = x, y, d, l_1, l_2, \text{ or } \mu$

$$t = t_1 - t_0 \quad (\text{decimal hours}) \text{ and } t_0 = 4.00 \text{ TDT}$$

The polynomial Besselian elements were derived from a least-squares fit to elements rigorously calculated at five separate times over a six hour period centered at t_0 . Thus, the equation and elements are valid over the period $1.00 \leq t_1 \leq 7.00$ TDT.

⁴ The nominal value for atmospheric refraction at the horizon is 34 arc-minutes, but this value can vary by a factor of 2 depending on atmospheric conditions. For an eclipse in the horizon, the umbral path is shifted in the direction opposite from the Sun.

⁵ ΔT is the difference between Terrestrial Dynamical Time and Universal Time ($\Delta T = \text{TDT} - \text{UT}$).

Table 2.1 lists all contacts of penumbral and antumbral shadows with Earth. They include TDT times and geodetic coordinates with and without corrections for ΔT . The contacts are defined:

- P1** — Instant of first external tangency of penumbral shadow cone with Earth's limb.
(partial eclipse begins)
- P4** — Instant of last external tangency of penumbral shadow cone with Earth's limb.
(partial eclipse ends)
- U1** — Instant of first external tangency of antumbral shadow cone with Earth's limb.
(annular eclipse begins)
- U4** — Instant of last external tangency of antumbral shadow cone with Earth's limb.
(annular eclipse ends)

Similarly, the southern extremes of the penumbral and antumbral paths, and extreme limits of the antumbral central line are given. The IAU (International Astronomical Union) longitude convention is used throughout this publication (i.e., for longitude, east is positive and west is negative; for latitude, north is positive and south is negative).

The path of the antumbral shadow is delineated at one minute intervals in Universal Time in Table 1.3. Coordinates of the terminator limit, the antumbral limit and the central line are listed to the nearest tenth of an arc-minute (~185 m at the Equator). The Sun's altitude, path width and antumbral duration are calculated for the central line position. Table 1.4 presents a physical ephemeris for the antumbral shadow at one minute intervals in UT. The central line coordinates are followed by the topocentric ratio of the apparent diameters of the Moon and Sun, the eclipse obscuration⁶, and the Sun's altitude and azimuth at that instant. The antumbral shadow's instantaneous velocity with respect to Earth's surface are included. Finally, the central line duration of the antumbral phase is given.

Local circumstances for each central line position listed in Tables 1.4 are presented in Table 1.5. The first three columns give the Universal Time of maximum eclipse, the central line duration of annularity and the altitude of the Sun at that instant. The following columns list each of the four eclipse contact times followed by their related contact position angles and the corresponding altitude of the Sun. The four contacts identify significant stages in the progress of the eclipse. They are defined as follows:

- First Contact** — Instant of first external tangency between the Moon and Sun.
(partial eclipse begins)
- Second Contact** — Instant of first internal tangency between the Moon and Sun.
(central or antumbral eclipse begins; annular eclipse begins)
- Third Contact** — Instant of last internal tangency between the Moon and Sun.
(central or antumbral eclipse ends; annular eclipse ends)
- Fourth Contact** — Instant of last external tangency between the Moon and Sun.
(partial eclipse ends)

The position angles **P** and **V** identify the point along the Sun's disk where each contact occurs⁷. Second and third contact altitudes are omitted since they are always within 1° of the altitude at maximum eclipse.

⁶ Eclipse obscuration is defined as the fraction of the Sun's surface area occulted by the Moon.

⁷ **P** is defined as the contact angle measured counter-clockwise from the *north* point of the Sun's disk. **V** is defined as the contact angle measured counter-clockwise from the *zenith* point of the Sun's disk.

1.07 LOCAL CIRCUMSTANCES TABLES FOR MAY 31

Local circumstances for ~330 cities and locations in the UK, Iceland, Europe and Asia are presented in Tables 1.6 through 1.15. These tables give the local circumstances at each contact and at maximum eclipse⁸ for every location. The coordinates are listed along with the location's elevation (meters) above sea-level, if known. Otherwise, the local circumstances are calculated for sea-level. The Universal Time of each contact is given to a tenth of a second, along with position angles **P** and **V** and the altitude of the Sun. The position angles identify the point along the Sun's disk where each contact occurs and are measured counter-clockwise (i.e., eastward) from the north and zenith points, respectively. Locations outside the antumbral path miss the annular eclipse and only witness first and fourth contacts. The Universal Time of maximum eclipse (either partial or annular) is listed. Next, the position angles **P** and **V** of the Moon's disk with respect to the Sun are given, followed by the altitude and azimuth of the Sun at maximum eclipse. Finally, the corresponding eclipse magnitude and obscuration are listed. For annular eclipses, the eclipse magnitude is identical to the topocentric ratio of the Moon's and Sun's apparent diameters.

Two additional columns are included if the location lies within the path of annularity. The **antumbral depth** is a relative measure of a location's position with respect to the central line and path limits. It is a unitless parameter that is defined as:

$$u = 1 - \text{abs}(x/R) \quad [1.1]$$

where: **u** = antumbral depth
x = perpendicular distance from the shadow axis (kilometers)
R = radius of the antumbral shadow as it intersects Earth's surface (kilometers)

The antumbral depth for a location varies from 0.0 to 1.0. A position at the path limits corresponds to a value of 0.0 while a position on the central line has a value of 1.0. The parameter can be used to quickly determine the corresponding central line duration. Thus, it is a useful tool for evaluating the trade-off in duration of a location's position relative to the central line. Using the location's duration and antumbral depth, the central line duration is calculated as:

$$D = d / (1 - (1 - u)^2)^{1/2} \text{ seconds} \quad [1.2]$$

where: **D** = duration of annularity on the central line (seconds)
d = duration of annularity at location (seconds)
u = antumbral depth

The final column gives the duration of annularity. The effects of refraction have not been included in these calculations, nor have there been any corrections for center of figure or the lunar limb profile.

Locations were chosen based on general geographic distribution, population, and proximity to the path. The primary source for geographic coordinates is *The New International Atlas* (Rand McNally, 1991). Elevations for major cities were taken from *Climates of the World* (U.S. Dept. of Commerce, 1972). The city names and spellings presented here are for location purposes only and are not meant to be authoritative. They do not imply recognition of status of any location by the United States Government.

⁸ For partial eclipses, maximum eclipse is the instant when the greatest fraction of the Sun's diameter is occulted. For total eclipses, maximum eclipse is the instant of mid-totality.

1.08 LUNAR LIMB PROFILE FOR MAY 31

Eclipse contact times, magnitude and duration of annularity all depend on the angular diameters and relative velocities of the Moon and Sun. These calculations are limited in accuracy by the departure of the Moon's limb from a perfectly circular figure. The Moon's surface exhibits a rather dramatic topography, which manifests itself as an irregular limb when seen in profile. Most eclipse calculations assume some mean radius that averages high mountain peaks and low valleys along the Moon's rugged limb. Such an approximation is acceptable for many applications, but if higher accuracy is needed, the Moon's actual limb profile must be considered. Fortunately, an extensive body of knowledge exists on this subject in the form of Watts' limb charts [Watts, 1963]. These data are the product of a photographic survey of the marginal zone of the Moon and give limb profile heights with respect to an adopted smooth reference surface (or datum). Analyses of lunar occultations of stars by Van Flandern [1970] and Morrison [1979] have shown that the average cross-section of Watts' datum is slightly elliptical rather than circular. Furthermore, the implicit center of the datum (i.e., the center of figure) is displaced from the Moon's center of mass. Additional work by Morrison and Appleby [1981] shows that the radius of the datum varies with libration producing systematic errors in Watts' original limb profile heights that attain 0.4 arc-seconds at some position angles. Thus, corrections to Watts' limb data are necessary to ensure that the reference datum is a sphere with its center at the center of mass.

The Watts charts have been digitized and may be used to generate limb profiles for any libration. Ellipticity and libration corrections can be applied to refer the profile to the Moon's center of mass. Such a profile can then be used to correct eclipse predictions which have been generated using a mean lunar limb.

The lunar limb profile in Figure 1.7 includes corrections for center of mass and ellipticity [Morrison and Appleby, 1981]. It is generated for the central line at 04:05 UT, corresponding to central Iceland. The Moon's topocentric libration (physical + optical) is $l = -2.46^\circ$ $b = +1.28^\circ$, and the topocentric semi-diameters of the Sun and Moon are 945.5 and 888.2 arc-seconds, respectively. The Moon's angular velocity with respect to the Sun is 0.539 arc-seconds per second.

The radial scale of the limb profile (bottom of Figure 1.7) is greatly exaggerated so that the true limb's departure from the mean lunar limb is readily apparent. The mean limb with respect to the center of figure of Watts' original data is shown (dashed) along with the mean limb with respect to the center of mass (solid). Note that all the predictions presented in this publication are calculated with respect to the latter limb unless otherwise noted. Position angles of various lunar features can be read using the protractor marks along the Moon's mean limb (center of mass). The position angles of second and third contact are clearly marked along with the north pole of the Moon's axis of rotation and the observer's zenith at mid-annularity. The dashed line identifies the contact point on the north limb corresponding to the path limit. To the upper left of the profile are the Sun's topocentric coordinates at maximum eclipse. They include the right ascension *R.A.*, declination *Dec.*, semi-diameter *S.D.* and horizontal parallax *H.P.* The corresponding topocentric coordinates for the Moon are to the upper right. Below and left of the profile are the geographic coordinates of the central line at 04:05 UT while the times of the eclipse contacts at that location appear to the lower right. Directly below the profile are the local circumstances at maximum eclipse. They include the Sun's altitude, azimuth, and central duration of annularity. The position angle of the path's southern limit axis is *PA(N.Limit)* and the angular velocity of the Moon with respect to the Sun is *A.Vel.(M:S)*. At the bottom left are a number of parameters used in the predictions, and the topocentric lunar librations appear at the lower right.

In investigations where accurate contact times are needed, the lunar limb profile can be used to correct the nominal or mean limb predictions. For any given position angle, there will be a high mountain (annular eclipses) or a low valley (total eclipses) in the vicinity that ultimately determines the true instant of contact. The difference, in time, between the Sun's position when tangent to the contact point on the mean limb and tangent to the highest mountain (annular) or lowest valley (total) at actual contact is the desired correction to the predicted contact time. On the exaggerated radial scale of Figure 1.7, the Sun's limb can be represented as an epicyclic curve that is tangent to the mean lunar limb at the point of contact. Using the digitized Watts' datum, an analytical solution is straightforward and robust. Curves of corrections to the times of second and third contact for most position angles have been computer generated and plotted. The circular protractor scale at the center represents the nominal contact time using a mean lunar limb. The departure of the contact correction curves from

this scale graphically illustrates the time correction to the mean predictions for any position angle as a result of the Moon's true limb profile. Time corrections external to the circular scale are added to the mean contact time; time corrections internal to the protractor are subtracted from the mean contact time. The magnitude of the time correction at a given position angle is measured using any of the four radial scales plotted at each cardinal point.

For example, Table 1.7 gives the following data for Reykjavik, Iceland:

Second Contact = 04:02:27.6 UT	P2=254°
Third Contact = 04:06:03.5 UT	P3=077°

Measuring the contact time corrections in Figure 1.7, the resulting contact times are:

C2=+3.2 seconds;	Second Contact	= 04:02:27.6 +3.2s	= 04:02:30.8 UT
C3=-5.2 seconds;	Third Contact	= 04:06:03.5 -5.2s	= 04:05:58.3 UT

The above corrected values are within 0.1 seconds of a rigorous calculation using the true limb profile.

1.09 INTRODUCTION TO WEATHER PROSPECTS FOR MAY 31

The two polar eclipses of 2003 occur in the springtimes of their opposing seasons. One cannot help but be struck by their meteorological parallels — both occur in a marine environment, both have a polar ice cap to consider as an observing venue, both occur in regions of the globe that are plagued by many active low pressure systems, and both are famously cloudy over much of the track. Of the two, the annular eclipse across Greenland, Iceland and northern Scotland offers the poorer weather prospects, though it is easier to reach than November's eclipse over Antarctica. The best possible escape from the gray skies and wet climate is to select a site on the Greenland ice cap where high altitude and a drier air may bring favor on eclipse day. The same is true in Antarctica.

Low pressure systems that develop and cross North America frequently turn to the northeast when they leave the continent, eventually ending their existence over the waters between Greenland and Iceland. This location is the home of the infamous Icelandic low, a semi-permanent depression that dictates not only the weather of its home island but also the meteorology of Britain and northern Europe. The low lies at the boundary of the cold Arctic airmass that lurks to the north and the warmer maritime climate that accompanies the Gulf Stream as it flows past Iceland in its clockwise circuit of the Atlantic.

The clash of warm and cold, both in the water and the atmosphere, generates a never-ending succession of mid-latitude frontal depressions that travel toward the British Isles. In Iceland, overcast skies with rain or snow are the norm, though precipitation amounts are not especially high. With its more southerly latitude, Scotland is able to tap occasionally into the drier air around the large high-pressure system that lingers near the Azores, and so the gloominess of north Atlantic weather is relieved occasionally by southerly breezes.

1.10 WEATHER PROSPECTS FOR GREENLAND

Greenland's population lives on the coastal margins of the island, especially on the western side where the ice cap lies farther back from the coast. The coasts are surmounted by the Greenland ice cap which rises to over 3000 m in mid-island. In May an east-west oriented high-pressure system lies across the north of the island while an extension of the Iceland low reaches to Cape Farewell at the southern tip. The northeasterly winds between these two semi-permanent systems bring a steady flow of cool and humid Arctic air against the sharply rising east coast. Nearly forty percent of weather observations at eclipse time at Angmagssalik (Table 1.16) have precipitation falling as a result of this onshore flow and the frequency of overcast skies is more than fifty percent.

On the west coast winds tend to be lighter and more variable, but Davis Strait is a favorite destination for lows traveling across North America, and so the coast is visited by a steady series of disturbances. Cloud cover from these systems plus a persistent fog and low cloud that arises from the cool waters of Davis Strait combine to make this side of the island as nearly as cloudy as the east. Cloud cover statistics derived from satellite images are subject to a number of complications at Greenland's latitude, but the data do show a tendency to slightly less cloud along the west coast.

Air on the ice cap is much colder and denser than that in the lowlands and there is a steady downhill flow of cold air toward the coast from the interior known as a katabatic wind. Though generally light, the katabatic flow can exceed 100 km/h when channeled by terrain. It is most common on the steep eastern coast where they are known as Pitera. Downslope winds such as these are warmed slightly and dried by compression and reach the coast as a cold but dry flow that can clear out some of the persistent clouds and bring good eclipse viewing conditions. Though they tend to be most common in the early morning, prediction is difficult, as they are highly variable from place to place.

On the west coast, a southeast Foehn wind often develops bringing warm dry weather as it descends from the mountain peaks. It is the Greenland counterpart of the Chinook of North America. Foehn winds may last for as long as three days and are frequently followed by precipitation. They are more efficient than katabatic winds in clearing out the persistent cloudiness along the coast. A cap cloud on the nearby mountains often heralds these winds.

For the hardest (and wealthiest) eclipse travelers, the interior ice cap likely offers the best chances for clear eclipse viewing. Observations from the cap are few in number and tend to be more concerned with temperature and wind rather than cloud cover. Automatic satellite measurements of cloudiness are unreliable because of the bright ice background and the cold temperatures of the plateau. A Russian study using ten years of imagery from 1971 to 1980 measured very good sky conditions on the ice cap — 60 to 68% of the observations had clear skies or scattered clouds and only 12 to 18% were overcast. The clouds over the ice cap are also likely to be thinner than that on the coast as the cold air inland is not capable of holding as much moisture as that at lower altitude.

1.11 WEATHER PROSPECTS FOR ICELAND

Iceland lies alongside one of the most active weather areas in the Northern Hemisphere. The Icelandic low, about 1000 km to the southwest, is the source of a frequent and endless supply of weather systems that move past the island, each one bringing its own retinue of cloud and precipitation. The Gulf Stream waters that bathe Iceland also warm the air and fill it with moisture. As this warm and humid air encounters the colder water from the Arctic basin west and north, fog and low clouds form and keep gray weather even when an active low is not present.

Southern regions are marginally more promising than those in the north, in large part because of the lower frequency of low cloud and fog. Prevailing winds tend to be from the easterly side, so that there is a modest downslope to the flow at Reykjavik and a consequent drying of the atmosphere. Clear skies are almost unknown, being less than 5% of observations at all stations save one. Because the eclipse occurs very early with the Sun only a few degrees above the northeast horizon, clear or scattered cloudiness is almost mandatory.

Satellite observations show a complex pattern of cloudiness around the island. The largest amounts are in the interior where the higher terrain promotes condensation in the atmosphere. The least cloud is found straddling the south shore, and reaches slightly inland near Keflavik and Eyrarbakki. On the basis of the available data, a location near Reykjavik would be the most promising, though a good eclipse expedition will follow the forecast rather than the climatology.

1.12 WEATHER PROSPECTS FOR SCOTLAND

In spite of its more southerly location, Scotland offers no better prospects for viewing the eclipse than Iceland or Greenland. In spite of this gloomy statement, there is approximately a one-third chance of a sunny morning for the event according to the cloud and sunshine statistics. Aberdeen sees 36% of possible sunshine in May and 34% in June, figures very close to the probability calculated in Table 1.16 (which are for the hour of the eclipse).

Once again the main culprit is the series of frequent frontal lows that pass across or north of the British Isles in their eastward migration. Virtually all of these lows will bring precipitation to northern Scotland but spring is the driest season with changeable weather and a chance of a dry spell. Inland areas tend to be cloudier

than the coast, in large part because of the higher terrain that promotes the lifting of the moist air masses and their conversion into cloudy weather.

Fog is also common on the Scottish coast, but highly variable from place to place. From the data in Table 1.16, it appears that locations along Moray Firth (Inverness, Lossiemouth) have a relatively low incidence of fog while those exposed to the North Sea (Aberdeen) are much more likely to encounter it. This does not seem to have much of an impact on the probability of seeing the eclipse, for the stations within and near the track are all remarkably alike. On the Scottish mainland the most promising site is at Lossiemouth with a score of 0.34 while the least promising sites have a score of 0.30. These differences are too small to recommend one over another.

1.13 WEATHER STRATEGIES

While the footprint of the lunar shadow on Earth is very large, the opportunities to view annularity are very limited. In Iceland, the distance from the capital Reykjavik to the opposite end of the island is only about 450 km (though much longer by road). Scotland's annular zone is barely more than 300 km across from the most southerly point to the mainland tip. Both of these distances are short enough to allow ready movement to a clear location on the basis of forecasts on the day before the eclipse. In Scotland, Inverness would seem to be a convenient staging point, and it has a small weather advantage to boot. In Iceland the same benefits can be extended to Reykjavik.

Rapid travel from site to site in Greenland is all but impossible unless by aircraft, and so the site selection must be on the basis of the climatology. The available evidence points to the interior ice cap as the best site by far on the entire track, but cost and opportunity will limit access there. Elsewhere in Greenland, the west coast holds more promise than the east, which dictates a site at Christianshab or Godhavn, the two largest communities within the annular zone. These sites are close to the observation sites of Egdesminde and Jacobshavn in Table 1. The Sun does not set on May 31 and so the lucky eclipse observer could be treated to a midnight sun in annular eclipse. A sequence of solar images with an eclipse just 2° above the north horizon would surely be one of the great eclipse photographs - except, perhaps, for those that can be obtained in Antarctica just six months later.

1.14 WEATHER WEB SITES FOR THE MAY 31 ANNULAR ECLIPSE

World —

1. <http://www.tvweather.com> — Links to current and past weather and climate around the world
2. <http://www.worldclimate.com/climate/index.htm> — World data base of temperature and rainfall
3. <http://www.accuweather.com> — Forecasts for many cities worldwide
4. <http://www.worldweather.org/> A site operated by the World Meteorological Organization with links to climate and meteorological data worldwide. This site is still being developed and in many instances only climate information is available.
5. <http://www.fnoc.navy.mil/PUBLIC/WXMAP/index.html> — U.S. Navy weather center (Fleet Numerical Meteorology and Oceanographic Center - FNMOC). This site provides several (3) model outputs for many areas of the globe. While complex to use (meteorological expertise is a real bonus), it contains a wealth of model data. Look for relative humidity forecasts for 700 hPa (hectopascals) – this is a mid-level of the atmosphere and the relative humidity forecasts provide an indication of the forecast cloud cover from larger weather systems. Use the 70% contour as the outline of cloud areas. Areas with 90% or greater will likely have precipitation. Model forecasts for six days in advance for many parts of the world are available.

Scotland, Iceland and Greenland —

1. <http://weather.uwyo.edu/> - An impressive site at the University of Wyoming that allows you to build your own numerical model output. Choose “Forecasts from Numerical Models” and then “Aviation Model” to be given a choice of a model output over Scotland, Iceland, or Greenland (chose Europe). Choose 700 mb relative humidity. Values above 70% at 700 mb frequently indicate deep cloudiness.

2. <http://www.nottingham.ac.uk/meteosat> - Nottingham University site for obtaining satellite imagery over Scotland, Iceland and parts of Greenland. The two islands are quite distorted in the images as they lie well around the curve of the Earth from the satellite perspective.
3. <http://www.sat.dundee.ac.uk/pdus/> - Dundee University site of satellite imagery for Scotland, Iceland and Greenland. Select the AV subdirectory for visual images and the AI subdirectory for infrared pictures. These are large whole-Earth images whereas Nottingham's images are sectored and only a small part of the globe needs to be selected to see either Iceland or southern Greenland.
4. http://www.weatheroffice.ec.gc.ca/charts/index_e.html - The Meteorological Service of Canada site has satellite imagery of the Canadian Arctic and frequently most of Greenland. Select "Satellite Imagery" and look for the Canadian Arctic Composite image under HRPT (NOAA polar orbiting). Because the satellites used are polar orbiters instead of geostationary satellites, the images over Greenland are very detailed.
5. <http://www.met.no/satellit/> - The Norwegian Meteorological Institute satellite web page. Rectified images of Iceland are available. Choose "Europa, animasjon:" for an animated image of Europe and the north Atlantic. The satellite site is not in English.

Annular Solar Eclipse of 2003 May 31

FIGURE 1.1 - ORTHOGRAPHIC PROJECTION MAP OF THE ECLIPSE PATH

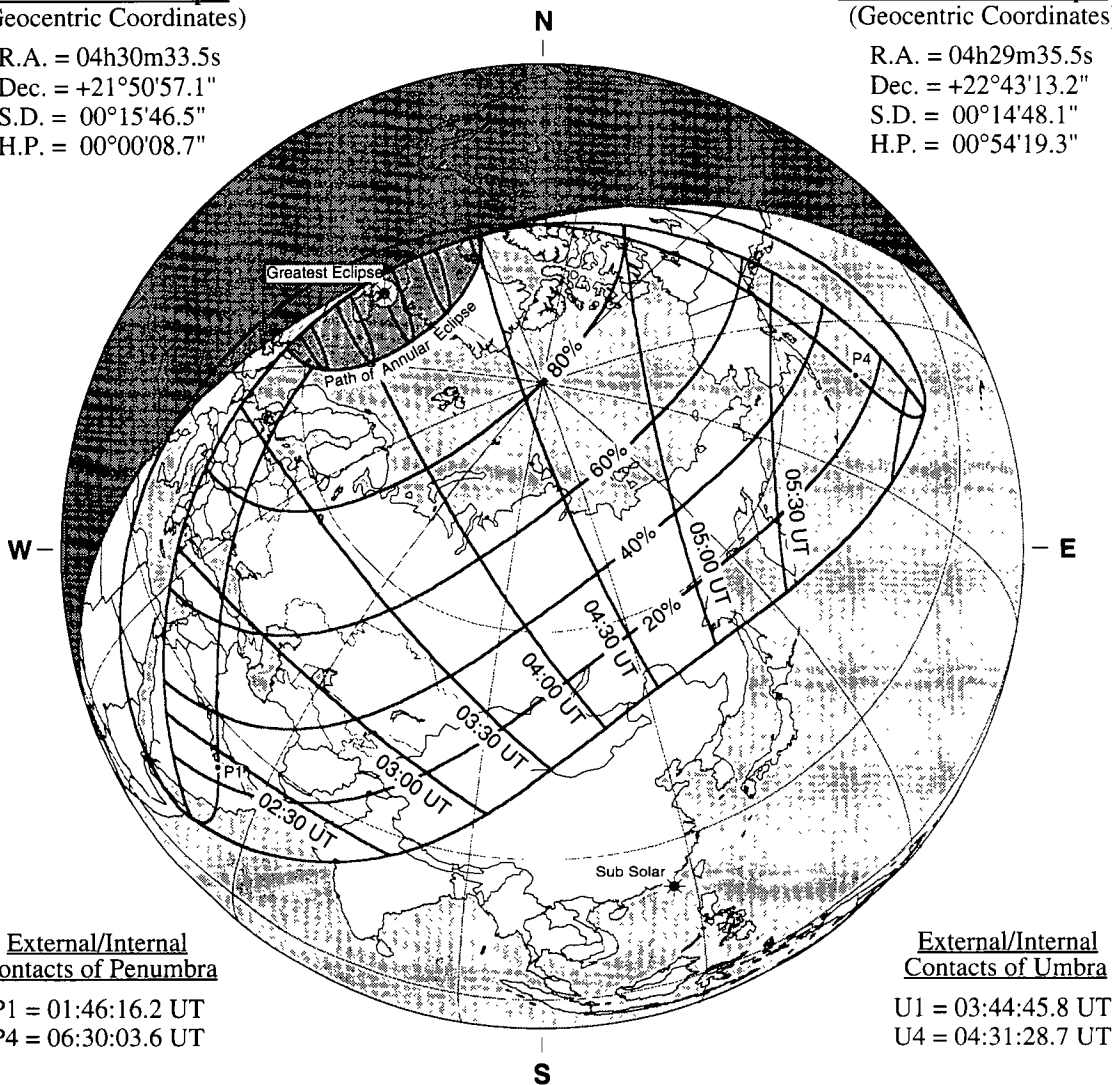
Geocentric Conjunction = 04:38:15.7 UT J.D. = 2452790.693236
 Greatest Eclipse = 04:08:17.7 UT J.D. = 2452790.672426
 Eclipse Magnitude = 0.93842 Gamma = 0.99598
 Saros Series = 147 Member = 22 of 80

Sun at Greatest Eclipse
(Geocentric Coordinates)

R.A. = 04h30m33.5s
 Dec. = +21°50'57.1"
 S.D. = 00°15'46.5"
 H.P. = 00°00'08.7"

Moon at Greatest Eclipse
(Geocentric Coordinates)

R.A. = 04h29m35.5s
 Dec. = +22°43'13.2"
 S.D. = 00°14'48.1"
 H.P. = 00°54'19.3"



External/Internal
Contacts of Penumbra

P1 = 01:46:16.2 UT
 P4 = 06:30:03.6 UT

External/Internal
Contacts of Umbra

U1 = 03:44:45.8 UT
 U4 = 04:31:28.7 UT

Local Circumstances at Greatest Eclipse

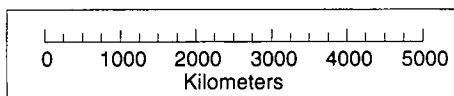
Lat. = 66°33.2'N Sun Alt. = 2.9°
 Long. = 024°30.0'W Sun Azm. = 35.1°
 Duration = 03m36.8s

Ephemeris & Constants

Eph. = DE200/LE200
 $\Delta T = 64.7$ s
 $k1 = 0.2725076$
 $k2 = 0.2722810$
 $\Delta b = 0.0''$ $\Delta l = 0.0''$

Geocentric Libration
(Optical + Physical)

$l = -2.60''$
 $b = -1.15''$
 $c = -7.26''$



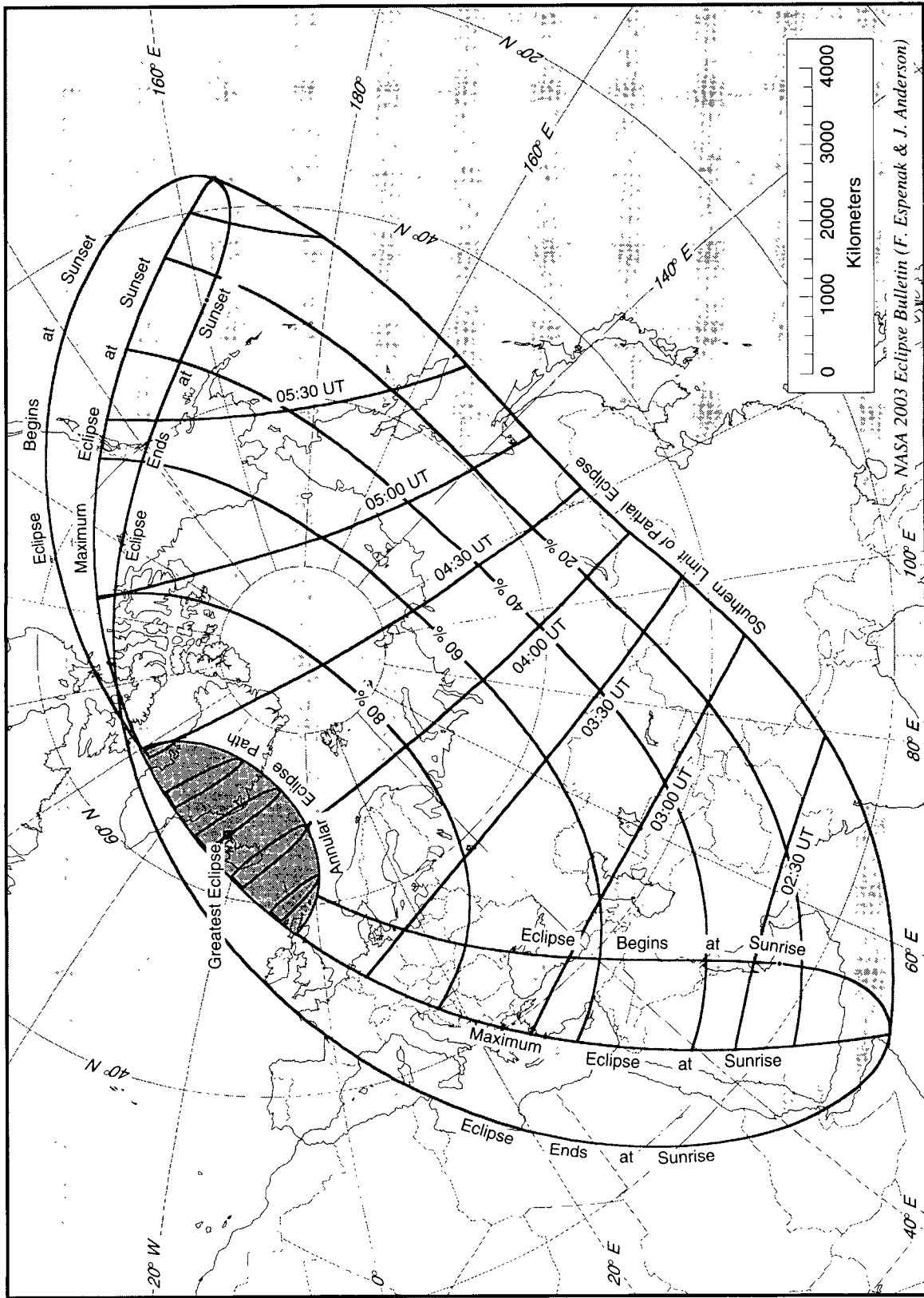
Brown Lun. No. = 995

NASA 2003 Eclipse Bulletin (F. Espenak & J. Anderson)

sunearth.gsfc.nasa.gov/eclipse/eclipse.html

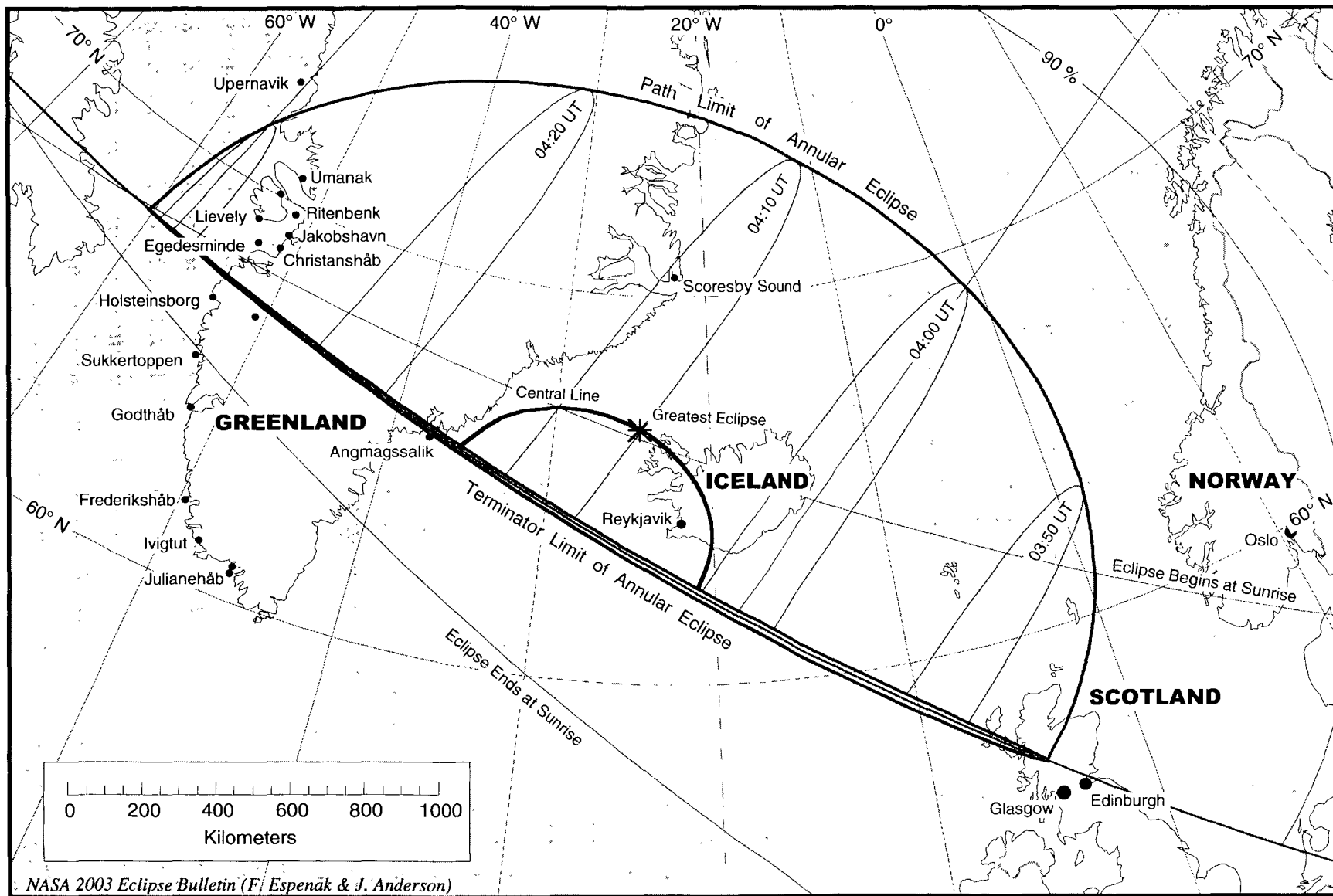
Annular Solar Eclipse of 2003 May 31

FIGURE 1.2 - STEREOGRAPHIC PROJECTION MAP OF THE ECLIPSE PATH



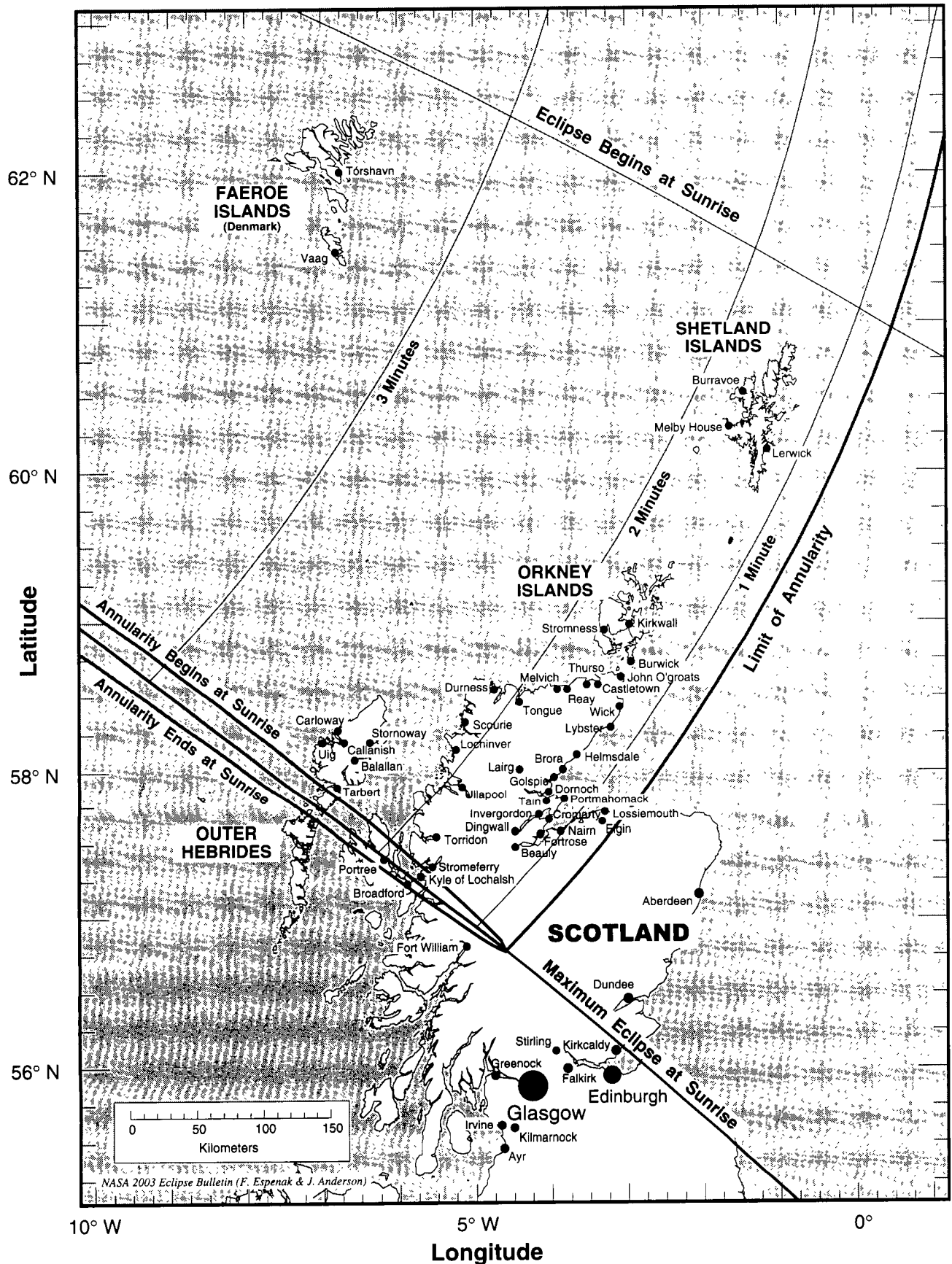
Annular Solar Eclipse of 2003 May 31

FIGURE 1.4 - THE PATH OF ANNULARITY



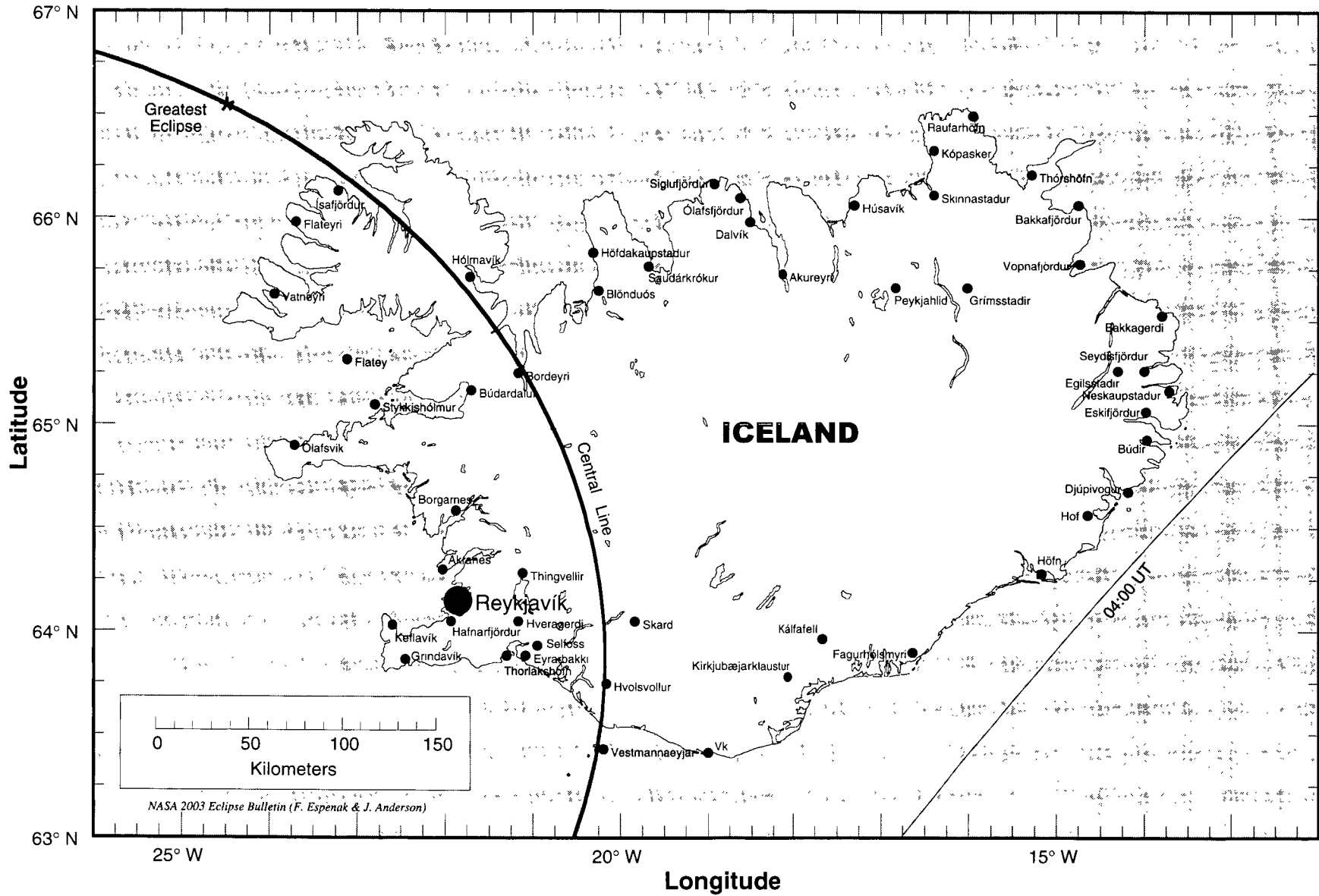
Annular Solar Eclipse of 2003 May 31

FIGURE 1.5 - THE PATH THROUGH SCOTLAND AND FAEROE ISLANDS



Annular Solar Eclipse of 2003 May 31

FIGURE 1.6 - THE PATH THROUGH ICELAND



Annular Solar Eclipse of 2003 May 31

FIGURE 1.7 - LUNAR LIMB PROFILE FOR MAY 31 AT 04:05 UT

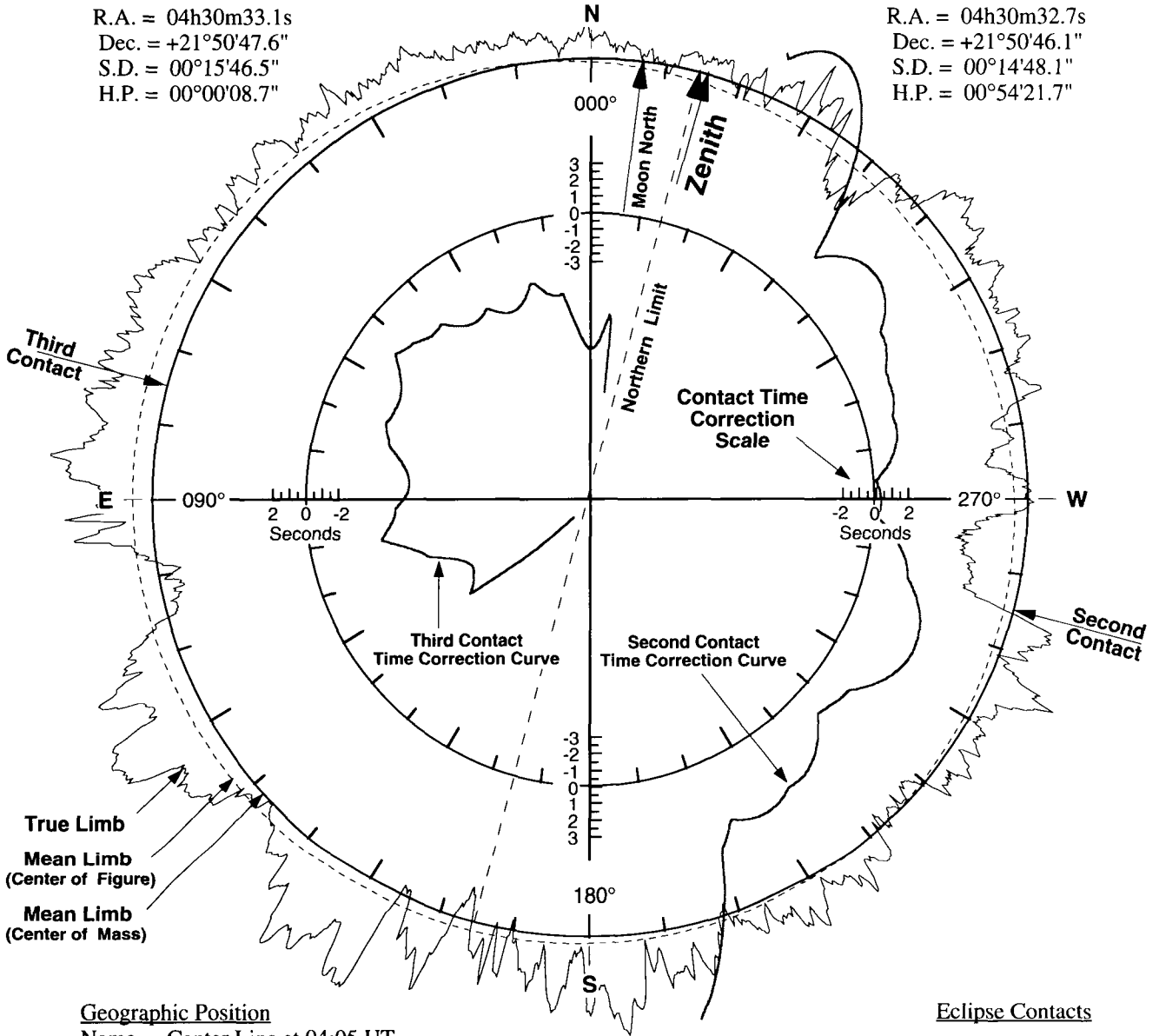
Sun at Maximum Eclipse
(Topocentric Coordinates)

R.A. = 04h30m33.1s
Dec. = +21°50'47.6"
S.D. = 00°15'46.5"
H.P. = 00°00'08.7"

Moon/Sun Ratio = 0.9383

Moon at Maximum Eclipse
(Topocentric Coordinates)

R.A. = 04h30m32.7s
Dec. = +21°50'46.1"
S.D. = 00°14'48.1"
H.P. = 00°54'21.7"



Geographic Position

Name = Center Line at 04:05 UT
Lat. = 65°15'55.6"N
Long. = 021°07'33.1"W
Elev. = 0.0 m

Ephemeris & Constants

Eph. = DE200/LE200
 $\Delta T = 64.7$ s
 $k1 = 0.2725076$
 $k2 = 0.2722810$
 $\Delta b = 0.00''$ $\Delta l = 0.00''$

Local Circumstances at Maximum Eclipse

Sun Alt. = 2.8°
Sun Azm. = 37.3°
PA(N.Limit) = 165.2°
Duration = 03m36.6s
A.Vel. (M:S) = 0.539"/s

Eclipse Contacts

C1 = —
C2 = 04:03:11.7 UT
C3 = 04:06:48.3 UT
C4 = 05:02:28.8 UT
 $\Delta C2 = 2.8$ s $\Delta C3 = -4.7$ s

Topocentric Libration
(Optical + Physical)

$l = -2.46^\circ$
 $b = -0.26^\circ$
 $c = -7.18^\circ$

cor.C2 = 04:03:14.5 UT (2.8s)

cor.C3 = 04:06:43.6 UT (-4.7s)

NASA 2003 Eclipse Bulletin (F. Espenak & J. Anderson)

TABLE 1.1

ELEMENTS OF THE ANNULAR SOLAR ECLIPSE OF 2003 MAY 31

Geocentric Conjunction 04:39:20.37 TDT J.D. = 2452790.693986
of Sun & Moon in R.A.: (=04:38:15.67 UT)

Instant of 04:09:22.42 TDT J.D. = 2452790.673176
Greatest Eclipse: (=04:08:17.72 UT)

Geocentric Coordinates of Sun & Moon at Greatest Eclipse (DE200/LE200):

<u>Sun:</u>	R.A. = 04h30m33.482s	<u>Moon:</u>	R.A. = 04h29m35.526s
	Dec. = +21°50'57.15"		Dec. = +22°43'13.15 "
Semi-Diameter =	15'46.51"	Semi-Diameter =	14'48.14"
Eq.Hor.Par. =	08.67"	Eq.Hor.Par. =	0°54'19.28 "
Δ R.A. =	10.215s/h	Δ R.A. =	126.148s/h
Δ Dec. =	21.78"/h	Δ Dec. =	436.27"/h

<u>Lunar Radius</u>	k1 = 0.2725076 (Penumbra)	<u>Shift in</u>	Δb = 0.00"
<u>Constants:</u>	k2 = 0.2722810 (Umbra)	<u>Lunar Position:</u>	Δl = 0.00"

<u>Geocentric Libration:</u>	l = -2.6°	Brown Lun. No. =	995
(Optical + Physical)	b = -1.2°	Saros Series =	147 (22/80)
	c = -7.2°	Ephemeris =	(DE200/LE200)

Eclipse Magnitude = 0.93842 Gamma = 0.99598 ΔT = 64.7 s

Polynomial Besselian Elements for: 2003 May 31 04:00:00.0 TDT (=t₀)

n	x	y	d	l ₁	l ₂	μ
0	-0.3238544	0.9452118	21.8459854	0.5644051	0.0181570	240.614990
1	0.4939022	0.1263288	0.0057463	-0.0000530	-0.0000527	14.999788
2	0.0000545	-0.0001691	-0.0000051	-0.0000098	-0.0000098	-0.000001
3	-0.0000056	-0.0000016	0.0000000	0.0000000	0.0000000	0.000000

Tan f₁ = 0.0046126 Tan f₂ = 0.0045896

At time 't₁' (decimal hours), each Besselian element is evaluated by:

$$a = a_0 + a_1*t + a_2*t^2 + a_3*t^3 \quad (\text{or } a = \sum [a_n*t^n]; n = 0 \text{ to } 3)$$

where: a = x, y, d, l₁, l₂, or μ
t = t₁ - t₀ (decimal hours) and t₀ = 4.000 TDT

The Besselian elements were derived from a least-squares fit to elements calculated at five uniformly spaced times over a six hour period centered at t₀. Thus the elements are valid over the period 1.00 ≤ t₁ ≤ 7.00 TDT.

Note that all times are expressed in Terrestrial Dynamical Time (TDT).

Saros Series 147: Member 22 of 80 eclipses in series.

TABLE 1.2

SHADOW CONTACTS AND CIRCUMSTANCES
ANNULAR SOLAR ECLIPSE OF 2003 MAY 31

$\Delta T = 64.7 \text{ s}$
 $= 000^{\circ}16'13.2''$

		Terrestrial Dynamical Time h m s	Latitude	Ephemeris Longitude†	True Longitude*
External/Internal Contacts of Penumbra:	P1	01:47:20.9	23°22.1'N	052°34.7'E	052°50.9'E
	P4	06:31:08.3	48°42.6'N	161°12.9'W	160°56.7'W
Extreme North/South Limits of Penumbral Path:	L1	02:12:58.5	10°51.5'N	051°44.0'E	052°00.2'E
	L2	06:05:33.5	37°05.6'N	164°20.8'W	164°04.6'W
External/Internal Contacts of Umbra:	U1	03:45:50.5	56°51.6'N	004°57.3'W	004°41.1'W
	U4	04:32:33.4	67°56.3'N	060°22.9'W	060°06.7'W
Extreme North/South Limits of Umbral Path:	N1	03:45:59.3	56°47.1'N	004°52.0'W	004°35.7'W
	N2	04:32:24.5	67°57.1'N	060°36.3'W	060°20.0'W
Extreme Limits of Central Line:	C1	04:03:10.5	62°24.9'N	021°31.5'W	021°15.2'W
	C2	04:15:14.7	65°29.0'N	035°57.4'W	035°41.2'W
Instant of Greatest Eclipse:	G0	04:09:22.4	66°33.2'N	024°46.3'W	024°30.0'W
Circumstances at Greatest Eclipse:	Sun's Altitude = 2.9°				
	Sun's Azimuth = 35.1° Central Duration = 03m36.8s				

† Ephemeris Longitude is the terrestrial dynamical longitude assuming a uniformly rotating Earth.

* True Longitude is calculated by correcting the Ephemeris Longitude for the non-uniform rotation of Earth.

(T.L. = E.L. + $1.002738 \cdot \Delta T / 240$, where ΔT (in seconds) = TDT - UT)

Note: Longitude is measured positive to the East.

Since ΔT is not known in advance, the value used in the predictions is an extrapolation based on pre-2003 measurements. Nevertheless, the actual value is expected to fall within ± 0.3 seconds of the estimated ΔT used here.

TABLE 1.3

PATH OF THE ANTUMBRAL SHADOW
ANNULAR SOLAR ECLIPSE OF 2003 MAY 31

Universal Time	Terminator Limit		Antumbral Limit		Central Line		Sun Path Alt °	Sun Path Width km	Central Durat.
	Latitude	Longitude	Latitude	Longitude	Latitude	Longitude			
Limits	56°47.1'N	004°35.7'W	56°47.1'N	004°35.7'W	62°24.9'N	021°15.2'W	0	-	-
03:45	56°49.0'N	004°40.3'W	57°19.1'N	003°40.2'W	-	-	-	-	-
03:46	57°10.5'N	005°32.3'W	59°16.8'N	000°59.9'W	-	-	-	-	-
03:47	57°31.8'N	006°24.9'W	60°26.5'N	000°05.6'E	-	-	-	-	-
03:48	57°52.9'N	007°18.3'W	61°24.0'N	000°46.0'E	-	-	-	-	-
03:49	58°13.8'N	008°12.3'W	62°14.9'N	001°12.2'E	-	-	-	-	-
03:50	58°34.5'N	009°07.1'W	63°01.4'N	001°28.4'E	-	-	-	-	-
03:51	58°54.9'N	010°02.7'W	63°44.8'N	001°36.9'E	-	-	-	-	-
03:52	59°15.2'N	010°59.1'W	64°25.7'N	001°39.1'E	-	-	-	-	-
03:53	59°35.1'N	011°56.2'W	65°04.7'N	001°35.7'E	-	-	-	-	-
03:54	59°54.9'N	012°54.1'W	65°42.0'N	001°27.3'E	-	-	-	-	-
03:55	60°14.4'N	013°52.9'W	66°17.9'N	001°14.2'E	-	-	-	-	-
03:56	60°33.6'N	014°52.5'W	66°52.5'N	000°56.5'E	-	-	-	-	-
03:57	60°52.5'N	015°53.0'W	67°25.9'N	000°34.5'E	-	-	-	-	-
03:58	61°11.2'N	016°54.4'W	67°58.3'N	000°08.2'E	-	-	-	-	-
03:59	61°29.7'N	017°56.6'W	68°29.7'N	000°22.4'W	-	-	-	-	-
04:00	61°47.8'N	018°59.8'W	69°00.2'N	000°57.3'W	-	-	-	-	-
04:01	62°05.7'N	020°03.9'W	69°29.7'N	001°36.6'W	-	-	-	-	-
04:02	62°23.2'N	021°09.0'W	69°58.3'N	002°20.4'W	-	-	-	-	-
04:03	62°40.4'N	022°15.0'W	70°26.0'N	003°08.8'W	63°54.6'N	020°11.7'W	2	-	03m36.1s
04:04	62°57.3'N	023°22.0'W	70°52.9'N	004°02.0'W	64°40.6'N	020°29.7'W	2	-	03m36.4s
04:05	63°13.9'N	024°30.0'W	71°18.7'N	005°00.1'W	65°15.9'N	021°07.6'W	3	-	03m36.6s
04:06	63°30.2'N	025°39.0'W	71°43.7'N	006°03.3'W	65°44.8'N	021°58.0'W	3	-	03m36.7s
04:07	63°46.1'N	026°49.0'W	72°07.6'N	007°11.8'W	66°08.7'N	022°58.5'W	3	-	03m36.8s
04:08	64°01.6'N	028°00.0'W	72°30.5'N	008°25.8'W	66°28.3'N	024°07.9'W	3	-	03m36.8s
04:09	64°16.8'N	029°12.1'W	72°52.2'N	009°45.4'W	66°43.4'N	025°25.7'W	3	-	03m36.7s
04:10	64°31.6'N	030°25.2'W	73°12.8'N	011°10.9'W	66°54.0'N	026°51.8'W	3	-	03m36.7s
04:11	64°46.0'N	031°39.4'W	73°32.1'N	012°42.4'W	66°59.2'N	028°26.6'W	3	-	03m36.6s
04:12	65°00.0'N	032°54.6'W	73°50.1'N	014°20.0'W	66°57.6'N	030°11.5'W	2	-	03m36.4s
04:13	65°13.6'N	034°10.9'W	74°06.6'N	016°03.9'W	66°45.2'N	032°10.1'W	2	-	03m36.1s
04:14	65°26.8'N	035°28.2'W	74°21.5'N	017°54.1'W	66°03.5'N	034°43.3'W	1	-	03m35.5s
04:15	65°39.6'N	036°46.6'W	74°34.7'N	019°50.5'W	-	-	-	-	-
04:16	65°51.9'N	038°06.0'W	74°46.0'N	021°53.2'W	-	-	-	-	-
04:17	66°03.7'N	039°26.5'W	74°55.3'N	024°01.9'W	-	-	-	-	-
04:18	66°15.1'N	040°48.0'W	75°02.3'N	026°16.3'W	-	-	-	-	-
04:19	66°26.0'N	042°10.4'W	75°06.9'N	028°36.0'W	-	-	-	-	-
04:20	66°36.5'N	043°33.9'W	75°08.9'N	031°00.6'W	-	-	-	-	-
04:21	66°46.4'N	044°58.4'W	75°08.0'N	033°29.4'W	-	-	-	-	-
04:22	66°55.8'N	046°23.8'W	75°03.9'N	036°01.6'W	-	-	-	-	-
04:23	67°04.7'N	047°50.1'W	74°56.2'N	038°36.4'W	-	-	-	-	-
04:24	67°13.0'N	049°17.3'W	74°44.7'N	041°12.9'W	-	-	-	-	-
04:25	67°20.8'N	050°45.4'W	74°28.8'N	043°50.1'W	-	-	-	-	-
04:26	67°28.1'N	052°14.3'W	74°07.7'N	046°27.0'W	-	-	-	-	-
04:27	67°34.8'N	053°44.0'W	73°40.6'N	049°02.8'W	-	-	-	-	-
04:28	67°40.9'N	055°14.4'W	73°05.8'N	051°36.7'W	-	-	-	-	-
04:29	67°46.5'N	056°45.4'W	72°20.6'N	054°08.1'W	-	-	-	-	-
04:30	67°51.4'N	058°17.1'W	71°18.4'N	056°37.7'W	-	-	-	-	-
04:31	67°55.8'N	059°49.4'W	69°34.4'N	059°11.3'W	-	-	-	-	-
Limits	67°57.1'N	060°20.0'W	67°57.1'N	060°20.0'W	65°29.0'N	035°41.2'W	0	-	-

TABLE 1.4

PHYSICAL EPHEMERIS OF THE ANTUMBRAL SHADOW
ANNULAR SOLAR ECLIPSE OF 2003 MAY 31

Universal Time	Central Line		Diameter Ratio	Eclipse Obscur.	Sun Alt °	Sun Azm °	Path Width km	Major Axis km	Minor Axis km	Umbra Veloc. km/s	Central Durat.
	Latitude	Longitude									
04:03	63°54.6'N	020°11.7'W	0.9380	0.8799	1.5	37.7	-	-	-	1.851	03m36.1s
04:04	64°40.6'N	020°29.7'W	0.9382	0.8802	2.1	37.6	-	-	-	1.338	03m36.4s
04:05	65°15.9'N	021°07.6'W	0.9383	0.8804	2.5	37.3	-	-	-	1.166	03m36.6s
04:06	65°44.8'N	021°58.0'W	0.9384	0.8805	2.7	36.8	-	-	-	1.090	03m36.7s
04:07	66°08.7'N	022°58.5'W	0.9384	0.8806	2.9	36.1	-	-	-	1.059	03m36.8s
04:08	66°28.3'N	024°07.9'W	0.9384	0.8806	2.9	35.3	-	-	-	1.057	03m36.8s
04:09	66°43.4'N	025°25.7'W	0.9384	0.8806	2.9	34.4	-	-	-	1.077	03m36.7s
04:10	66°54.0'N	026°51.8'W	0.9384	0.8806	2.8	33.3	-	-	-	1.123	03m36.7s
04:11	66°59.2'N	028°26.6'W	0.9383	0.8805	2.6	32.1	-	-	-	1.206	03m36.6s
04:12	66°57.6'N	030°11.5'W	0.9383	0.8803	2.2	30.8	-	-	-	1.364	03m36.4s
04:13	66°45.2'N	032°10.1'W	0.9381	0.8801	1.7	29.2	-	-	-	1.740	03m36.1s
04:14	66°03.5'N	034°43.3'W	0.9379	0.8796	0.7	27.1	-	-	-	4.724	03m35.5s

TABLE 1.5

LOCAL CIRCUMSTANCES ON THE CENTRAL LINE
ANNULAR SOLAR ECLIPSE OF 2003 MAY 31

Central Line Maximum Eclipse			First Contact				Second Contact			Third Contact			Fourth Contact			
U.T.	Durat.	Alt °	U.T.	P °	V °	Alt °	U.T.	P °	V °	U.T.	P °	V °	U.T.	P °	V °	Alt °
04:03	03m36.1s	2	-	-	-	-	04:01:12	255	272	04:04:48	75	92	05:00:09	75	96	6
04:04	03m36.4s	2	-	-	-	-	04:02:12	255	271	04:05:48	75	92	05:01:21	75	95	7
04:05	03m36.6s	3	-	-	-	-	04:03:12	255	271	04:06:48	75	91	05:02:29	75	95	7
04:06	03m36.7s	3	03:09:47	256	266	0	04:04:12	255	271	04:07:48	75	91	05:03:33	75	94	7
04:07	03m36.8s	3	03:10:43	256	266	1	04:05:12	255	270	04:08:48	75	90	05:04:35	75	94	7
04:08	03m36.8s	3	03:11:40	256	265	1	04:06:12	255	270	04:09:48	75	90	05:05:35	75	94	7
04:09	03m36.7s	3	03:12:40	256	265	1	04:07:12	255	269	04:10:48	75	90	05:06:32	75	93	7
04:10	03m36.7s	3	03:13:41	256	265	1	04:08:12	256	269	04:11:48	76	89	05:07:28	75	93	7
04:11	03m36.6s	3	03:14:44	256	264	1	04:09:12	256	269	04:12:48	76	89	05:08:22	75	93	6
04:12	03m36.4s	3	03:15:50	256	264	1	04:10:12	256	268	04:13:48	76	88	05:09:13	75	92	6
04:13	03m36.1s	2	-	-	-	-	04:11:12	256	268	04:14:48	76	88	05:09:59	75	92	5
04:14	03m35.5s	1	-	-	-	-	04:12:12	256	267	04:15:48	76	88	05:10:33	76	92	4

**Table 1.16 - Weather Statistics for
Annular Solar Eclipse of 2003 May 31**

Location	Latitude	Longitude	Percent Frequency of				obability	% hours with cloud < 0.3 & vis > 2	Monthly pcpn (mm)	% observations with precipitation	% observations with fog	Mean Wind	Prevailing direction		
			Clear	Scattered	Broken	Overcast & Obscured									
Greenland															
Angmagssalik	65.60	-37.63	10.0	18.7	17.3	53.9	0.27	17	58.4	38.0	15.5	11.1	vrbl	3	-2
Danmarkshaun	76.77	-18.67	19.6	26.3	17.7	36.4	0.42	30	5.1	22.1	18.9	10.0	W	-4	-9
Egedesminde *	68.70	-52.75	4.8	24.4	32.5	38.2	0.30	11	15.2	20.7	5.2	5.8	W	0	-4
Fredenskshab	62.00	-43.72	6.4	16.4	13.9	63.2	0.21	11		30.9	14.0	6.1	NW	3	-1
Godthab	64.17	-51.75	6.2	19.1	21.8	52.9	0.25	12	43.2	37.4	11.1	10.3	S	2	-2
Holsteinsborg	66.92	-53.67	13.5	21.1	20.7	44.8	0.33	21		24.3	5.4	5.0	ENE	2	-3
Jakobshavn *	69.25	-51.07	11.4	20.0	42.9	25.8	0.37	11		2 3.4	8.4	4.6	S	0	-4
Julianehab	60.72	-46.05	12.8	20.5	19.1	47.6	0.32	19		28.8	8.8	5.6	calm	6	1
Narsarsuaq	60.18	-45.42	6.7	25.9	28.1	39.2	0.32	19		3 3.7	2.2	6.7	ENE	8	2
Prins Christian	60.03	-43.12	14.8	20.1	16.7	48.4	0.33	22	177.8	31.1	5.6	12.1	N	3	0
Sonder Stromfjord	67.00	-50.80	7.8	29.6	42.2	20.4	0.40	20	12.7	21.5	0.2	6.9	ENE	6	-2
Upernavik	72.78	-56.17	12.2	25.8	22.9	39.1	0.36	21		18.4	4.4	5.5	calm	-2	-6
Iceland															
Akureyri *	65.68	-18.08	3.0	18.4	29.3	49.3	0.24	20	17.8	12.8	3.3	7.5	SE	9	3
Raufarhofn *	66.45	-15.95	6.8	15.1	22.3	55.9	0.23	11		17.3	19.1	9.1	SW	6	1
Blonduos *	65.67	-20.30	1.1	17	11.6	70.2	0.16	8		22.6	10.3	6.2	calm	7	3
Stykkisholmur *	65.08	-22.73	4.1	15.6	31.1	49.1	0.24	9	35.6	13.8	4.9	9.9	E	7	4
Hjardarnes *	65.25	-15.18	0.5	23.2	24.7	51.6	0.23	8	86.4	25.4	17.5	10.5	E	8	4
Reykjavik *	64.13	-21.54	0.9	26.9	35.2	36.9	0.29	13	43.2	34.3	7.4	9.3	E	8	4
Keflavik *	63.97	-22.60	2.4	20.7	32.3	44.7	0.26	10	76.2	23.1	8.2	10.0	NNE	4	4
Eyrbakkı *	63.87	-21.15	1.1	26.3	28.3	44.3	0.27	15		24.4	9.1	10.1	NE	9	5
Vestmannaeyjar *	63.40	-20.28	2.8	25.2	23.2	48.8	0.26	15	83.8	28.3	8.3	18.3	SE	7	4
Faeroes															
Thorshaun *	62.02	-6.77	4.6	12.4	28.3	54.6	0.21	7	78.7	32.3	9.9	8.0	calm	8	6
Jan Mayen *	70.93	-8.67	1.1	12.9	37.2	48.7	0.21	5	30.5	25.9	17.4	10.4	N	1	-2
United Kingdom															
Lerwick, Shetland Is. *	60.13	-1.18	0.6	21.2	39.1	39.1	0.26	9	55.9	27.4	19.1	10.8	N	9	6
Kirkwall, Orkney Is. *	58.95	-2.90	1.9	25.0	41.2	31.8	0.31	10		24.0	20.1	10.4	S	11	6
Wick *	58.45	-3.08	2.4	22.4	47.6	27.6	0.31	9		19.9	17.5	8.2	SE	11	6
Stornoway *	58.22	-6.32	2.3	32.0	36.5	29.2	0.34	17	55.9	27.1	6.7	8.6	vrbl	12	6
Aberdeen	57.20	-2.22	1.8	25.9	40.5	31.8	0.31	11	53.3	24.2	21.5	5.9	vrbl	13	6
Benbecula Island	57.47	-7.37	3.7	32.8	39.3	24.0	0.37	17		25.1	5.2	10.5	vrbl	12	7
Fort William	56.83	-5.10	2.7	26.6	42.3	28.4	0.33	10	99.1	11.9	0.5	4.9	calm	14	8
Invergordon Harbour *	57.68	-4.17	6.7	21.2	32.0	40.1	0.30	12		17.8	6.4	5.8	calm	13	8
Inverness *	57.53	-4.05	1.7	17.8	56.1	24.4	0.30	10	45.7	18.8	7.1	6.0	SW	13	7
Kinloss RAF *	57.65	-3.57	1.6	24.1	52.4	21.8	0.33	14	48.3	24.0	11.0	6.5	SW	13	6
Lossiemouth RAF *	57.72	-3.32	2.5	25.3	51.0	21.1	0.34	13	53.3	21.8	9.7	6.9	SW	13	6
Peterhead Harbour	57.50	-1.77	5.9	23.2	30.8	40.2	0.30	8		18	7.6	7.9	S	11	7
Edinburgh	55.95	-3.21	2.6	27.2	46.0	24.3	0.34	14	50.8	23.6	18.0	5.7	WSW	14	6
Manchester	53.21	-2.27	7.7	27.9	42.6	21.8	0.39	17	63.5	20.5	8.0	6.2	S	15	7
Leeds	53.48	-1.55	12.7	31.7	39.7	15.9	0.45	29		14.3	6.3	3.6	WNW	16	8
Birmingham	52.45	-1.73	7.8	30	36.1	26.1	0.38	19	55.9	21.8	26	5.7	vrbl	16	6
London	51.48	-0.45	15.2	27.1	32.9	24.9	0.43	24	45.7	18.3	9.7	5.2	N	17	8
Glasgow	55.87	-4.43	3.3	27.8	44	24.9	0.35	14		22.2	11.7	6	ENE	15	6

* indicates station is within annular zone

Key to table 1.16 appears on next page.

WEATHER STATISTICS FOR ANNULAR SOLAR ECLIPSE OF 2003 MAY 31

Key to Table 1.16

Percent Frequency of Clear, Scattered (2-4 tenths), Broken (5-9 tenths) and Overcast or Obscured Skies

These data are compiled from surface observations at the site. The time of the observation is usually 0300 UTC except for a few stations where observations at that time are missing. This is about one hour before the eclipse.

Probability

A rough calculation of the probability of seeing the eclipse based on the frequency of clear, scattered, broken or overcast cloud. It is essentially the sums of the frequency of the cloud category times a representative clear sky amount for the category.

% hours with cloud <0.3 and vis > 2

This the frequency of hours with less than 3 tenths cloud and visibilities of 3 miles or more. The time of observation is 0300 UTC except for a few cases as noted above.

Monthly pcpn

Average May precipitation in mm. Snow is melted and the water content measured.

% of observations with precipitation

The percent of observations at 0300 UTC in May in which precipitation is reported.

% of observations with fog

The percent of 0300 UTC observations with visibility less than 3 miles.

Mean wind

The average wind speed in May at 0300 UTC

Prevailing Direction

The most frequent wind direction. Where winds do not show a dominant direction, "vrbl" (variable) is shown. If calm winds are the most common condition and more than 20% of observations, "calm" is indicated.

Tmax

Mean daily high temperature (°C) for December.

Tmin

Mean daily minimum temperature (°C) for December.

2.00 TOTAL SOLAR ECLIPSE OF 2003 NOVEMBER 23

2.01 INTRODUCTION

On Sunday, 2003 November 23, a total eclipse of the Sun will be visible from a broad corridor that traverses portions of the Southern Hemisphere. The path of the Moon's umbral shadow begins in the Indian Ocean, crosses Antarctica, and ends at sunrise near the edge of the southern continent. A partial eclipse will be seen within the much broader path of the Moon's penumbral shadow, which includes Australia, New Zealand, Antarctica and southern South America (Figures 2.1 and 2.2).

The trajectory of the Moon's shadow takes it between the sunrise terminator and the South Pole. As viewed from the Sun's direction, the Moon's shadow passes around the "back" side of the pole between Earth's axis of rotation and the terminator. Consequently, the track of totality travels east to west rather than the usual west to east direction. Furthermore, the 500 kilometer wide path both begins and ends at sunrise, just like the May 31 annular eclipse. The unusual characteristics of these two events is directly attributed to their grazing geometries in Earth's polar regions coupled with the close temporal proximity of the eclipses with summer solstice in each hemisphere.

2.02 PATH OF TOTALITY

The path of the Moon's umbral shadow begins at 22:19 UT in the southern Indian Ocean about 1100 kilometers southeast of Kerguelen Island (Figure 2.2). Curving south, the five hundred kilometer wide umbral path reaches the coast of Antarctica at 22:35 UT. The Shackleton Ice Shelf and Russia's Mirny research station lie in the path where the central duration is 1 minute 55 seconds and the Sun stands 13° above the frozen landscape. Quickly moving inland, the elongated shadow sweeps over the desolate interior of the continent at velocities exceeding 1 kilometer per second (Figure 2.3). No other permanently staffed research stations are encountered for the next half hour.

The instant of greatest eclipse¹ occurs in Wilkes Land at 22:49:17 UT when the axis of the Moon's shadow passes closest to the center of Earth ($\gamma^2 = -0.964$). At this point, the duration of totality reaches its maximum of 1 minute 55 seconds with a Sun altitude of 15°. The duration and altitude slowly drop as the umbra's path curves from southwest to northwest. The umbra reaches the Antarctic coast in Queen Maud Land, which harbors several more research stations (Novolazarevskaya, Maitri). From Maitri, the 1 minute 19 second total phase occurs with the Sun just 2° above the horizon at 23:17 UT.

Two minutes later, the path ends and the shadow leaves Earth's surface (23:19 UT) one hour after it began. Over the course of its sixty minute trajectory, the Moon's umbra sweeps over a track approximately 5,000 kilometers long and covering 0.51% of Earth's surface area.

The rest of Antarctica will see a partial eclipse as well as most of New Zealand, Australia, southern Argentina and Chile (Figure 2.2). Outside of Antarctica, southwestern Australia will witness the largest eclipse. For instance, citizens of Perth will be treated to an early morning partial eclipse of magnitude 0.612. In contrast, the Cape York Peninsula in northeastern Australia lies beyond the penumbra's path and will miss the eclipse entirely.

¹ The instant of greatest eclipse occurs when the distance between the Moon's shadow axis and Earth's geocenter reaches a minimum. Although greatest eclipse differs slightly from the instants of greatest magnitude and greatest duration (for total eclipses), the differences are usually quite small.

² Minimum distance of the Moon's shadow axis from Earth's center in units of equatorial Earth radii.

2.03 ORTHOGRAPHIC PROJECTION MAP OF THE ECLIPSE PATH

Figure 2.1 is an orthographic projection map of Earth [adapted from Espenak, 1987] showing the path of penumbral (partial) and umbral (total) eclipse. The daylight terminator is plotted for the instant of greatest eclipse with north at the top. The sub-Earth point is centered over the point of greatest eclipse and is indicated with an asterisk-like symbol. The sub-solar point (Sun in zenith) at that instant is also shown.

The limits of the Moon's penumbral shadow define the region of visibility of the partial eclipse. This saddle shaped region often covers more than half of Earth's daylight hemisphere and consists of several distinct zones or limits. At the northern boundary lies the limit of the penumbra's path. Great loops at the western and eastern extremes of the penumbra's path identify the areas where the eclipse begins/ends at sunrise and sunset, respectively. Bisecting the 'eclipse begins/ends at sunrise and sunset' loops is the curve of maximum eclipse at sunrise (western loop) and sunset (eastern loop). The exterior tangency points **P1** and **P4** mark the coordinates where the penumbral shadow first contacts (partial eclipse begins) and last contacts (partial eclipse ends) Earth's surface. The path of the umbral shadow bisects the penumbral path from west to east and is shaded dark gray.

A curve of maximum eclipse is the locus of all points where the eclipse is at maximum at a given time. They are plotted at each half hour Universal Time (UT), and generally run in a north-south direction. The outline of the umbral shadow is plotted every ten minutes in UT. Curves of constant eclipse magnitude³ delineate the locus of all points where the magnitude at maximum eclipse is constant. These curves run exclusively between the curves of maximum eclipse at sunrise and sunset. Furthermore, they are quasi-parallel to the northern penumbral limit and the umbral path of total eclipse. The southern limit of the penumbra may be thought of as a curve of constant magnitude of 0%, while adjacent curves are for magnitudes of 20%, 40%, 60% and 80%. The northern and southern limits of the path of total eclipse are curves of constant magnitude of 100%.

At the top of Figure 2.1, the Universal Time of geocentric conjunction between the Moon and Sun is given followed by the instant of greatest eclipse. The eclipse magnitude is given for greatest eclipse. For central eclipses (both total and annular), it is equivalent to the geocentric ratio of diameters of the Moon and Sun. Gamma is the minimum distance of the Moon's shadow axis from Earth's center in units of equatorial Earth radii. The shadow axis passes south of Earth's geocenter for negative values of Gamma. Finally, the Saros series number of the eclipse is given along with its relative sequence in the series.

2.04 STEREOGRAPHIC MAP OF THE NOVEMBER 23 ECLIPSE PATH

The stereographic projection of Earth in Figure 2.2 depicts the path of penumbral and umbral eclipse in greater detail. The map is oriented with north up. International political borders are shown and circles of latitude and longitude are plotted at 20° increments. The region of penumbral or partial eclipse is identified by its northern limit, curves of eclipse begins or ends at sunrise and sunset, and curves of maximum eclipse at sunrise and sunset. Curves of constant eclipse magnitude are plotted for 20%, 40%, 60% and 80%, as are the limits of the path of total eclipse. Also included are curves of greatest eclipse at every half hour Universal Time.

Figures 2.1 and 2.2 may be used to quickly determine the approximate time and magnitude of maximum eclipse at any location within the eclipse path.

³ Eclipse magnitude is defined as the fraction of the Sun's diameter occulted by the Moon. It is strictly a ratio of *diameters* and should not be confused with eclipse obscuration, which is a measure of the Sun's surface *area* occulted by the Moon. Eclipse magnitude may be expressed as either a percentage or a decimal fraction (e.g.: 50% or 0.50).

2.05 DETAILED MAP OF THE PATH OF TOTALITY

The path of totality is plotted on a detailed map appearing in Figures 2.3. The map uses coastline data from the World Data Bank II (WDBII). The WDBII outline files are digitized from navigational charts to a working scale of approximately 1:3 million. Major scientific research stations are plotted to show their relative positions with respect to the path of totality. Only three of the several dozen stations actually lie within the track of total eclipse: Mirny, Novolazarevskaya, and Maitri. Local circumstances have been calculated for the research stations and can be found in Table 2.6.

Although no corrections have been made for center of figure or lunar limb profile, they have little or no effect at this scale. Atmospheric refraction⁴ has not been included because it depends on the atmospheric temperature-pressure profile, which cannot be predicted in advance. These maps are also available on the web at <http://sunearth.gsfc.nasa.gov/eclipse/TSE2003/TSE2003.html>.

2.06 ELEMENTS, SHADOW CONTACTS AND ECLIPSE PATH TABLES

The geocentric ephemeris for the Sun and Moon, various parameters, constants, and the Besselian elements (polynomial form) are given in Table 2.1. The eclipse elements and predictions were derived from the DE200 and LE200 ephemerides (solar and lunar, respectively) developed jointly by the Jet Propulsion Laboratory and the U.S. Naval Observatory for use in the *Astronomical Almanac* for 1984 and thereafter. Unless otherwise stated, all predictions are based on center of mass positions for the Moon and Sun with no corrections made for center of figure, lunar limb profile or atmospheric refraction. The predictions depart from normal IAU convention through the use of a smaller constant for the mean lunar radius k for all umbral contacts (see: LUNAR LIMB PROFILE). Times are expressed in either Terrestrial Dynamical Time (TDT) or in Universal Time (UT), where the best value of ΔT ⁵ available at the time of preparation is used.

From the polynomial form of the Besselian elements, any element can be evaluated for any time t_1 (in decimal hours) via the equation:

$$\mathbf{a} = \mathbf{a}_0 + \mathbf{a}_1 * \mathbf{t} + \mathbf{a}_2 * \mathbf{t}^2 + \mathbf{a}_3 * \mathbf{t}^3 \quad (\text{or } \mathbf{a} = \sum [\mathbf{a}_n * \mathbf{t}^n]; n = 0 \text{ to } 3)$$

where: $\mathbf{a} = x, y, d, l_1, l_2, \text{ or } \mu$

$$\mathbf{t} = t_1 - t_0 \text{ (decimal hours) and } t_0 = 23.00 \text{ TDT}$$

The polynomial Besselian elements were derived from a least-squares fit to elements rigorously calculated at five separate times over a six hour period centered at t_0 . Thus, the equation and elements are valid over the period $20.00 \leq t_1 \leq 02.00$ TDT (Nov 23 to Nov 24).

⁴ The nominal value for atmospheric refraction at the horizon is 34 arc-minutes, but this value can vary by a factor of 2 depending on atmospheric conditions. For an eclipse in the horizon, the umbral path is shifted in the direction opposite from the Sun.

⁵ ΔT is the difference between Terrestrial Dynamical Time and Universal Time.

Table 2.2 lists all external and internal contacts of penumbral and umbral shadows with Earth. They include TDT times and geodetic coordinates with and without corrections for ΔT . The contacts are defined:

- P1** — Instant of first external tangency of penumbral shadow cone with Earth's limb.
(partial eclipse begins)
- P4** — Instant of last external tangency of penumbral shadow cone with Earth's limb.
(partial eclipse ends)
- U1** — Instant of first external tangency of umbral shadow cone with Earth's limb.
(umbral eclipse begins)
- U2** — Instant of first internal tangency of umbral shadow cone with Earth's limb.
- U3** — Instant of last internal tangency of umbral shadow cone with Earth's limb.
- U4** — Instant of last external tangency of umbral shadow cone with Earth's limb.
(umbral eclipse ends)

Similarly, the northern and southern extremes of the penumbral and umbral paths, and extreme limits of the umbra's central line are given. The IAU (International Astronomical Union) longitude convention is used throughout this publication (i.e., for longitude, east is positive and west is negative; for latitude, north is positive and south is negative).

The path of the umbral shadow is delineated at two minute intervals in Universal Time in Table 2.3. Coordinates of the northern limit, the southern limit and the central line are listed to the nearest tenth of an arc-minute (~185 m at the Equator). The Sun's altitude, path width and umbral duration are calculated for the central line position. Table 2.4 presents a physical ephemeris for the umbral shadow at two minute intervals in UT. The central line coordinates are followed by the topocentric ratio of the apparent diameters of the Moon and Sun, the eclipse obscuration⁶, and the Sun's altitude and azimuth at that instant. The central path width, the umbral shadow's major and minor axes and its instantaneous velocity with respect to Earth's surface are included. Finally, the central line duration of the umbral phase is given.

Local circumstances for each central line position listed in Tables 2.3 and 2.4 are presented in Table 2.5. The first three columns give the Universal Time of maximum eclipse, the central line duration of totality and the altitude of the Sun at that instant. The following columns list each of the four eclipse contact times followed by their related contact position angles and the corresponding altitude of the Sun. The four contacts identify significant stages in the progress of the eclipse. They are defined as follows:

- First Contact** — Instant of first external tangency between the Moon and Sun.
(partial eclipse begins)
- Second Contact** — Instant of first internal tangency between the Moon and Sun.
(central or umbral eclipse begins; total or annular eclipse begins)
- Third Contact** — Instant of last internal tangency between the Moon and Sun.
(central or umbral eclipse ends; total or annular eclipse ends)
- Fourth Contact** — Instant of last external tangency between the Moon and Sun.
(partial eclipse ends)

The position angles **P** and **V** identify the point along the Sun's disk where each contact occurs⁷. Second and third contact altitudes are omitted since they are always within 1° of the altitude at maximum eclipse.

⁶ Eclipse obscuration is defined as the fraction of the Sun's surface area occulted by the Moon.

⁷ P is defined as the contact angle measured counter-clockwise from the *north* point of the Sun's disk.

V is defined as the contact angle measured counter-clockwise from the *zenith* point of the Sun's disk.

2.07 LOCAL CIRCUMSTANCES TABLES FOR NOVEMBER 23

Local circumstances for ~140 cities and locations in Antarctica, Australia, New Zealand and South America are presented in Tables 2.6 through 2.10. These tables give the local circumstances at each contact and at maximum eclipse⁸ for every location. The coordinates are listed along with the location's elevation (meters) above sea-level, if known. The Universal Time of each contact is given to a tenth of a second, along with position angles **P** and **V** and the altitude of the Sun. The position angles identify the point along the Sun's disk where each contact occurs and are measured counter-clockwise (i.e., eastward) from the north and zenith points, respectively. Locations outside the umbral path miss the umbral eclipse and only witness first and fourth contacts. The Universal Time of maximum eclipse (either partial or total) is listed to a tenth of a second. Next, the position angles **P** and **V** of the Moon's disk with respect to the Sun are given, followed by the altitude and azimuth of the Sun at maximum eclipse. Finally, the corresponding eclipse magnitude and obscuration are listed. For total eclipses, the eclipse magnitude is identical to the topocentric ratio of the Moon's and Sun's apparent diameters.

Two additional columns are included if the location lies within the path of the Moon's umbral shadow. The **umbral depth** is a relative measure of a location's position with respect to the central line and path limits. It is a unitless parameter which is defined as:

$$u = 1 - \text{abs}(x/R) \quad [2.1]$$

where: **u** = umbral depth
x = perpendicular distance from the shadow axis (kilometers)
R = radius of the umbral shadow as it intersects Earth's surface (kilometers)

The umbral depth for a location varies from 0.0 to 1.0. A position at the path limits corresponds to a value of 0.0 while a position on the central line has a value of 1.0. The parameter can be used to quickly determine the corresponding central line duration. Thus, it is a useful tool for evaluating the trade-off in duration of a location's position relative to the central line. Using the location's duration and umbral depth, the central line duration is calculated as:

$$D = d / (1 - (1 - u)^2)^{1/2} \text{ seconds} \quad [2.2]$$

where: **D** = duration of totality on the central line (seconds)
d = duration of totality at location (seconds)
u = umbral depth

The final column gives the duration of totality. The effects of refraction have not been included in these calculations, nor have there been any corrections for center of figure or the lunar limb profile.

The geographic coordinates of cities are from *The New International Atlas* (Rand McNally, 1991). Coordinates in Antarctica are from www.scar.org/Antarctic%20Info/wintering_stations_2000.htm. The city names and spellings presented here are for location purposes only and are not meant to be authoritative. They do not imply recognition of status of any location by the United States Government.

⁸For partial eclipses, maximum eclipse is the instant when the greatest fraction of the Sun's diameter is occulted. For total eclipses, maximum eclipse is the instant of mid-totally.

2.08 LUNAR LIMB PROFILE FOR NOVEMBER 23

Eclipse contact times, magnitude and duration of totality all depend on the angular diameters and relative velocities of the Moon and Sun. These calculations are limited in accuracy by the departure of the Moon's limb from a perfectly circular figure. The Moon's surface exhibits a rather dramatic topography, which manifests itself as an irregular limb when seen in profile. Most eclipse calculations assume some mean radius that averages high mountain peaks and low valleys along the Moon's rugged limb. Such an approximation is acceptable for many applications, but if higher accuracy is needed, the Moon's actual limb profile must be considered. Fortunately, an extensive body of knowledge exists on this subject in the form of Watts' limb charts [Watts, 1963]. These data are the product of a photographic survey of the marginal zone of the Moon and give limb profile heights with respect to an adopted smooth reference surface (or datum). Analyses of lunar occultations of stars by Van Flandern [1970] and Morrison [1979] have shown that the average cross-section of Watts' datum is slightly elliptical rather than circular. Furthermore, the implicit center of the datum (i.e., the center of figure) is displaced from the Moon's center of mass. Additional work by Morrison and Appleby [1981] shows that the radius of the datum varies with libration producing systematic errors in Watts' original limb profile heights that attain 0.4 arc-seconds at some position angles. Thus, corrections to Watts' limb data are necessary to ensure that the reference datum is a sphere with its center at the center of mass.

The Watts charts have been digitized and may be used to generate limb profiles for any libration. Ellipticity and libration corrections can be applied to refer the profile to the Moon's center of mass. Such a profile can then be used to correct eclipse predictions which have been generated using a mean lunar limb.

The lunar limb profile in Figure 2.5 includes corrections for center of mass and ellipticity [Morrison and Appleby, 1981]. It is generated for the central line at 22:40 UT which is close to Russia's Mirny research base. The Moon's topocentric libration (physical + optical) is $l=+0.21^\circ$ $b=+0.29^\circ$, and the topocentric semi-diameters of the Sun and Moon are 971.8 and 1008.4 arc-seconds, respectively. The Moon's angular velocity with respect to the Sun is 0.632 arc-seconds per second.

The radial scale of the limb profile (bottom of Figure 2.5) is greatly exaggerated so that the true limb's departure from the mean lunar limb is readily apparent. The mean limb with respect to the center of figure of Watts' original data is shown (dashed) along with the mean limb with respect to the center of mass (solid). Note that all the predictions presented in this publication are calculated with respect to the latter limb unless otherwise noted. Position angles of various lunar features can be read using the protractor marks along the Moon's mean limb (center of mass). The position angles of second and third contact are clearly marked along with the north pole of the Moon's axis of rotation and the observer's zenith at mid-totality. The dashed line with arrows at either end identifies the contact points on the limb corresponding to the northern and southern limits of the path. To the upper left of the profile are the Sun's topocentric coordinates at maximum eclipse. They include the right ascension *R.A.*, declination *Dec.*, semi-diameter *S.D.* and horizontal parallax *H.P.* The corresponding topocentric coordinates for the Moon are to the upper right. Below and left of the profile are the geographic coordinates of the center line at 22:40 UT while the times of the four eclipse contacts at that location appear to the lower right. Directly below the profile are the local circumstances at maximum eclipse. They include the Sun's altitude and azimuth, the path width, and central duration. The position angle of the path's northern/southern limit axis is *PA(N.Limit)* and the angular velocity of the Moon with respect to the Sun is *A.Vel.(M:S)*. At the bottom left are a number of parameters used in the predictions, and the topocentric lunar librations appear at the lower right.

In investigations where accurate contact times are needed, the lunar limb profile can be used to correct the nominal or mean limb predictions. For any given position angle, there will be a high mountain (annular eclipses) or a low valley (total eclipses) in the vicinity that ultimately determines the true instant of contact. The difference, in time, between the Sun's position when tangent to the contact point on the mean limb and tangent to the highest mountain (annular) or lowest valley (total) at actual contact is the desired correction to the predicted contact time. On the exaggerated radial scale of Figure 2.4, the Sun's limb can be represented as an epicyclic curve that is tangent to the mean lunar limb at the point of contact. Using the digitized Watts' datum, an analytical solution is straightforward and robust. Curves of corrections to the times of second and third contact for most position angles have been computer generated and plotted. The circular protractor scale at the center represents the nominal contact time using a mean lunar limb. The departure of the contact correction curves from

this scale graphically illustrates the time correction to the mean predictions for any position angle as a result of the Moon's true limb profile. Time corrections external to the circular scale are added to the mean contact time; time corrections internal to the protractor are subtracted from the mean contact time. The magnitude of the time correction at a given position angle is measured using any of the four radial scales plotted at each cardinal point.

For example, Table 2.6 gives the following data for the Antarctic base Mirny:

Second Contact	= 22:37:37.0 UT	P2=117°
Third Contact	= 22:39:30.7 UT	P3=283°

Using Figure 18, the measured time corrections and the resulting contact times are:

C2=+0.5 seconds;	Second Contact	= 22:37:37.0 +0.5s	= 22:37:37.5 UT
C3=-4.3 seconds;	Third Contact	= 22:39:30.7 -4.3s	= 22:39:26.4 UT

The above corrected values are within 0.1 seconds of a rigorous calculation using the true limb profile.

2.09 SKY DURING TOTALITY

The total phase of an eclipse is accompanied by the onset of a rapidly darkening sky whose appearance resembles evening twilight about half an hour after sunset. The effect presents an excellent opportunity to view planets and bright stars in the daytime sky. Aside from the sheer novelty of it, such observations are useful in gauging the apparent sky brightness and transparency during totality.

During the total solar eclipse of 2003, the Sun is in northern Scorpius near the border with Libra. From Antarctica, three naked eye planets and a number of bright stars will be above the horizon within the umbral path. Figure 2.5 depicts the appearance of the sky during totality as seen from the central line at 22:40 UT. This is close to Russia's Mirny research base, where the early morning eclipse occurs low in the southeastern sky.

The most conspicuous planet visible during totality will be Venus ($m_v = -3.8$) located 25° east of the Sun in Ophiuchus. Mercury ($m_v = -0.4$) lies between the Sun and Venus at a solar elongation of 16° east. Jupiter ($m_v = -1.8$) is over a magnitude brighter than Mercury but it will be located in Leo in the northeastern sky 75° away from the Sun. From the central line at 22:40 UT, Venus, Mercury and Jupiter will have altitudes above the horizon of 9.4°, 12.6° and 12.7°, respectively. For comparison, the Sun's altitude will be 14°. Saturn and Mars are both below the horizon.

A number of the bright stars may also be visible in the twilight sky during the total eclipse. Antares ($m_v = +1.06$) is 10° southeast of the Sun. The great southern stars Alpha ($m_v = +0.14$) and Beta ($m_v = +0.58$) Centauri are high in the sky about 44° from the Sun. Canopus is near the zenith about 100° away and Achernar ($m_v = +0.45$) stands high in the southwest. Sirius ($m_v = -1.44$) and the bright stars of Orion lie in the northwest quadrant of the sky. It should be noted that star visibility requires a very dark and cloud free sky during totality.

The following ephemeris [using Bretagnon and Simon, 1986] gives the positions of the naked eye planets during the eclipse. *Delta* is the distance of the planet from Earth (A.U.'s), *App. Mag.* is the apparent visual magnitude of the planet, and *Solar Elong* gives the elongation or angle between the Sun and planet.

Ephemeris: 2003 Nov 23 23:00:00 UT				Equinox = Mean Date			
Planet	RA	Declination	Delta	App. Mag.	Apparent Diameter "	Phase	Solar Elong °
Sun	15h56m25s	-20°24'28"	0.98745	-26.7	1943.7	-	-
Moon	15h55m35s	-21°22'40"	0.00239	-	2009.3	0.00	1.0W
Mercury	17h04m34s	-25°03'35"	1.28941	-0.4	5.2	0.89	16.4E
Venus	17h43m08s	-24°32'35"	1.49229	-3.8	11.2	0.91	25.0E
Mars	23h16m20s	-05°57'46"	0.79238	-0.6	11.8	0.87	106.4E
Jupiter	11h11m23s	+06°20'50"	5.56825	-1.8	35.4	0.99	74.9W
Saturn	6h53m56s	+22°08'25"	8.26635	+0.1	20.1	1.00	138.8W

2.10 INTRODUCTION TO WEATHER PROSPECTS FOR NOVEMBER 23

This will probably be the first eclipse to be systematically observed from Antarctica - the coldest, windiest, highest and driest place on the Earth. The meteorology is simple because it is dominated by one factor: cold. Cold air forms in the center of the Antarctic Plateau, close to the south pole, and flows outward to the margins of the continent. The flow is primarily katabatic, driven by gravity as the heavy frigid air moves downhill toward the sea. Where the terrain funnels and confines this steady flow, wind speeds reach exceptional values, among the strongest ever recorded.

Weather stations are isolated and mostly confined to the shores. Inland, automatic stations measure a small selection of the possible variables: wind, temperature, pressure but not cloud cover, humidity, visibility or precipitation. It doesn't matter much - in the cold air absolute humidities are always low and precipitation is sparse. Data are often missing and frequently suspect. The length of the climatological record is short so that the statistics represent more "what is possible or typical" rather than give a serious account of the average conditions.

On the coast and at a very few inland locations, humans supplement the machine measurements, and the full suite of observations is available. For the eclipse observer, cloud cover is usually paramount, but in the extremes of the White Continent, temperature, wind and wind chill demand the attention of eclipse planners far more than in any other location in the world. While Mongolia and Siberia offered the possibility of extreme cold in the 1997 eclipse, Antarctica in 2003 virtually guarantees it.

The eclipse track is not forgiving, and there are only four venues from which it can be realistically observed. Two of these are at coastal locations, one near the Russian base at Mirny and the other near the western limit of the eclipse where a collection of German, Indian, Japanese and Russian bases congregate. The third site is "inland", at whatever point adventure and finances can take an eclipse expedition. The fourth possibility is aboard an icebreaker at sea or near the coast along the sunrise portion of the path.

2.11 WEATHER PATTERNS

Antarctic winds flow outward from a cold high pressure system overlying the continent, turning gradually toward the west as they approach the coast. Descending from the 3000 meter mid-continent plateau, the air is dried even farther, bringing bright sunny skies to the continental margins. In some regions the winds are exceptionally strong - over 100 km/h - as the local topography squeezes and redirects them. Blizzards and blowing snow are common in such circumstances.

As the cold outflow moves over the relatively warm waters surrounding the continent, the air is rapidly saturated with moisture. Clouds form quickly bringing snow showers to the coastal regions and offshore ice fields. The wind shear along the edges of the cold air outbreaks and the strong temperature contrast between air and water helps to create a continuous supply of small scale lows along the coast.

Farther offshore, the southeast winds flowing off of the continent gradually abate and the westerly global flow asserts itself. This change in wind direction creates a zone of intense low-pressure development. The lows that form tend to travel east and southward, gradually moving toward the Antarctic coast where they weaken and die. Some stronger lows can penetrate into the continent, but these are rare, though the lack of observation and measurement makes the exact frequency of such systems uncertain. Even though the low itself may be confined to coastal waters, the higher clouds from such systems can penetrate well inland.

Lows moving along the coast tend to bring onshore winds as they approach and offshore southerlies as they depart. The first pushes moist air against the land and brings extensive stratiform cloudiness and continuous precipitation - either rain or snow - while the latter reinforces the normal cold outflow with its sunny skies from the continent margins.

The interior of the continent offers a considerably more relaxed climatology, notwithstanding the low temperatures. Water vapor is in short supply and weather systems from the north have difficulty scaling the steep slopes of the coast. Unfortunately observations of cloud cover are almost non-existent in central Antarctica, and satellite observations are limited by the lack of contrast between the icy surface and the clouds and the long polar nights. The Russian base at Vostok is the only one in the vicinity of the eclipse track that can provide cloud data but their statistics are probably representative of the conditions over much of the mid-continent portion of the track.

Temperatures along the coast are relatively warm and have the potential to rise above zero, but those inland are much lower. The coldest temperatures are a result of the long Antarctic nights, low humidity, high albedo, low cloud cover and high altitude of the interior that allows the surface to radiate energy into space with little interruption. The warmest temperatures that are found in the interior (-18° C at Vostok) are a result of advection from coastal regions. On the eclipse track the coldest temperatures tend to be found near the Australian automatic weather stations LGB20 and LGB35. Fortunately such temperatures come with much better prospects for clear skies. Since warm temperatures on the coast are associated with cloudy weather, falling temperatures will be preferred on eclipse day as these bring in the drier air from the interior.

Though winds inland are about half the strength of those on the coast, the lower temperatures in the interior dominate the calculation of wind chill to bring values which can reach into the minus sixties. Frostbite can occur in less than four minutes in such weather. While the actual temperatures are considerably warmer, observers will probably want to limit their outdoor exposure while waiting for the lunar shadow, or at least make sure they have some shelter from the wind.

2.12 COAST OF QUEEN MARY LAND — MIRNY

Mirny is the main Russian base in the Antarctic, situated on the coast of Queen Mary Land on a small peninsula that juts northward into the Davis Sea. Established in 1956, the station has the distinction of being best placed within the eclipse track, for the central line lies only a few tens of kilometers to the east. The station buildings, a collection of two-story rectangular blocks topped by various instrument domes, lies on four rocky outcrops about 20 meters above sea level. South of the station, the land rises to a height of 1500 meters within 100 km. A few small rocky islands lie offshore, but land-fast ice is observable much of the year. The 24-hour polar day begins on December 10 at Mirny, and so eclipse day will be one with long daylight and a short twilight.

Mirny's weather is governed by strong downslope winds and a high frequency of offshore low pressure systems. While the blizzard season is receding in November, winds at eclipse time average a brisk 41 km/h (Table 2.11) with the highest reported value in the past 15 years reaching over 110 km/h. Temperatures are modest by Antarctic standards, with an average of -7°C and a range from minus 20 to the freezing point at eclipse time. The high winds bring a significant wind chill to the station however, and eclipse observers will have to dress accordingly. By Canadian and north European winter standards, the average eclipse-day conditions at Mirny appear to be relatively tolerable though the wind speeds are higher than is typical of the Earth's northern hemisphere.

Cloud cover at Mirny averages 6.4 tenths, a large value when compared with opportunities at past eclipses but comparable to the other coastal stations on and near the track. The distribution of cloudiness is a typical U-shape (Figure 2.5), with a high frequencies of low and high cloudiness and smaller frequencies of intervening

values. If we make the assumption that the probability of seeing the eclipse is proportional to the frequency of the various levels of cloud cover, then Mirny offers a 36% chance of a successful expedition. This is slightly optimistic as no account has been taken of the low 13° altitude of the Sun.

Low-pressure disturbances moving toward the station can bring heavy clouds and precipitation for several days in a row but November is approaching the driest months of the year and these are relatively uncommon. Eclipse observers will be looking for southerly katabatic winds blowing from the high plateau, for such winds bring dry cold air and clear skies. Such winds are more frequent in the evening and overnight, which favors the sunset portion of the eclipse track rather than the morning portion at Mirny. The wind speed is critical however, for even under clear skies, blizzard conditions can develop if winds are too strong - anything above 35 km/h brings poor visibility and blowing snow. Heavy snow is rare during the summer months from November to February. Fog and ice crystal haze are rare at any time.

2.13 INTERIOR OF ANTARCTICA

While human observations are in limited supply, several automatic weather stations lie within the track of the eclipse and can provide temperature and wind information. These stations, LGB20, LGB35 and LGB59 (Table 2.11) show a considerably colder climate than the coastal regions. Though winds are frequently lighter on the interior plateau, wind chill values are colder because of the lower initial temperature. Observing from distant inland sites along the eclipse track will require special care for equipment and people.

The interior stations have a short period of record - from 4 to 10 years - and the climatology of the interior is only poorly revealed. For the three Australian automatic stations, average temperatures at eclipse time ranged from -28°C to -33°C. Extreme temperatures dropped as low as -41.5°C at LGB20. Wind chill values are 15 to 20 degrees colder on average, reaching below -60°C at LGB20. At LGB20 and LGB35, wind speeds are relatively low, about half of those at LGB59. The explanation likely lies in the configuration of the surrounding terrain. The prevailing wind direction at LGB59 is also at odds with most of the other interior stations, being northerly rather than the more typical southerly outflow.

For cloud cover statistics we are forced to rely on the data collected at Vostok, which lies considerably farther inland and at a higher altitude. Here we see a complete reversal of the cloud patterns of the coast, with clear skies being the most frequent report. The mean cloudiness of 3.4 tenths is nearly half that of Mirny, and the probability of seeing the eclipse rises to 66%. While inland sites on the track are probably not quite this favorable, the implications cannot be ignored - for this eclipse, inland areas are most likely to see the event by a considerable margin.

The impact of frontal cloudiness and weather systems is muted by distance from the oceans and the high altitude of the interior. Most of the clouds are at mid and high levels where, being composed entirely of ice crystals, they are frequently semi-transparent. This implies that the probability of seeing the eclipse is greater than the formal calculation (66%) would suggest.

The atmospheric transparency of inland Antarctica is legendary. The air is unpolluted except for occasional water vapor and ice crystals. Snowstorms are rare and tend to be at a minimum in the spring. During calm and clear weather, ice crystals are frequent, bringing a hazy sky and occasional ice fog. Both of these phenomena are more likely in winter than summer but their main effect on the eclipse will be to produce a halo around the sun. Drifting snow is common, occurring on nearly one third of the days at Vostok.

2.14 COAST OF QUEEN MAUD LAND — MAITRI, NEUMAYER, AND NOVOLAZAREVSKAJA

The eclipse track comes to an end just beyond Antarctica's coast and the solar altitude is very low for observation sites in this area. The Russian base Novolazarevskaja and the near-by Indian base at Maitri are the two stations within the path, and von Neumayer (Germany) lies just to the west. Maitri and Novolazarevskaja, four kilometers apart, are situated on the rocky ground of the Schirmacher oasis, a group of low-lying hills interspersed with many glacial lakes. Neumayer lies on a flat ice shelf in Atka Bay, buried beneath the snow and ice. Those with an urge to see the station first hand can go to http://www.awi-bremerhaven.de/NM_WebCam/

for hourly photographs from their web cam. These stations are 80 to 100 kilometers from open water because of the presence of the ice shelf at the foot of the continent.

Temperature, wind chill and wind statistics for the sunset stations are similar to those at Mirny but cloud statistics are more variable. Neumayer is one of the grayest locations on the track with an average cloudiness of 7.6 tenths. Novolazarevskaja averages 5.7 tenths and Maitri only 3.9 tenths, a rather discordant amount given their proximity to the others. The reason for the much lower cloud cover at Maitri may be due to local conditions that favor downslope winds or to the short period of record that just happens to lie in a relatively sunny time. A comparison of hourly reports from Maitri with those at Novolazarevskaja shows a few large differences but a near-zero bias, so the second explanation would seem to be the most reasonable. The cloud climatology of the Russian base with its longer period of record seems to be more reliable for planning purposes.

With this in mind, cloudiness patterns along the eclipse sunset coast are similar to those at Mirny (Figure 2.5). Most of the cloud is at mid and high levels, a factor that does not augur well for such a low altitude eclipse. The formal probability of seeing the eclipse is calculated to be between 27 and 52 percent, with the 44% at Novolazarevskaja being the most representative figure. These must be regarded as too large in view of the very low angle toward the eclipse.

2.15 SELECTING A SITE

Antarctic eclipse adventurers are likely to have little choice in their selection of an observing site, as most travel will be to existing bases. Most sites offer some alternative locations relatively nearby: at Novolazarevskaja the airport is 15 km inland from the base, and most other sites have inland and upland scientific bases. Where movement is possible, it is best to look for a spot where the southeast katabatic winds are most favored, in the northwest lee of a plateau for instance.

In interior regions, site selection will be more versatile, as almost all access will be by plane. Flat vistas where the winds are lightest should be easy to locate - a high spot might even be best, as winds will tend to flow downhill and away. Satellite imagery (most big bases have it) can be used to predict cloud motion and help select a site with a high prospect of clear skies.

The interior offers the best chances and the biggest challenges. Prospects for clear skies are twice those of the coast, depending on the distance and altitude at the site. Coastal regions offer more comfort and easier access, but at the expense of a high cloud frequency. Mirny seems to be the best lowland site, in large part because of the higher Sun. Observers there should attempt to move as far inland as possible to take advantage of the better weather away from the coast.

2.16 - WEATHER WEB SITES FOR NOVEMBER 23 TOTAL ECLIPSE

World —

1. <http://www.tvweather.com> - Links to current and past weather and climate around the world
2. <http://www.worldclimate.com/climate/index.htm> - World data base of temperature and rainfall
3. <http://www.accuweather.com> - Forecasts for many cities worldwide
4. <http://www.worldweather.org/> A site operated by the World Meteorological Organization with links to the climate and meteorological data worldwide. This site is still being developed and in many instances only climate information is available.
5. <http://www.fnoc.navy.mil/PUBLIC/WXMAP/index.html> - U.S. Navy weather center (Fleet Numerical Meteorology and Oceanographic Center - FNMOC). This site provides several (3) model outputs for many areas of the globe. While complex to use (meteorological expertise is a real bonus), it contains a wealth of model data. Look for relative humidity forecasts for 700 hPa (hectoPascals) - this is a mid-level of the atmosphere and the relative humidity forecasts provide an indication of the forecast cloud cover from larger weather systems. Use the 70% contour as the outline of cloud areas. Areas with 90% or greater will likely have precipitation. Model forecasts for six days in advance for many parts of the world are available.

Antarctica —

1. <http://weather.uwyo.edu/> - An impressive site at the University of Wyoming that allows you to build your own numerical model output. Choose “Forecasts from Numerical Models” and then “Aviation Model” to be given a choice of a model output over Antarctica. For coastal Antarctica, choose 700 mb relative humidity. For the interior of Antarctica choose 500 mb relative humidity. Values above 70% at 700 mb frequently indicate deep cloudiness but values over 80% are likely required for cloud over the cold dome of Antarctica.
2. <http://www.people.fas.harvard.edu/~dbaron/sat/comp/> - Latest composite (assembled from several satellite passes over several hours) over Antarctica. Choose “Antarctica Composite Images” and select from available links. Because of the low latitude of the continent, there are frequently holes in the coverage, but eclipse areas are usually well shown. A Japanese mirror site provides animated views but the speed of animation is very quick and requires careful orientation and study.
3. <http://uwamrc.ssec.wisc.edu/amrhome.html> - The Antarctic Meteorology Research Centre. This site provides links to polar orbiting satellite imagery and current weather observations.

Total Solar Eclipse of 2003 Nov 23

FIGURE 2.1 - ORTHOGRAPHIC PROJECTION MAP OF THE ECLIPSE PATH

Geocentric Conjunction = 23:20:14.6 UT J.D. = 2452967.472391
 Greatest Eclipse = 22:49:16.7 UT J.D. = 2452967.450887

Eclipse Magnitude = 1.03788 Gamma = -0.96381

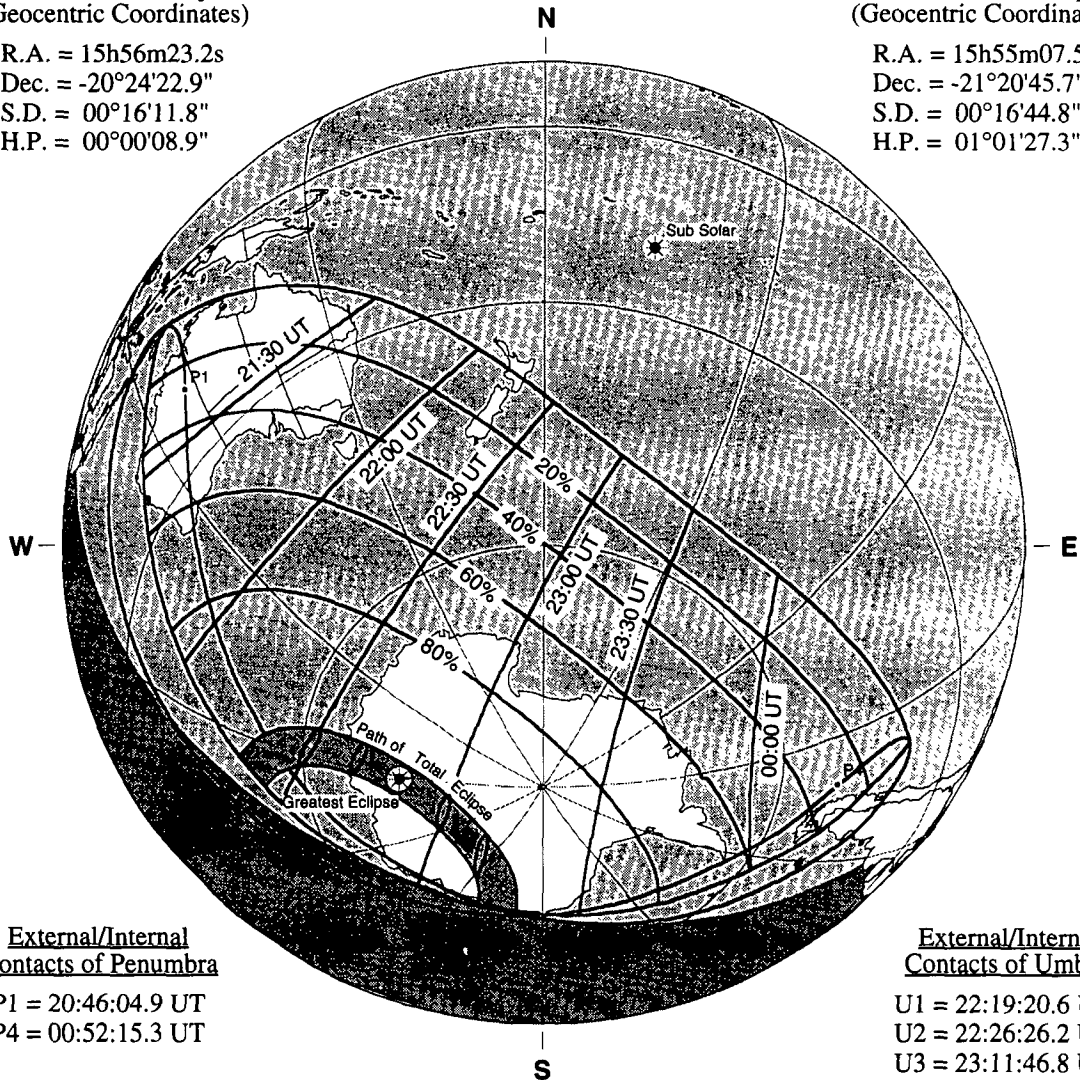
Saros Series = 152 Member = 12 of 70

Sun at Greatest Eclipse
(Geocentric Coordinates)

R.A. = 15h56m23.2s
 Dec. = -20°24'22.9"
 S.D. = 00°16'11.8"
 H.P. = 00°00'08.9"

Moon at Greatest Eclipse
(Geocentric Coordinates)

R.A. = 15h55m07.5s
 Dec. = -21°20'45.7"
 S.D. = 00°16'44.8"
 H.P. = 01°01'27.3"



External/Internal
Contacts of Penumbra

P1 = 20:46:04.9 UT
 P4 = 00:52:15.3 UT

External/Internal
Contacts of Umbra

U1 = 22:19:20.6 UT
 U2 = 22:26:26.2 UT
 U3 = 23:11:46.8 UT
 U4 = 23:18:52.7 UT

Local Circumstances at Greatest Eclipse

Lat. = 72°40.0'S Sun Alt. = 14.9°
 Long. = 088°23.5'E Sun Azm. = 111.2°
 Path Width = 495.5 km Duration = 01m57.3s

Ephemeris & Constants

Eph. = DE200/LE200
 $\Delta T = 65.0$ s
 $k1 = 0.2725076$
 $k2 = 0.2722810$
 $\Delta b = 0.0''$ $\Delta l = 0.0''$

Geocentric Libration
(Optical + Physical)

$l = 0.01^\circ$
 $b = 1.28^\circ$
 $c = 10.41^\circ$

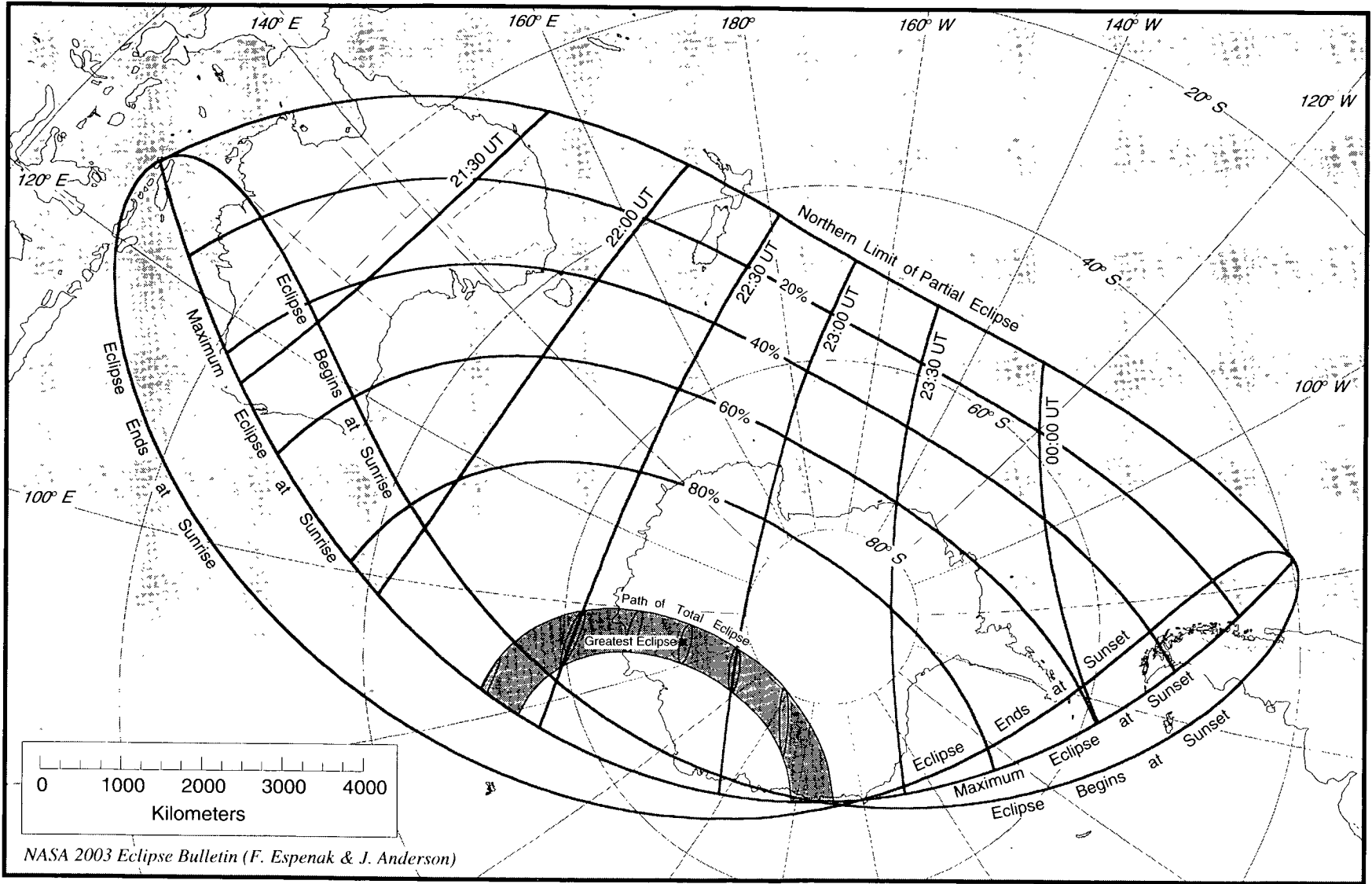
Brown Lun. No. = 1001

NASA 2003 Eclipse Bulletin (F. Espenak & J. Anderson)

sunearth.gsfc.nasa.gov/eclipse/eclipse.html

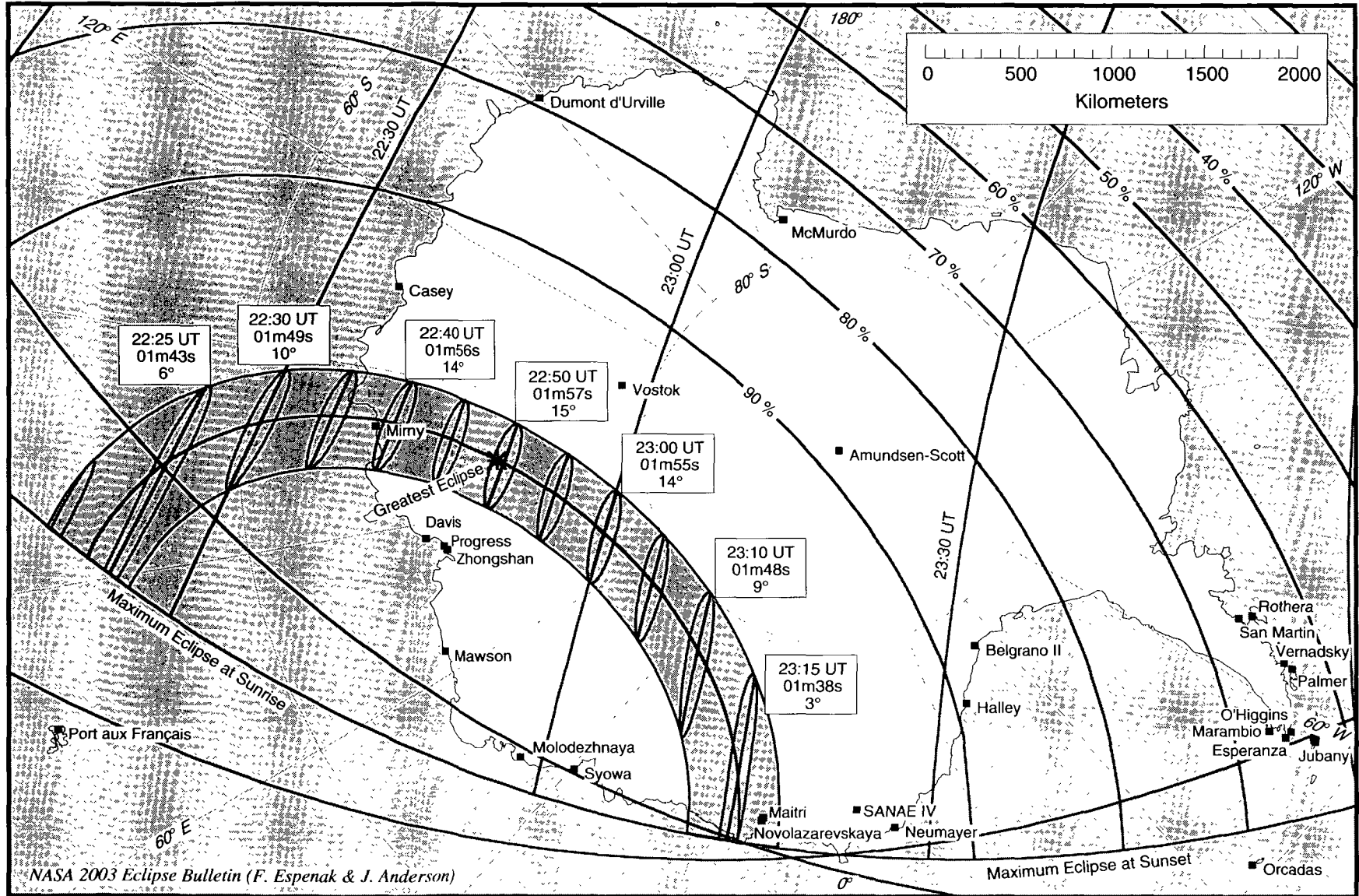
Total Solar Eclipse of 2003 November 23

FIGURE 2.2 - STEREOGRAPHIC PROJECTION MAP OF THE ECLIPSE PATH



Total Solar Eclipse of 2003 November 23

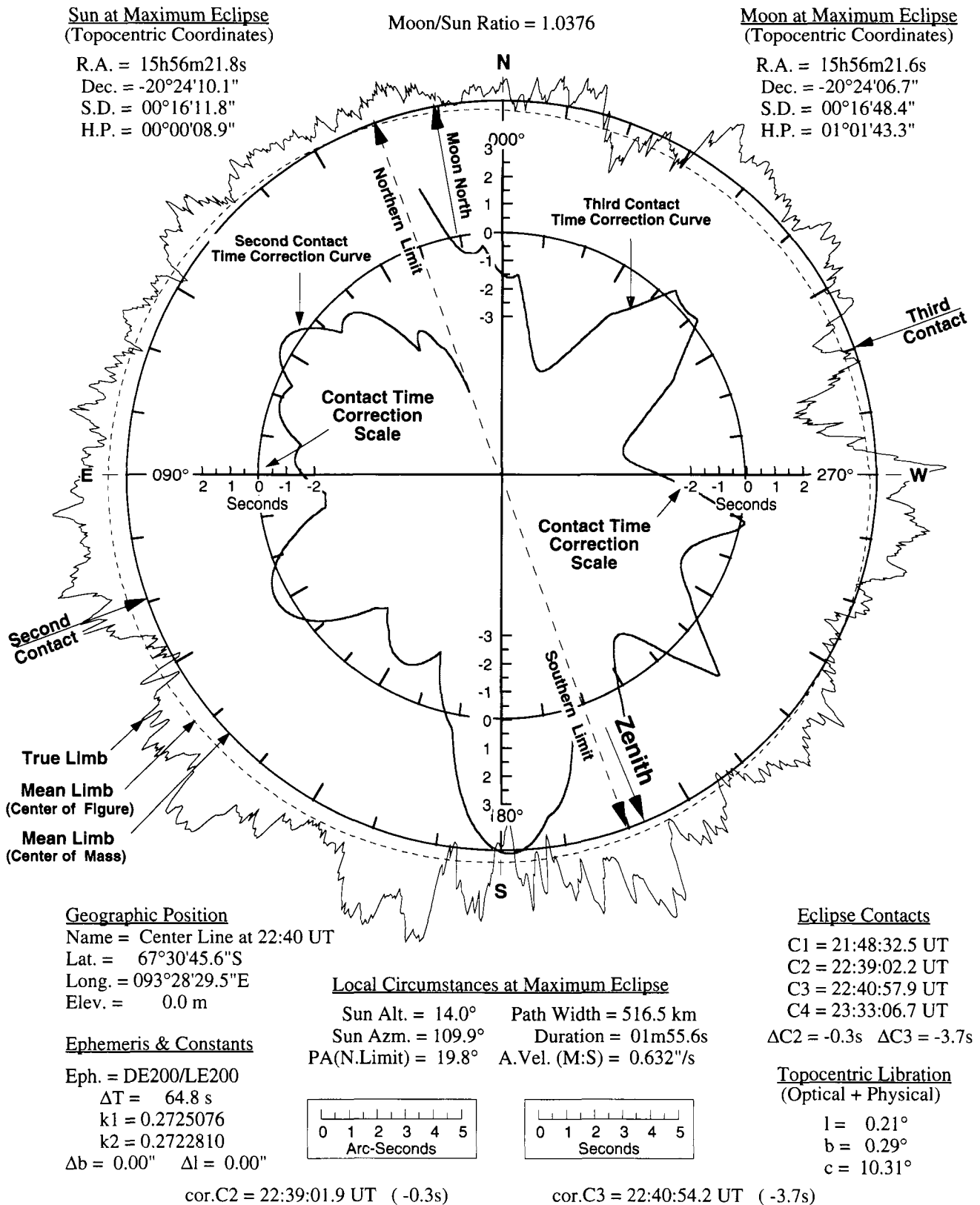
FIGURE 2.3 - THE ECLIPSE PATH THROUGH ANTARCTICA



NASA 2003 Eclipse Bulletin (F. Espenak & J. Anderson)

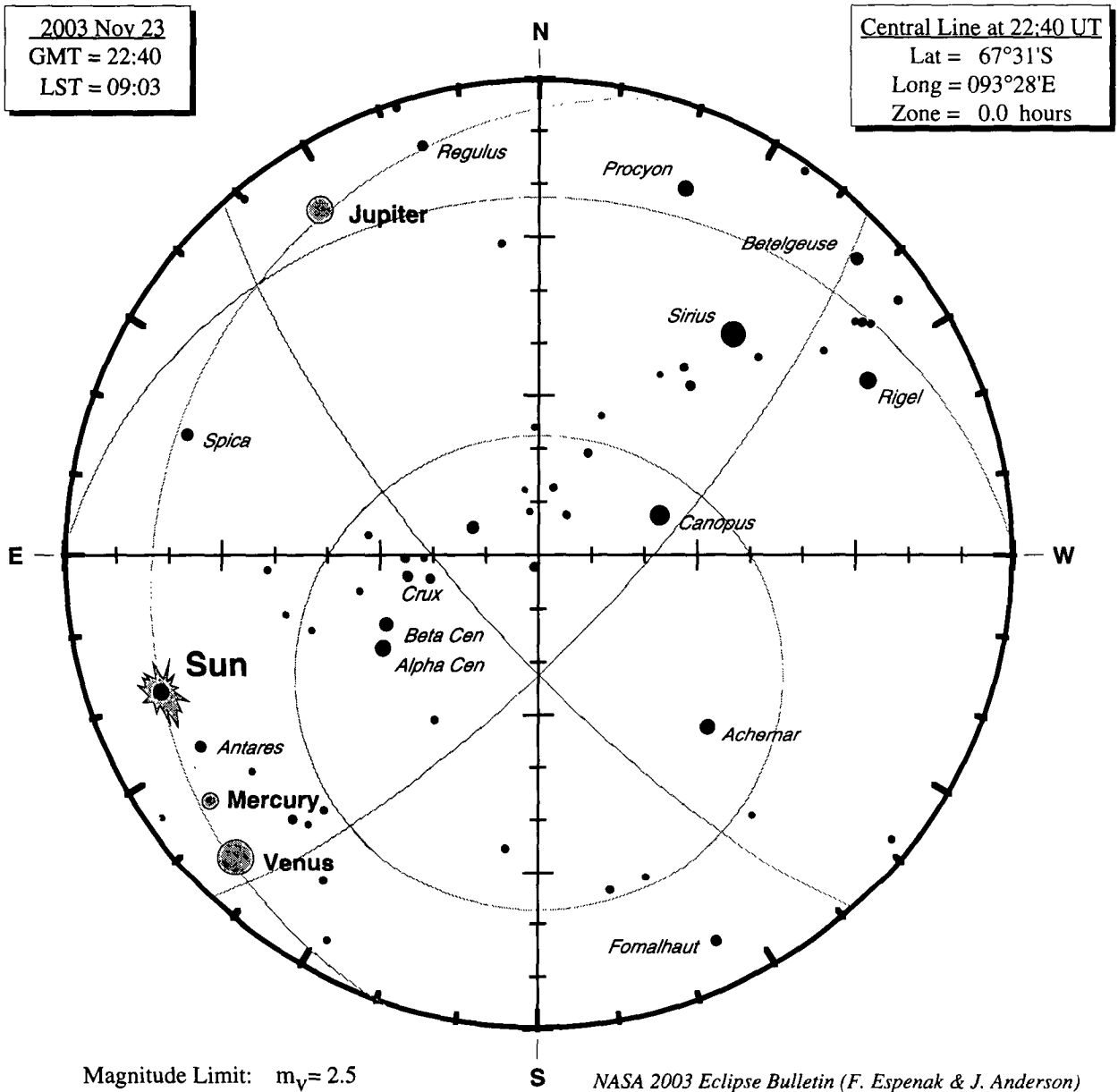
Total Solar Eclipse of 2003 November 23

FIGURE 2.4 - LUNAR LIMB PROFILE FOR NOV 23 AT 22:40 UT



Total Solar Eclipse of 2003 November 23

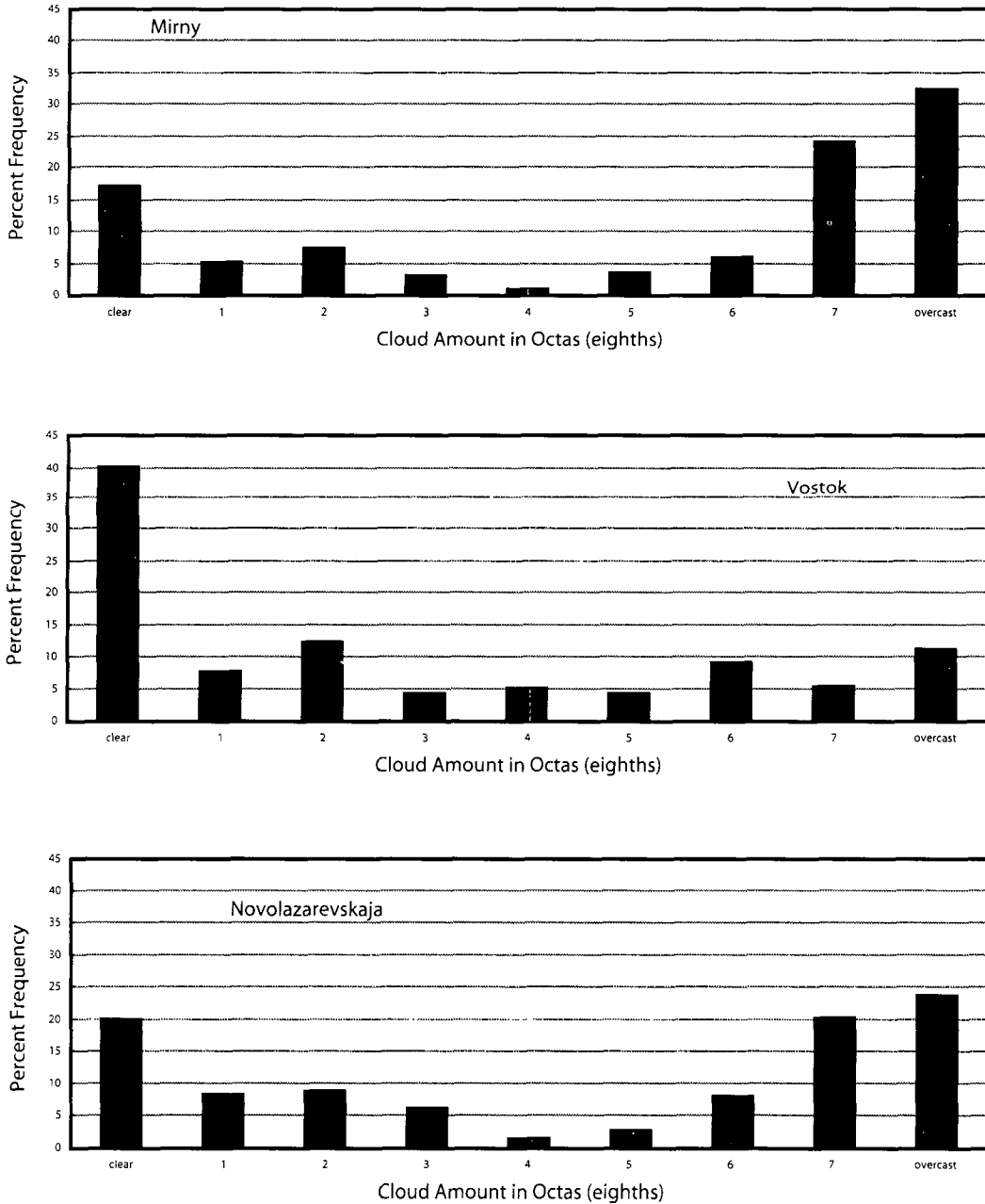
FIGURE 2.5 - SKY DURING TOTALITY AS SEEN FROM CENTRAL LINE AT 22:40 UT



The sky during totality as seen from the central line in Antarctica at 22:40 UT. The most conspicuous planets visible during the total eclipse will be Venus ($m_v = -3.8$), Mercury ($m_v = -0.4$) and Jupiter ($m_v = -1.8$) located 25° east, 16° east and 75° west of the Sun, respectively. Bright stars which might be visible include Antares ($m_v = +1.06$), Alpha ($m_v = +0.14$) and Beta ($m_v = +0.58$) Centauri, Canopus ($m_v = -0.62$), Achernar ($m_v = +0.45$) and Sirius ($m_v = -1.44$).

<http://sunearth.gsfc.nasa.gov/eclipse/TSE2003/TSE2003.html>

**Figure 2.6 - Cloud Statistics for Three Stations
for the Total Solar Eclipse of 2003 Nov 23**



These graphs show the frequency of various cloud amounts at selected stations within or near the eclipse path. At Mirny and Novolazarevskaja the distribution has a “U” shape, with higher values at low and high cloudiness. This is typical of most cloud distributions around the globe. At Vostok the distribution is more one-sided, with clear skies having the highest frequency. The sites chosen reflect the coastal and inland cloud climatologies along the track. Data are taken from the archives of the British Antarctic Society.

TABLE 2.1

ELEMENTS OF THE TOTAL SOLAR ECLIPSE OF 2003 NOVEMBER 23

Geocentric Conjunction 23:21:19.59 TDT J.D. = 2452967.473143
of Sun & Moon in R.A.: (=23:20:14.79 UT)

Instant of 22:50:21.65 TDT J.D. = 2452967.451639
Greatest Eclipse: (=22:49:16.85 UT)

Geocentric Coordinates of Sun & Moon at Greatest Eclipse (DE200/LE200):

<u>Sun:</u>	R.A. = 15h56m23.195s	<u>Moon:</u>	R.A. = 15h55m07.521s
	Dec. = -20°24'22.85"		Dec. = -21°20'45.70"
	Semi-Diameter = 16'11.82"		Semi-Diameter = 16'44.76"
	Eq.Hor.Par. = 08.91"		Eq.Hor.Par. = 1°01'27.25"
	Δ R.A. = 10.562s/h		Δ R.A. = 157.138s/h
	Δ Dec. = -30.99"/h		Δ Dec. = -673.37"/h

<u>Lunar Radius</u>	k1 = 0.2725076 (Penumbra)	<u>Shift in</u>	Δb = 0.00"
<u>Constants:</u>	k2 = 0.2722810 (Umbra)	<u>Lunar Position:</u>	Δl = 0.00"

<u>Geocentric Libration:</u>	l = 0.0°	Brown Lun. No. = 1001
(Optical + Physical)	b = 1.3°	Saros Series = 152 (12/70)
	c = 10.3°	Ephemeris = (DE200/LE200)

Eclipse Magnitude = 1.03788 Gamma = -0.96381 ΔT = 64.8 s

Polynomial Besselian Elements for: 2003 Nov 23 23:00:00.0 TDT (=t₀)

n	x	y	d	l ₁	l ₂	μ
0	-0.1979529	-0.9479029	-20.4053841	0.5373482	-0.0087654	168.398682
1	0.5568983	-0.1739249	-0.0081768	-0.0000032	-0.0000032	14.998531
2	0.0000570	0.0001989	0.0000050	-0.0000131	-0.0000130	-0.000003
3	-0.0000094	0.0000031	0.0000000	0.0000000	0.0000000	0.000000

Tan f₁ = 0.0047348 Tan f₂ = 0.0047112

At time 't₁' (decimal hours), each Besselian element is evaluated by:

$$a = a_0 + a_1*t + a_2*t^2 + a_3*t^3 \quad (\text{or } a = \sum [a_n*t^n]; n = 0 \text{ to } 3)$$

where: a = x, y, d, l₁, l₂, or μ
t = t₁ - t₀ (decimal hours) and t₀ = 23.000 TDT

The Besselian elements were derived from a least-squares fit to elements calculated at five uniformly spaced times over a six hour period centered at t₀. Thus the elements are valid over the period 20.00 ≤ t₁ ≤ 02.00 TDT (Nov 23 to Nov 24).

Note that all times are expressed in Terrestrial Dynamical Time (TDT).

Saros Series 152: Member 12 of 70 eclipses in series.

TABLE 2.2

**SHADOW CONTACTS AND CIRCUMSTANCES
TOTAL SOLAR ECLIPSE OF 2003 NOVEMBER 23**

$\Delta T = 64.8 \text{ s}$
 $= 000^{\circ}16'14.7''$

		Terrestrial Dynamical Time h m s	Latitude	Ephemeris Longitude†	True Longitude*
External/Internal					
Contacts of Penumbra:	P1	20:47:09.9	20°08.9'S	126°58.2'E	127°14.4'E
	P4	00:53:20.3	51°16.4'S	079°04.0'W	078°47.8'W
Extreme					
North/South Limits of Penumbral Path:	N1	21:10:09.3	07°41.8'S	126°10.8'E	126°27.1'E
	S1	00:30:23.4	39°47.4'S	082°55.9'W	082°39.7'W
External/Internal					
Contacts of Umbra:	U1	22:20:25.6	50°59.5'S	084°09.8'E	084°26.0'E
	U2	22:27:31.2	54°07.1'S	078°46.9'E	079°03.1'E
	U3	23:12:51.8	69°07.0'S	021°11.7'E	021°27.9'E
	U4	23:19:57.7	69°34.8'S	008°40.1'E	008°56.4'E
Extreme					
North/South Limits of Umbral Path:	N1	22:20:31.6	50°55.9'S	084°12.2'E	084°28.4'E
	S1	22:27:26.8	54°09.8'S	078°44.5'E	079°00.8'E
	N2	23:19:51.7	69°34.9'S	008°29.3'E	008°45.5'E
	S2	23:12:56.3	69°06.3'S	021°19.6'E	021°35.8'E
Extreme Limits					
of Central Line:	C1	22:23:45.0	52°27.4'S	081°43.3'E	081°59.5'E
	C2	23:16:38.1	69°26.9'S	014°32.8'E	014°49.1'E
Instant of					
Greatest Eclipse:	G0	22:50:21.7	72°40.0'S	088°07.2'E	088°23.4'E
Circumstances at					
Greatest Eclipse:	Sun's Altitude = 14.9°		Path Width = 495.5 km		
	Sun's Azimuth = 111.2°		Central Duration = 01m57.3 s		

† Ephemeris Longitude is the terrestrial dynamical longitude assuming a uniformly rotating Earth.

* True Longitude is calculated by correcting the Ephemeris Longitude for the non-uniform rotation of Earth.

(T.L. = E.L. + 1.002738* ΔT /240, where ΔT (in seconds) = TDT - UT)

Note: Longitude is measured positive to the East.

Since ΔT is not known in advance, the value used in the predictions is an extrapolation based on pre-2003 measurements. Nevertheless, the actual value is expected to fall within ± 0.5 seconds of the estimated ΔT used here.

TABLE 2.3

**PATH OF THE UMBRAL SHADOW
TOTAL SOLAR ECLIPSE OF 2003 NOVEMBER 23**

Universal Time	Northern Limit		Southern Limit		Central Line		Sun Path Alt °	Sun Path Width km	Central Durat. s
	Latitude	Longitude	Latitude	Longitude	Latitude	Longitude			
Limits	50°55.9'S	084°28.4'E	54°09.8'S	079°00.8'E	52°27.4'S	081°59.5'E	0	497	01m33.8s
22:24	57°29.2'S	094°55.6'E	-	-	55°32.6'S	087°36.8'E	5	534	01m40.7s
22:26	59°06.0'S	096°23.1'E	-	-	57°43.2'S	090°14.1'E	7	544	01m44.6s
22:28	60°34.4'S	097°26.9'E	57°24.6'S	084°15.8'E	59°27.7'S	091°46.4'E	9	545	01m47.4s
22:30	61°57.3'S	098°13.7'E	59°27.2'S	086°14.5'E	61°00.4'S	092°46.8'E	10	543	01m49.5s
22:32	63°16.3'S	098°46.9'E	61°07.9'S	087°18.0'E	62°26.1'S	093°25.7'E	11	539	01m51.2s
22:34	64°32.4'S	099°08.2'E	62°37.9'S	087°51.1'E	63°47.0'S	093°47.8'E	12	533	01m52.7s
22:36	65°46.3'S	099°18.4'E	64°01.1'S	088°02.0'E	65°04.2'S	093°55.2'E	13	528	01m53.9s
22:38	66°58.3'S	099°17.8'E	65°19.5'S	087°54.1'E	66°18.7'S	093°48.7'E	13	522	01m54.8s
22:40	68°08.8'S	099°06.2'E	66°34.1'S	087°28.7'E	67°30.8'S	093°28.5'E	14	516	01m55.6s
22:42	69°18.1'S	098°42.8'E	67°45.4'S	086°45.8'E	68°40.8'S	092°54.0'E	14	511	01m56.3s
22:44	70°26.1'S	098°06.5'E	68°53.8'S	085°44.7'E	69°49.0'S	092°04.0'E	15	506	01m56.7s
22:46	71°33.0'S	097°15.6'E	69°59.3'S	084°24.0'E	70°55.4'S	090°57.0'E	15	502	01m57.1s
22:48	72°38.7'S	096°08.0'E	71°01.9'S	082°41.6'E	71°59.8'S	089°30.4'E	15	498	01m57.2s
22:50	73°43.2'S	094°40.6'E	72°01.2'S	080°34.6'E	73°02.2'S	087°41.4'E	15	494	01m57.2s
22:52	74°46.2'S	092°49.6'E	72°56.7'S	077°59.9'E	74°02.0'S	085°26.1'E	15	491	01m57.1s
22:54	75°47.3'S	090°30.1'E	73°47.7'S	074°53.7'E	74°58.8'S	082°39.9'E	15	489	01m56.8s
22:56	76°46.0'S	087°35.7'E	74°33.0'S	071°12.2'E	75°51.6'S	079°17.4'E	14	487	01m56.4s
22:58	77°41.3'S	083°58.7'E	75°11.2'S	066°51.8'E	76°39.4'S	075°12.7'E	14	486	01m55.8s
23:00	78°32.0'S	079°30.0'E	75°40.2'S	061°50.4'E	77°20.4'S	070°20.2'E	14	485	01m55.0s
23:02	79°16.3'S	074°00.5'E	75°57.4'S	056°08.4'E	77°52.6'S	064°36.2'E	13	485	01m54.1s
23:04	79°51.6'S	067°22.9'E	75°59.4'S	049°50.3'E	78°13.2'S	058°00.8'E	12	486	01m52.9s
23:06	80°14.8'S	059°36.4'E	75°41.5'S	043°05.3'E	78°18.6'S	050°41.2'E	11	487	01m51.5s
23:08	80°21.9'S	050°52.3'E	74°56.2'S	036°06.3'E	78°05.0'S	042°53.0'E	10	489	01m49.8s
23:10	80°09.0'S	041°37.0'E	73°26.4'S	029°04.7'E	77°27.2'S	034°58.7'E	9	493	01m47.7s
23:12	79°31.7'S	032°28.1'E	-	-	76°17.2'S	027°22.6'E	7	497	01m45.0s
23:14	78°25.3'S	024°02.4'E	-	-	74°13.6'S	020°22.7'E	5	502	01m41.3s
Limits	69°34.9'S	008°45.5'E	69°06.3'S	021°35.8'E	69°26.9'S	014°49.1'E	0	504	01m33.8s

TABLE 2.4

**PHYSICAL EPHEMERIS OF THE UMBRAL SHADOW
TOTAL SOLAR ECLIPSE OF 2003 NOVEMBER 23**

Universal Time	Central Line		Diameter Ratio	Eclipse Obscur.	Sun Alt °	Sun Azm °	Path Width km	Major Axis km	Minor Axis km	Umbra Veloc. km/s	Central Durat.
	Latitude	Longitude									
22:22.7	52°27.4'S	081°59.5'E	1.0331	1.0674	0.0	124.9	497.4	-	111.7	-	01m33.8s
22:24	55°32.6'S	087°36.8'E	1.0346	1.0704	4.6	120.0	533.8	-	116.6	3.218	01m40.7s
22:26	57°43.2'S	090°14.1'E	1.0354	1.0721	7.2	117.3	544.0	969.9	119.2	2.032	01m44.6s
22:28	59°27.7'S	091°46.4'E	1.0360	1.0733	8.9	115.4	545.4	792.0	121.0	1.637	01m47.4s
22:30	61°00.4'S	092°46.8'E	1.0364	1.0742	10.2	113.9	542.9	696.8	122.4	1.435	01m49.5s
22:32	62°26.1'S	093°25.7'E	1.0368	1.0749	11.3	112.7	538.6	636.7	123.5	1.312	01m51.2s
22:34	63°47.0'S	093°47.8'E	1.0370	1.0754	12.1	111.7	533.4	595.4	124.4	1.232	01m52.7s
22:36	65°04.2'S	093°55.2'E	1.0373	1.0759	12.9	110.9	527.7	565.7	125.1	1.178	01m53.9s
22:38	66°18.7'S	093°48.7'E	1.0374	1.0763	13.5	110.3	522.0	543.8	125.7	1.140	01m54.8s
22:40	67°30.8'S	093°28.5'E	1.0376	1.0766	13.9	109.9	516.5	527.5	126.2	1.115	01m55.6s
22:42	68°40.8'S	092°54.0'E	1.0377	1.0768	14.3	109.7	511.2	515.6	126.6	1.098	01m56.3s
22:44	69°49.0'S	092°04.0'E	1.0378	1.0770	14.6	109.7	506.3	507.2	126.8	1.088	01m56.7s
22:46	70°55.4'S	090°57.0'E	1.0378	1.0771	14.7	110.0	501.8	501.8	127.0	1.085	01m57.1s
22:48	71°59.8'S	089°30.4'E	1.0379	1.0772	14.8	110.6	497.8	499.1	127.1	1.087	01m57.2s
22:50	73°02.2'S	087°41.4'E	1.0379	1.0772	14.8	111.5	494.3	499.0	127.1	1.095	01m57.2s
22:52	74°02.0'S	085°26.1'E	1.0379	1.0771	14.8	112.9	491.3	501.4	127.0	1.107	01m57.1s
22:54	74°58.8'S	082°39.9'E	1.0378	1.0770	14.6	114.8	488.8	506.5	126.9	1.125	01m56.8s
22:56	75°51.6'S	079°17.4'E	1.0377	1.0769	14.3	117.3	486.9	514.6	126.6	1.150	01m56.4s
22:58	76°39.4'S	075°12.7'E	1.0376	1.0766	14.0	120.5	485.6	526.2	126.2	1.181	01m55.8s
23:00	77°20.4'S	070°20.2'E	1.0375	1.0763	13.5	124.5	484.9	542.0	125.8	1.222	01m55.0s
23:02	77°52.6'S	064°36.2'E	1.0373	1.0759	12.9	129.4	484.9	563.2	125.2	1.274	01m54.1s
23:04	78°13.2'S	058°00.8'E	1.0371	1.0755	12.2	135.1	485.6	592.0	124.5	1.344	01m52.9s
23:06	78°18.6'S	050°41.2'E	1.0368	1.0749	11.4	141.5	487.1	631.8	123.6	1.438	01m51.5s
23:08	78°05.0'S	042°53.0'E	1.0365	1.0742	10.3	148.5	489.4	689.5	122.5	1.572	01m49.8s
23:10	77°27.2'S	034°58.7'E	1.0360	1.0734	9.0	155.5	492.7	779.7	121.2	1.780	01m47.7s
23:12	76°17.2'S	027°22.6'E	1.0355	1.0723	7.4	162.3	497.1	944.1	119.4	2.160	01m45.0s
23:14	74°13.6'S	020°22.7'E	1.0347	1.0707	5.0	168.5	502.5	-	116.9	3.175	01m41.3s
23:15.6	69°26.9'S	014°49.1'E	1.0331	1.0674	0.0	173.3	504.5	-	111.7	-	01m33.8s

TABLE 2.5

LOCAL CIRCUMSTANCES ON THE CENTRAL LINE
TOTAL SOLAR ECLIPSE OF 2003 NOVEMBER 23

Central Line Maximum Eclipse			First Contact				Second Contact			Third Contact			Fourth Contact			
U.T.	Durat.	Alt	U.T.	P	V	Alt	U.T.	P	V	U.T.	P	V	U.T.	P	V	Alt
		°		°	°	°		°	°		°	°		°	°	°
22:24	01m40.7s	5	-	-	-	-	22:23:10	110	258	22:24:50	290	78	23:14:19	110	256	11
22:26	01m44.6s	7	21:36:50	289	82	2	22:25:08	110	259	22:26:52	290	79	23:17:06	111	257	14
22:28	01m47.4s	9	21:38:18	290	83	4	22:27:06	110	261	22:28:54	290	81	23:19:38	111	259	15
22:30	01m49.5s	10	21:39:52	290	84	5	22:29:05	110	262	22:30:55	290	82	23:22:02	111	260	16
22:32	01m51.2s	11	21:41:31	290	85	6	22:31:04	110	263	22:32:56	290	83	23:24:21	111	261	17
22:34	01m52.7s	12	21:43:13	290	86	7	22:33:04	110	264	22:34:56	290	84	23:26:37	110	263	18
22:36	01m53.9s	13	21:44:57	289	87	8	22:35:03	110	265	22:36:57	290	85	23:28:49	110	264	18
22:38	01m54.8s	14	21:46:44	289	88	9	22:37:03	110	266	22:38:57	290	86	23:30:59	110	265	19
22:40	01m55.6s	14	21:48:33	289	89	10	22:39:02	110	267	22:40:58	290	87	23:33:07	110	266	19
22:42	01m56.3s	14	21:50:23	289	90	10	22:41:02	110	268	22:42:58	290	88	23:35:12	110	267	19
22:44	01m56.7s	15	21:52:15	289	91	11	22:43:02	109	269	22:44:58	290	89	23:37:15	110	268	19
22:46	01m57.1s	15	21:54:09	289	92	11	22:45:02	109	270	22:46:59	289	90	23:39:17	110	269	19
22:48	01m57.2s	15	21:56:05	289	93	11	22:47:01	109	271	22:48:59	289	91	23:41:16	110	270	19
22:50	01m57.2s	15	21:58:02	289	94	12	22:49:01	109	272	22:50:59	289	92	23:43:14	109	271	19
22:52	01m57.1s	15	22:00:01	289	95	12	22:51:02	109	273	22:52:59	289	93	23:45:10	109	272	18
22:54	01m56.8s	15	22:02:01	288	96	12	22:53:02	109	274	22:54:58	289	94	23:47:04	109	273	18
22:56	01m56.4s	14	22:04:04	288	97	12	22:55:02	108	275	22:56:58	288	95	23:48:56	109	274	17
22:58	01m55.8s	14	22:06:08	288	98	12	22:57:02	108	276	22:58:58	288	96	23:50:46	109	275	17
23:00	01m55.0s	14	22:08:14	288	99	11	22:59:03	108	277	23:00:58	288	97	23:52:34	108	276	16
23:02	01m54.1s	13	22:10:22	288	100	11	23:01:03	108	278	23:02:57	288	98	23:54:20	108	276	15
23:04	01m52.9s	12	22:12:33	287	101	11	23:03:04	108	279	23:04:56	288	99	23:56:03	108	277	14
23:06	01m51.5s	11	22:14:47	287	102	10	23:05:04	107	280	23:06:56	287	99	23:57:44	108	278	13
23:08	01m49.8s	10	22:17:04	287	103	9	23:07:05	107	280	23:08:55	287	100	23:59:21	107	278	12
23:10	01m47.7s	9	22:19:25	286	104	8	23:09:06	107	281	23:10:54	287	101	00:00:53	107	279	11
23:12	01m45.0s	7	22:21:54	286	105	7	23:11:08	106	282	23:12:53	286	102	00:02:19	107	279	9
23:14	01m41.3s	5	22:24:36	286	106	5	23:13:09	106	283	23:14:51	286	103	00:03:32	106	280	6

**Table 2.11 - Antarctic Station Climatology for the
Total Solar Eclipse of 2003 Nov 23**

Station	POR (years)	Ave. Temp. (°C)	Min. Temp. (°C)	Max. Temp. (°C)	Ave. Wind Chill (°C)	Min. Wind Chill (°C)	Ave. Wind Speed (km/h)	Max. Wind Speed (km/h)	Prevail. Wind Direction	Average Cloud Cover (tenths)	Most Frequent Cloud Cover (tenths)	Eclipse Observing Probability (%)
von Neumayer	15	-9.8	-24.3	1.0	-17.9	-36.0	29	113	E	7.6	10.0	27
Maitri *	5	-5.3	-11.9	4.1	-13.2	-27.0	32	111	S	3.9	10.0	52
Novolazarevskaja *	15	-5.7	-16.3	4.0	-13.2	-27.7	36	100	E - SE	5.7	10.0	44
Asuka	5	-14.5	-28.4	-5.6	-26.5	-37.5	42	80	SE			
Syowa	4	-7.5	-15.2	-1.4	-15	-24.3	27	78	N - NE	6.4	8.8	36
Relay Station	6	-41.1	-50.6	-28.6	-58.3	-70.2	25	61	W-SW			
LGB20 *	9	-32.6	-41.5	-18.2	-44.5	-63.3	16	46	S-SW			
LGB10	6	-32.5	-42.4	-17.1	-42.0	-59.9	20	50	S - SW			
GEO3	4	-22.0	-31.7	-11.3	-36.6	-45.4	41	87	S			
Mawson	15	-5.9	-14.9	5.2	-16	-29.6	51	139	SE	6.1	10.0	39
LGB35 *	7	-27.9	-36.9	-16.3	-43.2	-58.2	18	56	SE			
Zhongshan	4	-5.3	-13.1	0	-13.4	-26.4	37	130	E	6.1	10	39
LGB59 *	4	-28.8	-37.1	-18.5	-44.7	-57.1	36	61	NE			
Davis	15	-4.3	-14.3	5.6	-10.4	-23.8	13	53	E - NE	6.6	8.8	34
Mirnij *	15	-7.5	-19.7	0.3	-17	-33.8	41	111	E - SE	6.4	10.0	37
Vostok	15	-39.5	-53.7	-25.7	-53.7	-73.6	17	41	S - SW	3.4	0.0	66
GC46	2	-40.2	-53.6	-31.8	-55.7	-73.6	20	33	SE			
Casey	15	-4.3	-13.4	5.1	-10.5	-23.6	23	126	E - NE	6.9	8.8	31

* indicates stations within the eclipse track

Key to Table 2.11

Data for this table was taken from the archive of the British Antarctic Society. They are based on hourly observations taken at 00 hour UTC between November 9 and December 9 for a variable number of years.

POR

Period of record, or the length of time in years for which meteorological data are available.

Ave. Temp.

The mean of the temperatures at 00 UTC between November 9 and December 9 for the period of record, in degrees Celsius. Many values are missing from Antarctic stations, but most means are based on at least 90 reports.

Min. Temp.

The lowest temperature (°C) in the data collected during the period of record.

Max. Temp.

The highest temperature (°C) in the data collected during the period of record.

Ave. Wind Chill

Mean wind chill (°C) calculated using the new wind chill formula developed by Environment Canada and U. S. National Weather Service. The formula can be found at <http://windchill.ec.gc.ca>.

Min. Wind Chill

Coldest wind chill – the lowest wind chill value (°C) calculated during the period of record.

Ave. Wind Speed

The mean wind speed (km/h) for the period of record.

Max. Wind Speed

The greatest wind speed (km/h) for the period of record.

Prevail. Wind Direction

Prevailing wind direction – the most common wind direction or directions in the record.

Average Cloud Cover

Mean cloud amount in tenths in the record. Cloud observations are recorded in octas (eighths); these values are converted from those records. Obscured conditions are included in the overcast category. These make up only a small percentage of the observations.

Most Frequent Cloud Cover

The cloud amount that had the highest frequency in the period of record.

Eclipse Observing Probability

The summed product of the cloud amount times its frequency. It assumes that the sun is high (above 45°) and that all observed cloud is opaque. It provides a good comparison between observing sites.

3.00 ECLIPSE RESOURCES

3.01 EYE SAFETY AND SOLAR ECLIPSES

B. Ralph Chou, MSc, OD

Associate Professor, School of Optometry, University of Waterloo
Waterloo, Ontario, Canada N2L 3G1

A solar eclipse offers students a unique opportunity to see a natural phenomenon that illustrates the basic principles of mathematics and science that are taught through elementary and secondary school. Indeed, many scientists (including astronomers!) have been inspired to study science as a result of seeing a total solar eclipse. Teachers can use eclipses to show how the laws of motion and the mathematics of orbital motion can predict the occurrence of eclipses. The use of pinhole cameras and telescopes or binoculars to observe an eclipse leads to an understanding of the optics of these devices. The rise and fall of environmental light levels during an eclipse illustrate the principles of radiometry and photometry, while biology classes can observe the associated behavior of plants and animals. It is also an opportunity for children of school age to contribute actively to scientific research - observations of contact timings at different locations along the eclipse path are useful in refining our knowledge of the orbital motions of the moon and earth, and sketches and photographs of the solar corona can be used to build a three-dimensional picture of the sun's extended atmosphere during the eclipse.

However, observing the Sun can be dangerous if you do not take the proper precautions. The solar radiation that reaches the surface of the earth includes ultraviolet (UV) radiation at wavelengths longer than 290 nm, to radio waves in the meter range. The tissues in the eye transmit a substantial part of the radiation between 380 and 1400 nm to the light-sensitive retina at the back of the eye. While environmental exposure to UV radiation is known to contribute to the accelerated aging of the outer layers of the eye and the development of cataracts, the concern over improper viewing of the Sun during an eclipse is for the development of "eclipse blindness" or retinal burns.

Exposure of the retina to intense visible light causes damage to its light-sensitive rod and cone cells. The light triggers a series of complex chemical reactions within the cells which damages their ability to respond to a visual stimulus, and in extreme cases, can destroy them. The result is a loss of visual function which may be either temporary or permanent, depending on the severity of the damage. When a person looks repeatedly or for a long time at the Sun without proper protection for the eyes, this photochemical retinal damage may be accompanied by a thermal injury - the high level of visible light causes heating that literally cooks the exposed tissue. This thermal injury or photocoagulation destroys the rods and cones, creating a small blind area. The danger to vision is significant because photic retinal injuries occur without any feeling of pain (the retina has no pain receptors), and the visual effects do not occur for at least several hours after the damage is done (Pitts, 1993). Viewing the sun through binoculars, a telescope or other optical devices without proper protective filters can result in thermal retinal injury because of the high irradiance level due to visible light, as well as near infrared radiation, in the magnified image.

The only time that the Sun can be viewed safely with the naked eye is during a total eclipse, when the moon completely covers the Sun. ***It is never safe to look at an annular eclipse or the partial phases of any eclipse without the proper equipment and techniques.*** Even when 99.9% of the Sun's surface (the photosphere) is obscured during the partial phases of a solar eclipse, the remaining crescent Sun is still intense enough to cause a retinal burn, even though illumination levels are comparable to twilight (Chou, 1981, 1996; Marsh, 1982). Failure to use proper observing methods may result in permanent eye damage or severe visual loss. This can have important adverse effects on career choices and earning potential, since it has been shown that most individuals who sustain eclipse-related eye injuries are children and young adults (Penner and McNair, 1966; Chou and Krailo, 1981).

The same techniques for observing the Sun outside of eclipses are used to view and photograph annular solar eclipses and the partly eclipsed Sun (Sherrod, 1981; Pasachoff, 2000; Pasachoff & Covington, 1993; Reynolds & Sweetsir, 1995). The safest and most inexpensive method is by projection. A pinhole or small opening is used

to form an image of the Sun on a screen placed about a meter behind the opening. Multiple openings in perfboard, a loosely woven straw hat, or even between interlaced fingers can be used to cast a pattern of solar images on a screen. A similar effect is seen on the ground below a broad-leaved tree: the many “pinholes” formed by overlapping leaves creates hundreds of crescent-shaped images. Binoculars or a small telescope mounted on a tripod can also be used to project a magnified image of the Sun onto a white card. All of these methods can be used to provide a safe view of the partial phases of an eclipse to a group of observers, but care must be taken to ensure that no-one looks through the device. The main advantage of the projection methods is that nobody is looking directly at the Sun. The disadvantage of the pinhole method is that the screen must be placed at least a meter behind the opening to get a solar image that is large enough to see easily.

The Sun can only be viewed directly when filters specially designed to protect the eyes are used. Most of these filters have a thin layer of chromium alloy or aluminum deposited on their surfaces that attenuates both visible and near-infrared radiation. A safe solar filter should transmit less than 0.003% (density~4.5)¹ of visible light (380 to 780 nm) and no more than 0.5% (density~2.3) of the near-infrared radiation (780 to 1400 nm). Figure 3.1 shows transmittance curves for a selection of safe solar filters.

One of the most widely available filters for safe solar viewing is shade number 14 welder’s glass, which can be obtained from welding supply outlets. A popular inexpensive alternative is aluminized polyester² that has been made specially for solar observation. (“Space blankets” and aluminized polyester used in gardening are NOT suitable for this purpose!) Unlike the welding glass, aluminized polyester can be cut to fit any viewing device, and doesn’t break when dropped. It has recently been pointed out that some aluminized polyester filters may have large (up to approximately 1 mm in size) defects in their aluminum coatings that may be hazardous. A microscopic analysis of examples of such defects shows that despite their appearance, the defects arise from a hole in one of the two aluminized polyester films used in the filter. There is no large opening completely devoid of the protective aluminum coating. While this is a quality control problem, the presence of a defect in the aluminum coating does not necessarily imply that the filter is hazardous. When in doubt, an aluminized polyester solar filter that has coating defects larger than 0.2 mm in size, or more than a single defect in any 5 mm circular zone of the filter, should not be used.

An alternative to aluminized polyester solar filter material that has become quite popular is “black polymer” in which carbon particles are suspended in a resin matrix. This material is somewhat stiffer than polyester and requires a special holding cell if it is to be used at the front of binoculars, telephoto lenses or telescopes. Intended mainly as a visual filter, the polymer gives a yellow image of the Sun (aluminized polyester produces a blue-white image). This type of filter may show significant variations in density of the tint across its extent; some areas may appear much lighter than others. Lighter areas of the filter transmit more infrared radiation than may be desirable. A recent development is a filter that consists of aluminum-coated black polymer. Combining the best features of polyester and black polymer, this new material may eventually replace both as the filter of choice in solar eclipse viewers. The transmittance curve of one of these hybrid filters (Polymer Plus™ by Thousand Oaks Optical) is shown in Figure 3.1. Another material, Baader AstroSolar Safety Film, can be used for both visual and photographic solar observations. It is an ultrathin resin film with excellent optical quality and less scattered light than most polyester filters.

¹ In addition to the term transmittance (in percent), the energy transmission of a filter can also be described by the term density (unitless) where density ‘d’ is the common logarithm of the reciprocal of transmittance ‘t’ or $d = \log_{10}[1/t]$. A density of ‘0’ corresponds to a transmittance of 100%; a density of ‘1’ corresponds to a transmittance of 10%; a density of ‘2’ corresponds to a transmittance of 1%, etc....

² Aluminized polyester is popularly known as mylar. DuPont actually owns the trademark “Mylar™” and does not manufacture this material for use as a solar filter.

Many experienced solar observers use one or two layers of black-and-white film that has been fully exposed to light and developed to maximum density. The metallic silver contained in the film emulsion is the protective filter; however any black-and-white negative with images in it is not suitable for this purpose. More recently, solar observers have used floppy disks and compact disks (CDs and CD-ROMs) as protective filters by covering the central openings and looking through the disk media. However, the optical quality of the solar image formed by a floppy disk or CD is relatively poor compared to aluminized polyester or welder's glass. Some CDs are made with very thin aluminum coatings that are not safe - if you can see through the CD in normal room lighting, don't use it!! No filter should be used with an optical device (e.g., binoculars, telescope, camera) unless it has been specifically designed for that purpose and is mounted at the front end. Some sources of solar filters are listed below.

Unsafe filters include color film, black-and-white film that contains no silver, film negatives with images on them, smoked glass, sunglasses (single or multiple pairs), photographic neutral density filters and polarizing filters. Most of these transmit high levels of invisible, infrared radiation which can cause a thermal retinal burn (see Figure 3.1). The fact that the Sun appears dim, or that you feel no discomfort when looking at the Sun through the filter, is no guarantee that your eyes are safe. Solar filters designed to thread into eyepieces that are often provided with inexpensive telescopes are also unsafe. These glass filters often crack unexpectedly from overheating when the telescope is pointed at the Sun, and retinal damage can occur faster than the observer can move the eye from the eyepiece. Avoid unnecessary risks. Your local planetarium, science central, or amateur astronomy club can provide additional information on how to observe the eclipse safely.

There are some concerns that UVA radiation (wavelengths between 315 and 380 nm) in sunlight may also adversely affect the retina (Del Priore, 1991). While there is some experimental evidence for this, it only applies to the special case of aphakia, where the natural lens of the eye has been removed because of cataract or injury, and no UV-blocking spectacle, contact or intraocular lens has been fitted. In an intact normal human eye, UVA radiation does not reach the retina because it is absorbed by the crystalline lens. In aphakia, normal environmental exposure to solar UV radiation may indeed cause chronic retinal damage. However, the solar filter materials discussed in this article attenuate solar UV radiation to a level well below the minimum permissible occupational exposure for UVA (ACGIH, 1994), so an aphakic observer is at no additional risk of retinal damage when looking at the Sun through a proper solar filter.

In the days and weeks before a solar eclipse occurs, there are often news stories and announcements in the media, warning about the dangers of looking at the eclipse. Unfortunately, despite the good intentions behind these messages, they frequently contain misinformation, and may be designed to scare people from seeing the eclipse at all. However, this tactic may backfire, particularly when the messages are intended for students. A student who heeds warnings from teachers and other authorities not to view the eclipse because of the danger to vision, and learns later that other students did see it safely, may feel cheated out of the experience. Having now learned that the authority figure was wrong on one occasion, how is this student going to react when other health-related advice about drugs, AIDS, or smoking is given? Misinformation may be just as bad, if not worse than no information (Pasachoff, 2001).

3.02 SOURCES FOR SOLAR FILTERS

A brief list of sources for solar filters appears below. For additional sources, see advertisements in *Astronomy* and/or *Sky & Telescope* magazines. The inclusion of any source on this list does not imply an endorsement of that source by the authors or NASA.

- American Paper Optics, 3080 Bartlett Corporate Drive, Bartlett, TN 38133. (800)767-8427
- Celestron International, 2835 Columbia St., Torrance, CA 90503. (310) 328-9560
- Meade Instruments Corporation, 16542 Millikan Ave., Irvine, CA 92714. (714) 756-2291
- Orion Telescopes and Binoculars, P.O. Box 1815, Santa Cruz, CA 95061-1815. (800) 447-1001
- Pocono Mountain Optics, 104 NP 502 Plaza, Moscow, PA 18444. (717) 842-1500
- Rainbow Symphony, Inc., 6860 Canby Ave., #120, Reseda, CA 91335 (800) 821-5122 *
- Thousand Oaks Optical, Box 5044-289, Thousand Oaks, CA 91359. (805) 491-3642 *

- Khan Scope Centre, 3243 Dufferin Street, Toronto, Ontario, Canada M6A 2T2 (416) 783-4140
- Perceptor Telescopes TransCanada, Brownsville Junction Plaza, Box 38,
Schomberg, Ontario, Canada L0G 1T0 (905) 939-2313
- Starfield Scientific, PO Box 232, Port Kembla, NSW 2505, Australia 0425 235804

* sources for inexpensive hand held solar filters and eclipse glasses

3.03 IAU SOLAR ECLIPSE EDUCATION COMMITTEE

In order to ensure that astronomers and public health authorities have access to information on safe viewing practices, the Commission on Astronomy Education and Development of the International Astronomical Union, the international organization for professional astronomers, set up a Solar Eclipse Education Committee. Under Prof. Jay M. Pasachoff of Williams College, the Committee has assembled information on safe methods of observing the Sun and solar eclipses, eclipse-related eye injuries, and samples of educational materials on solar eclipses (see: <http://www.eclipses.info>).

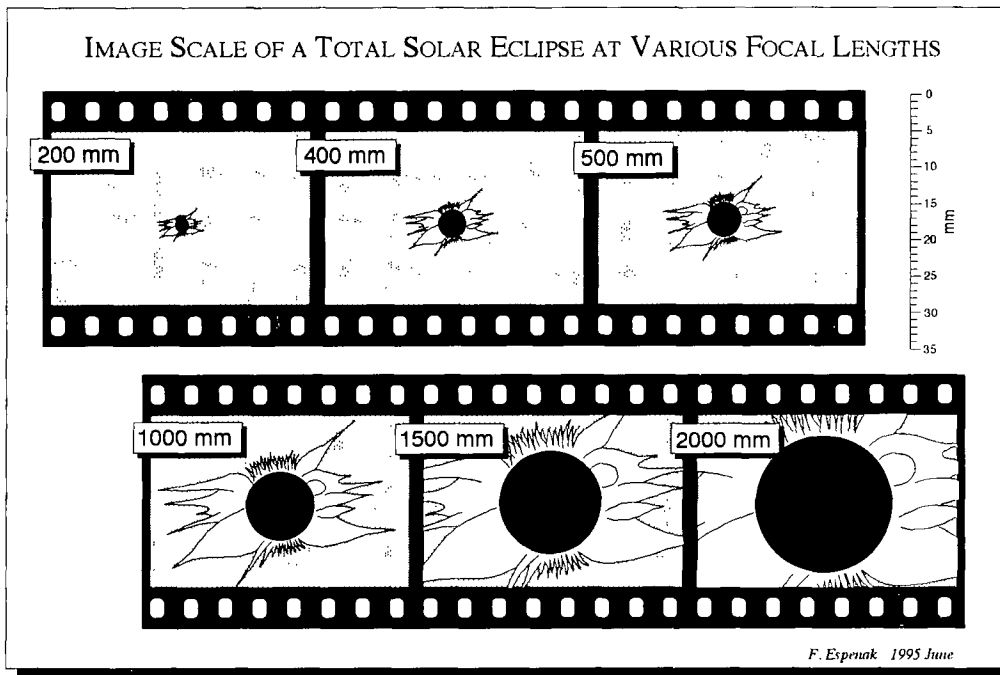
For more information, contact Prof. Jay M. Pasachoff, Hopkins Observatory, Williams College, Williamstown, MA 01267, USA (e-mail: jay.m.pasachoff@williams.edu). Information on safe solar filters can be obtained by contacting Dr. B. Ralph Chou (e-mail: bchou@sciborg.uwaterloo.ca).

3.04 ECLIPSE PHOTOGRAPHY

From a photographic perspective, annular eclipses are similar to partial eclipses. They both require the use of safe solar filters as described in the previous section. The partial phases of total eclipses also require filters. Only the total phase can be viewed and photographed without a filter.

Almost any kind of camera with manual controls can be used to capture these rare events. However, a lens with a fairly long focal length is recommended to produce as large an image of the Sun as possible. A standard 50 mm lens yields a minuscule 0.5 mm image, while a 200 mm telephoto or zoom produces a 1.9 mm image. A better choice would be one of the small, compact catadioptric or mirror lenses that have become widely available in the past ten years. The focal length of 500 mm is most common among such mirror lenses and yields a solar image of 4.6 mm. Adding a 2x tele-converter will produce a 1000 mm focal length, which doubles the Sun's size to 9.2 mm. Focal lengths in excess of 1000 mm usually fall within the realm of amateur telescopes. If full disk photography of the Sun on 35 mm format is planned, the focal length of the optics must not exceed 2600 mm. However, since most cameras don't show the full extent of the image in their viewfinders, a more practical limit is about 2000 mm. Longer focal lengths permit photography of only a magnified portion of the Sun's disk. For November's total eclipse, a focal length no longer than 1500 mm is recommended in order to capture the solar corona. However, a focal length of 1000 mm requires less critical framing and can capture some of the longer coronal streamers. For any particular focal length, the diameter of the Sun's image is approximately equal to the focal length divided by 109 (Table 3.1).

A solar filter must be used on the lens throughout the partial phases (and annularity) for both photography and viewing. Such filters can be obtained through manufacturers and dealers listed in *Sky & Telescope* and *Astronomy* magazines (see: SOURCES FOR SOLAR FILTERS). These filters typically attenuate the Sun's visible and infrared energy by a factor of 100,000. However, the actual filter factor and choice of ISO film speed will play critical roles in determining the correct photographic exposure. Almost any speed film can be used since the Sun gives off abundant light. The easiest method for determining the correct exposure is accomplished by running a calibration test on the uneclipsed Sun. Shoot a roll of film of the mid-day Sun at a fixed aperture (f/8 to f/16) using every shutter speed between 1/1000 and 1/4 second. After the film is developed, note the best exposures and use them to photograph all the partial phases. The Sun's surface brightness remains constant throughout the eclipse, so no exposure compensation is needed except for the crescent phases (and annularity) which require two more stops due to solar limb darkening. Bracketing by several stops is also necessary if haze or clouds



interfere on eclipse day. This is especially true for the May 31 annular eclipse which occurs low on the horizon. A camera with a built in spot meter would be of great value in determining the exposure. If the haze is thick enough, you may need to remove the solar filter in order to see and photograph the annular eclipse, but extreme caution must be used.

For November's eclipse, the most spectacular and awe inspiring phase is totality. For two brief minutes, the Sun's pearly white corona, red prominences and chromosphere are visible. The most important point to remember is that during the total phase, all solar filters must be removed! The corona is a million times fainter than the photosphere, so photographs of the corona must be made without a filter. It is completely safe to view the totally eclipsed Sun directly with the naked eye. No filters are needed and they will only hinder your view. The average brightness of the corona varies inversely with the distance from the Sun's limb. The inner corona is far brighter than the outer corona. Thus, no single exposure can capture its full dynamic range. The best strategy is to choose one aperture or *f*/number and bracket the exposures over a range of shutter speeds (i.e., 1/1000 down to 1 second). Rehearsing this sequence is highly recommended since great excitement accompanies totality and there is little time to think.

Exposure times for various film speeds (ISO), apertures (*f*/number) and features (chromosphere, prominences, inner, middle and outer corona) are summarized in Table 3.2. The table was developed from eclipse photographs made by Espenak and photographs published in *Sky and Telescope*. To use the table, first select the ISO film speed in the upper left column. Next, move to the right to the desired aperture or *f*/number for the chosen ISO. The shutter speeds in that column may be used as starting points for photographing various features and phenomena tabulated in the 'Subject' column at the far left. For example, to photograph prominences using ISO 400 at *f*/16, the table recommends an exposure of 1/1000. Alternatively, you can calculate the recommended shutter speed using the 'Q' factors tabulated along with the exposure formula at the bottom of Table 3.2. Keep in mind that these exposures are based on a clear sky and a corona of average brightness. You should bracket your exposures one or more stops to take into account the actual sky conditions and the variable nature of these phenomena.

Finally, an eclipse effect that is easily captured with point-and-shoot or automatic cameras should not be overlooked. Use a kitchen sieve or colander and allow its shadow to fall on a piece of white card-board placed several feet away. The holes in the utensil act like pinhole cameras and each one projects its own image of the Sun. The effect can also be duplicated by forming a small aperture with one's hands and watching the ground below. The pinhole camera effect becomes more prominent with increasing eclipse magnitude. Virtually any

camera can be used to photograph the phenomenon, but automatic cameras must have their flashes turned off since this would otherwise obliterate the pinhole images.

If photography is done aboard a ship at sea, this puts certain limits on the focal length and shutter speeds that can be used. General recommendations are difficult to make since it depends on the stability of the ship as well as wave heights encountered on eclipse day. Certainly telescopes with focal lengths of 1000 mm or more can be ruled out since their small fields of view would require the ship to remain virtually motionless and this is rather unlikely even given calm seas. A 500 mm lens might be a safe upper limit in focal length. ISO 400 is a good film speed choice for photography at sea. For the total eclipse, shutter speeds as slow as 1/8 or 1/4 may be tried if the ocean is calm day. Otherwise, stick with a 1/15 or 1/30 and shoot a sequence through 1/1000 second. It might be good insurance to bring a wider 200 mm lens just in case the seas are rougher than expected. New image stabilized lenses from Canon and Nikon may also be helpful aboard ship by allowing the use of slower shutter speeds.

Cold weather and below freezing temperatures will be the greatest challenge especially for travelers to the total eclipse in Antarctica (see *ECLIPSES AT COLD TEMPERATURES*). The best advice is to keep observing and photography plans very simple and uncomplicated.

For more information on eclipse photography, observations and eye safety, see *FURTHER READING* in the *BIBLIOGRAPHY*.

3.05 ECLIPSES AT COLD TEMPERATURES

Along the coast of Antarctica, the average and even the coldest temperatures do not constitute a particularly difficult challenge for astronomy. Commercial telescopes and telescope equipment work reasonably well and cameras will usually function without fatal complaint. The wind chill values will make instruments cool quickly and steal the heat from any warming devices, but will not reduce the temperatures below the ambient values. Battery power is a different story. The power supplied by internal batteries of many cameras and camcorders begins to fail when temperatures fall below -10°C . Batteries must be kept warmer than this if they are to function.

Antarctica's interior temperatures are a far more challenging adversary. Commercial telescopes begin to fail at about -30°C , especially after several hours at those temperatures. Only manual cameras can be trusted, although shutters begin to lock up or fail at -35°C . Chemical warming packs will not work unless boosted by being tucked up against a warm human body, especially if the wind chill is significant. In such a cold weather venue, photographic plans should be modest.

Eyepieces will be quick to frost over when an errant breath of moist air condenses on their cold surfaces, so a spare should be kept within easy reach inside a pocket. Camera viewfinders are similarly affected. Metal stings immediately, and so a thin inner glove can permit fine adjustments possible at the last critical moments. Latex medical gloves can prevent hands from sticking to metal, but these provide no warmth and leave hands feeling clammy. However, they do prevent the skin from drying and cracking.

Cold and dry air brings static electrical discharges within the camera body that can leave jagged streaks across film that is advanced too rapidly. Motor driven cameras are most likely to suffer this fate. All film should be advanced slowly and carefully to avoid the discharges and breaking the brittle film. With average temperatures, cameras and telescopes should be able to tough it out in the interior. Below normal temperatures will be too much without supplementary heating but even something as simple as covering equipment in a black cloth to absorb whatever energy the Sun can offer may bring sufficient warming to make eclipse observation and photography more successful.

Cameras are best kept inside a coat against the skin and brought out for photography when needed. The eclipse is short and warm equipment will not cool so quickly that it fails in the time available. Attaching cameras to telescopes is more difficult, but even at -30°C , bare hands can be used for a half-minute to make a final adjustments. Small parts don't have a great heat capacity and won't usually burn in a short minute but large metal objects can produce a very quick frostbite.

Winds can play havoc with eclipse plans, especially along coastal Antarctica where average speeds are nearly twice those inland. For the most part prevailing winds tend to come out of the south and southeast, the same direction in which the Sun lies during the eclipse. Windbreaks will have to be selected carefully to avoid blocking the eclipse if they can be used at all.

Warmth is critical if the eclipse is to be enjoyed and in Antarctic conditions this means several layers of clothing. For average conditions on the coast with modest winds the following might suffice:

- Long underwear or tights under loose-fitting pants
- Two pair of socks, one light and the other heavier, made of wool or similar material
- T-shirt and regular shirt
- Light undercoat – a summer jacket would do here
- Well-insulated winter coat. Synthetic fillings are no match for goose down.
- Pair of light bicycle gloves covered by more substantial mitts or gloves
- Hat that can cover the ears
- Insulated boots

For colder interior temperatures the following should be added or substituted:

- Winter boots with high tops, thick insoles and warm liners
- Outer wind pants, preferably filled with down, and loose fitting (snowmobile pants)
- Heavy mitts with lighter gloves inside
- Chemical hand-warmers, tucked into a convenient pocket or loose-fitting boot. Be careful!
- Long down-filled winter coat with a hood. Don't keep the hood up when working with equipment as it will trap moisture that can freeze on optical surfaces.
- Balaclava to cover the face, except for eyes and mouth

3.06 IAU WORKING GROUP ON ECLIPSES

Professional scientists are asked to send descriptions of their eclipse plans to the Working Group on Eclipses of the International Astronomical Union, so that they can keep a list of observations planned. Send such descriptions, even in preliminary form, to:

International Astronomical Union Working Group on Eclipses

Prof. Jay M. Pasachoff, Chair

Williams College-Hopkins Observatory

Williamstown, MA 01267, USA

web: www.williams.edu/astronomy/IAU_eclipses

email: jay.m.pasachoff@williams.edu

FAX: (413) 597-3200

The members of the Working Group on Eclipses of the Solar Division of the International Astronomical Union are: Jay M. Pasachoff (USA), Chair; F. Clette (Belgium), F. Espenak (USA); Iraida Kim (Russia); Francis Podmore (Zimbabwe); V. Rusin (Slovakia); Jagdev Singh (India); Yoshinori Suematsu (Japan); consultant: J. Anderson (Canada).

The web site of the Program Group on Public Education at the Times of Eclipses of the Education and Development commission of the IAU is www.eclipses.info.

3.07 INTERNATIONAL SOLAR ECLIPSE CONFERENCE

An international Solar Eclipse Conference 2004 (SEC2004) will be held on 2004 Aug 20-22 at Open University, Milton Keynes, England. The main objective of the conference is to bring together professionals and amateurs to discuss all aspects of solar eclipses. Two days of lectures will be given in each of the following disciplines: predictions, mathematics, solar physics, weather forecasting, eye safety, diameter measuring, edge and central, and ancient eclipse research. Both past and future solar eclipses will be discussed, as well as the 2004 transit of Venus. For registration and more details, contact Patrick Poitevin (email: solareclipsewebpages@btopenworld.com) or visit the SEC2004 web page:

http://solareclipsewebpages.users.btopenworld.com/SEC_files/SEC2004.html

3.08 NASA ECLIPSE BULLETINS ON INTERNET

To make the NASA solar eclipse bulletins accessible to as large an audience as possible, these publications are also available via the Internet. This was made possible through the efforts and expertise of Dr. Joe Gurman (GSFC/Solar Physics Branch).

NASA eclipse bulletins can be read or downloaded via the World-Wide Web using a Web browser (e.g.: Netscape, Microsoft Explorer, etc.) from the GSFC SDAC (Solar Data Analysis Center) Eclipse Information home page, or from top-level URL's for the currently available eclipse bulletins themselves:

http://umbra.nascom.nasa.gov/eclipse/	(SDAC Eclipse Information)
http://umbra.nascom.nasa.gov/eclipse/941103/rp.html	(1994 Nov 3)
http://umbra.nascom.nasa.gov/eclipse/951024/rp.html	(1995 Oct 24)
http://umbra.nascom.nasa.gov/eclipse/970309/rp.html	(1997 Mar 9)
http://umbra.nascom.nasa.gov/eclipse/980226/rp.html	(1998 Feb 26)
http://umbra.nascom.nasa.gov/eclipse/990811/rp.html	(1999 Aug 11)
http://umbra.nascom.nasa.gov/eclipse/010621/rp.html	(2001 Jun 21)
http://umbra.nascom.nasa.gov/eclipse/021204/rp.html	(2002 Dec 04)
http://umbra.nascom.nasa.gov/eclipse/2003/rp.html	(2003 eclipses)

The original Microsoft Word text files, GIF and PICT figures (Macintosh format) are also available via anonymous ftp. They are stored as BinHex-encoded, StuffIt-compressed Mac folders with .hqx suffixes. For PC's, the text is available in a zip-compressed format in files with the .zip suffix. There are three sub directories for figures (GIF format), maps (JPEG format), and tables (html tables, easily readable as plain text). Some of the newer bulletins are also available in pdf format.

Current plans call for making all future NASA eclipse bulletins available over the Internet, at or before publication of each. The primary goal is to make the bulletins available to as large an audience as possible. Thus, some figures or maps may not be at their optimum resolution or format. Comments and suggestions are actively solicited to fix problems and improve on compatibility and formats.

3.09 FUTURE ECLIPSE PATHS ON INTERNET

Presently, the NASA eclipse bulletins are published 12 to 24 months before each eclipse. However, there have been a growing number of requests for eclipse path data with an even greater lead time. To accommodate the demand, predictions have been generated for all central solar eclipses from 1991 through 2030. All predictions are based on $j=2$ ephemerides for the Sun [Newcomb, 1895] and Moon [Brown, 1919, and Eckert, Jones and Clark, 1954]. The value used for the Moon's secular acceleration is $n\text{-dot} = -26 \text{ arc-sec/cy}^2$, as deduced by

Morrison and Ward [1975]. A correction of $-0.6''$ was added to the Moon's ecliptic latitude to account for the difference between the Moon's central of mass and central of figure. The value for ΔT is from direct measurements during the 20th century and extrapolation into the 21st century. The value used for the Moon's mean radius is $k=0.272281$.

The umbral path characteristics have been predicted at 2 minute intervals of time compared to the 6 minute interval used in *Fifty Year Canon of Solar Eclipses: 1986–2035* [Espenak, 1987]. This should provide enough detail for making preliminary plots of the path on larger scale maps. Global maps using an orthographic projection also present the regions of partial and total (or annular) eclipse. The index page for the path tables and maps is:

<http://sunearth.gsfc.nasa.gov/eclipse/SEpath/SEpath.html>

3.10 SPECIAL WEB SITES FOR 2003 SOLAR ECLIPSES

Two special web sites have been set up to supplement this bulletin with additional predictions, tables and data for the solar eclipses of 2003. The URL's of these two web sites are:

<http://sunearth.gsfc.nasa.gov/eclipse/ASE2003/ASE2003.html>

<http://sunearth.gsfc.nasa.gov/eclipse/TSE2003/TSE2003.html>

3.11 PREDICTIONS FOR ECLIPSE EXPERIMENTS

This publication provides comprehensive information on the 2003 solar eclipses to both the professional and amateur/lay communities. However, certain investigations and eclipse experiments may require additional information which lies beyond the scope of this work. We invite the international professional community to contact us for assistance with any aspect of eclipse prediction including predictions for locations not included in this publication, or for more detailed predictions for a specific location (e.g.: lunar limb profile and limb corrected contact times for an observing site).

This service is offered for the 2003 eclipses as well as for previous eclipses in which analysis is still in progress. To discuss your needs and requirements, please contact Fred Espenak (espenak@gsfc.nasa.gov).

3.12 MEAN LUNAR RADIUS

A fundamental parameter used in eclipse predictions is the Moon's radius k , expressed in units of Earth's equatorial radius. The Moon's actual radius varies as a function of position angle and libration due to the irregularity in the limb profile. From 1968 through 1980, the Nautical Almanac Office used two separate values for k in their predictions. The larger value ($k=0.2724880$), representing a mean over topographic features, was used for all penumbral (exterior) contacts and for annular eclipses. A smaller value ($k=0.272281$), representing a mean minimum radius, was reserved exclusively for umbral (interior) contact calculations of total eclipses [*Explanatory Supplement*, 1974]. Unfortunately, the use of two different values of k for umbral eclipses introduces a discontinuity in the case of hybrid or annular-total eclipses.

In August 1982, the International Astronomical Union (IAU) General Assembly adopted a value of $k=0.2725076$ for the mean lunar radius. This value is now used by the Nautical Almanac Office for all solar eclipse predictions [Fiala and Lukac, 1983] and is currently the best mean radius, averaging mountain peaks and low valleys along the Moon's rugged limb. The adoption of one single value for k eliminates the discontinuity in the case of annular-total eclipses and ends confusion arising from the use of two different values. However, the use of even the best 'mean' value for the Moon's radius introduces a problem in predicting the true character and duration of umbral eclipses, particularly total eclipses. A total eclipse can be defined as an eclipse in which the Sun's disk is completely occulted by the Moon. This cannot occur so long as any photospheric rays are visible

through deep valleys along the Moon's limb [Meeus, Grosjean and Vanderleen, 1966]. But the use of the IAU's mean k guarantees that some annular or annular-total eclipses will be misidentified as total. A case in point is the eclipse of 3 October 1986. Using the IAU value for k , the *Astronomical Almanac* identified this event as a total eclipse of 3 seconds duration when it was, in fact, a beaded annular eclipse. Since a smaller value of k is more representative of the deeper lunar valleys and hence the minimum solid disk radius, it helps ensure the correct identification of an eclipse's true nature.

Of primary interest to most observers are the times when umbral eclipse begins and ends (second and third contacts, respectively) and the duration of the umbral phase. When the IAU's value for k is used to calculate these times, they must be corrected to accommodate low valleys (total) or high mountains (annular) along the Moon's limb. The calculation of these corrections is not trivial but must be performed, especially if one plans to observe near the path limits [Herald, 1983]. For observers near the center line of a total eclipse, the limb corrections can be more closely approximated by using a smaller value of k which accounts for the valleys along the profile.

This publication uses the IAU's accepted value of $k=0.2725076$ for all penumbral (exterior) contacts. In order to avoid eclipse type misidentification and to predict central durations which are closer to the actual durations at total eclipses, we depart from standard convention by adopting the smaller value of $k=0.272281$ for all umbral (interior) contacts. This is consistent with predictions in *Fifty Year Canon of Solar Eclipses: 1986–2035* [Espenak, 1987]. Consequently, the smaller k produces shorter umbral durations and narrower paths for total eclipses when compared with calculations using the IAU value for k . Similarly, predictions using a smaller k result in longer umbral durations and wider paths for annular eclipses than do predictions using the IAU's k .

3.13 ALGORITHMS, EPHEMERIDES AND PARAMETERS

Algorithms for the eclipse predictions were developed by Espenak primarily from the *Explanatory Supplement* [1974] with additional algorithms from Meeus, Grosjean and Vanderleen [1966] and Meeus [1982]. The solar and lunar ephemerides were generated from the JPL DE200 and LE200, respectively. All eclipse calculations were made using a value for the Moon's radius of $k=0.2722810$ for umbral contacts, and $k=0.2725076$ (adopted IAU value) for penumbral contacts. Center of mass coordinates were used except where noted. Extrapolating from 2002 to 2003, a value for ΔT of 64.7 and 64.8 seconds for the May and November eclipses, respectively, was used to convert the predictions from Terrestrial Dynamical Time to Universal Time. The international convention of presenting date and time in descending order has been used throughout the bulletin (i.e., *year, month, day, hour, minute, second*).

The primary source for geographic coordinates used in the local circumstances tables is *The New International Atlas* (Rand McNally, 1991). Coordinates for research stations in Antarctica are from www.scar.org/Antarctic%20Info/wintering_stations_2000.htm. Elevations for major cities were taken from *Climates of the World* (U.S. Dept. of Commerce, 1972).

All eclipse predictions presented in this publication were generated on a Macintosh G4 iMac computer. Word processing and page layout for the publication were done using Microsoft Word v5.1. Figures were annotated with Claris MacDraw Pro 1.5. Meteorological diagrams and tables were prepared using Microsoft Excel 98.

The names and spellings of countries, cities and other geopolitical regions are not authoritative, nor do they imply any official recognition in status. Corrections to names, geographic coordinates and elevations are actively solicited in order to update the data base for future eclipses. All calculations, diagrams and opinions presented in this publication are those of the authors and they assume full responsibility for their accuracy.

FIGURE 3.1 - SPECTRAL RESPONSE OF SOME COMMONLY AVAILABLE SOLAR FILTERS

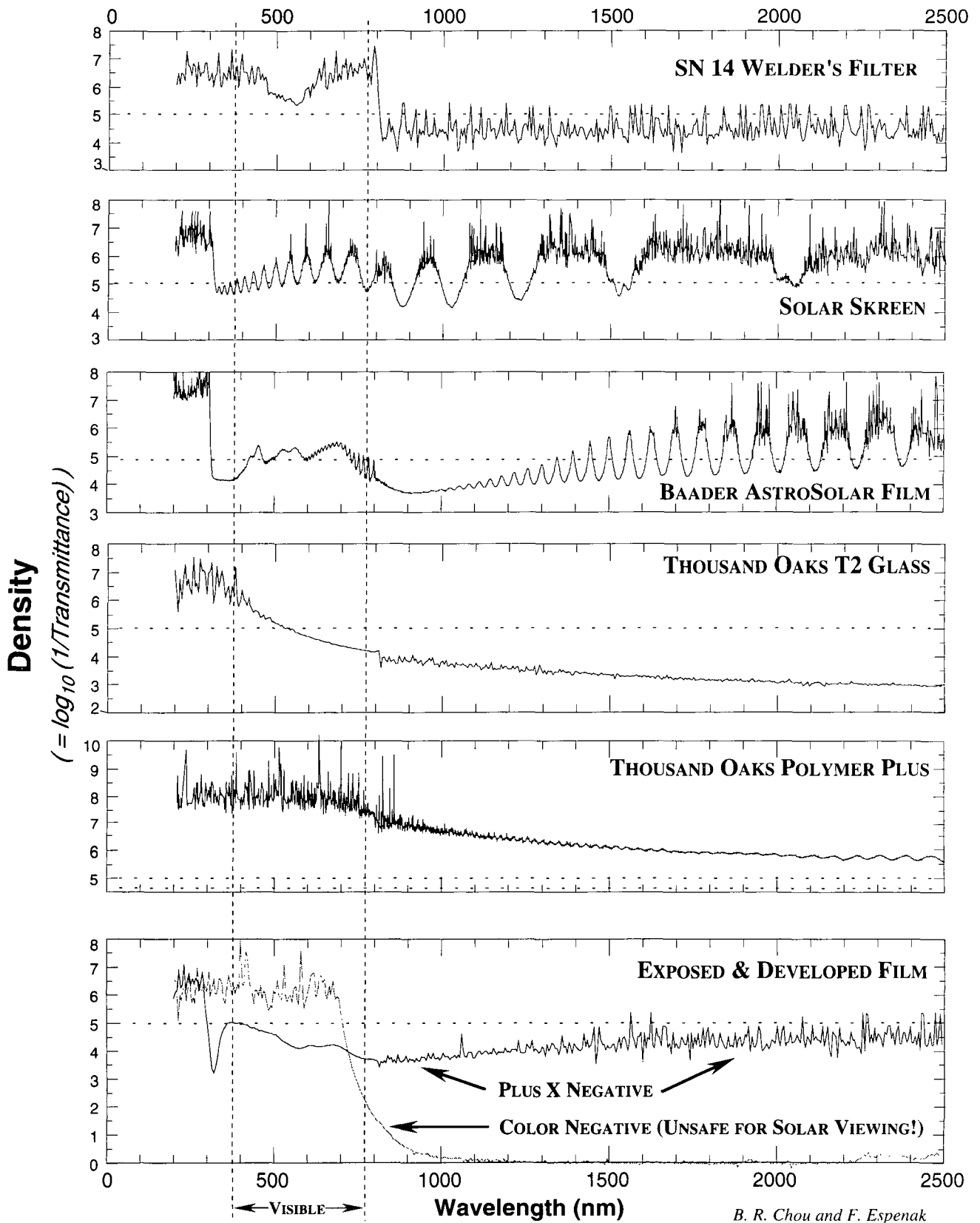


TABLE 3.1
35 MM FIELD OF VIEW AND SIZE OF SUN'S IMAGE
FOR VARIOUS PHOTOGRAPHIC FOCAL LENGTHS

<u>Focal Length</u>	<u>Field of View</u>	<u>Size of Sun</u>
28 mm	49° x 74°	0.2 mm
35 mm	39° x 59°	0.3 mm
50 mm	27° x 40°	0.5 mm
105 mm	13° x 19°	1.0 mm
200 mm	7° x 10°	1.8 mm
400 mm	3.4° x 5.1°	3.7 mm
500 mm	2.7° x 4.1°	4.6 mm
1000 mm	1.4° x 2.1°	9.2 mm
1500 mm	0.9° x 1.4°	13.8 mm
2000 mm	0.7° x 1.0°	18.4 mm
2500 mm	0.6° x 0.8°	22.9 mm

Image Size of Sun (mm) = Focal Length (mm) / 109

TABLE 3.2
SOLAR ECLIPSE EXPOSURE GUIDE

<u>ISO</u>	<u>f/Number</u>									
25	1.4	2	2.8	4	5.6	8	11	16	22	32
50	2	2.8	4	5.6	8	11	16	22	32	44
100	2.8	4	5.6	8	11	16	22	32	44	64
200	4	5.6	8	11	16	22	32	44	64	88
400	5.6	8	11	16	22	32	44	64	88	128
800	8	11	16	22	32	44	64	88	128	176
1600	11	16	22	32	44	64	88	128	176	224

<u>Subject</u>	<u>Q</u>	<u>Shutter Speed</u>												
Solar Eclipse														
Partial ¹ - 4.0 ND	11	—	—	—	1/4000	1/2000	1/1000	1/500	1/250	1/125	1/60	1/30	1/15	1/8
Partial ¹ - 5.0 ND	8	1/4000	1/2000	1/1000	1/500	1/250	1/125	1/60	1/30	1/15	1/8	1/4	1/2	1/1
Baily's Beads ²	11	—	—	—	1/4000	1/2000	1/1000	1/500	1/250	1/125	1/60	1/30	1/15	1/8
Chromosphere	10	—	—	1/4000	1/2000	1/1000	1/500	1/250	1/125	1/60	1/30	1/15	1/8	1/4
Prominences	9	—	1/4000	1/2000	1/1000	1/500	1/250	1/125	1/60	1/30	1/15	1/8	1/4	1/2
Corona - 0.1 Rs	7	1/2000	1/1000	1/500	1/250	1/125	1/60	1/30	1/15	1/8	1/4	1/2	1/1	1/1
Corona - 0.2 Rs ³	5	1/500	1/250	1/125	1/60	1/30	1/15	1/8	1/4	1/2	1/1	1/1	1/1	1/1
Corona - 0.5 Rs	3	1/125	1/60	1/30	1/15	1/8	1/4	1/2	1/1	1/1	1/1	1/1	1/1	1/1
Corona - 1.0 Rs	1	1/30	1/15	1/8	1/4	1/2	1/1	1/1	1/1	1/1	1/1	1/1	1/1	1/1
Corona - 2.0 Rs	0	1/15	1/8	1/4	1/2	1/1	1/1	1/1	1/1	1/1	1/1	1/1	1/1	1/1
Corona - 4.0 Rs	-1	1/8	1/4	1/2	1/1	1/1	1/1	1/1	1/1	1/1	1/1	1/1	1/1	1/1
Corona - 8.0 Rs	-3	1/2	1/1	1/1	1/1	1/1	1/1	1/1	1/1	1/1	1/1	1/1	1/1	1/1

Exposure Formula: $t = f^2 / (I \times 2^Q)$ where: t = exposure time (sec)
 $f = f/\text{number}$ or focal ratio
 $I = \text{ISO film speed}$
 $Q = \text{brightness exponent}$

Abbreviations: ND = Neutral Density Filter.
Rs = Solar Radii.

Notes: ¹ Exposures for partial phases are also good for annular eclipses.
² Baily's Beads are extremely bright and change rapidly.
³ This exposure also recommended for the 'Diamond Ring' effect.

F. Esperak - 2002

REQUEST FORM FOR NASA ECLIPSE BULLETINS

NASA eclipse bulletins contain detailed predictions, maps and meteorology for future central solar eclipses of interest. Published as part of NASA's Technical Publication (TP) series, the bulletins are prepared in cooperation with the Working Group on Eclipses of the International Astronomical Union and are provided as a public service to both the professional and lay communities, including educators and the media. In order to allow a reasonable lead time for planning purposes, subsequent bulletins will be published 12 to 24 months before each event. Comments, suggestions and corrections are solicited to improve the content and layout in subsequent editions of this publication series.

Single copies of the bulletins are available at no cost and may be ordered by sending a 9 x 12 inch SASE (self addressed stamped envelope) with sufficient postage for each bulletin (12 oz. or 340 g). Use stamps only since cash or checks cannot be accepted. Requests within the U. S. may use the Postal Service's Priority Mail for \$3.95. Please print either the eclipse date (year & month) or NASA publication number in the lower left corner of the SASE and return with this completed form to either of the authors. Requests from outside the U. S. and Canada may use ten international postal coupons to cover postage. Exceptions to the postage requirements will be made for international requests where political or economic restraints prevent the transfer of funds to other countries. Professional researchers and scientists are exempt from the SASE requirements provided the request comes on their official or institutional stationery.

Permission is freely granted to reproduce any portion of this NASA Reference Publication. All uses and/or publication of this material should be accompanied by an appropriate acknowledgment of the source.

Request for: NASA TP-2002-211618 — Annular and Total Solar Eclipses of 2003

Name of Organization: _____

(in English, if necessary): _____

Name of Contact Person: _____

Address: _____

City/State/ZIP: _____

Country: _____

E-mail: _____

Type of organization: University/College Observatory Library
(check all that apply) Planetarium Publication Media
 Professional Amateur Individual

Size of Organization: _____ (Number of Members)

Activities: _____

Return Requests and Comments to:	Fred Espenak NASA/GSFC Code 693 Greenbelt, MD 20771 USA	or	Jay Anderson Environment Canada 123 Main Street, Suite 150 Winnipeg, MB, CANADA R3C 4W2
-------------------------------------	---	----	---

E-mail:	espenak@gsfc.nasa.gov	E-mail:	jander@cc.umanitoba.ca
Fax:	(301) 286-0212	Fax:	(204) 983-0109

2002 Oct

REPORT DOCUMENTATION PAGE

Form Approved
OMB No. 0704-0188

Public reporting burden for this collection of information is estimated to average 1 hour per response, including the time for reviewing instructions, searching existing data sources, gathering and maintaining the data needed, and completing and reviewing the collection of information. Send comments regarding this burden estimate or any other aspect of this collection of information, including suggestions for reducing this burden, to Washington Headquarters Services, Directorate for Information Operations and Reports, 1215 Jefferson Davis Highway, Suite 1204, Arlington, VA 22202-4302, and to the Office of Management and Budget, Paperwork Reduction Project (0704-0188), Washington, DC 20503.

1. AGENCY USE ONLY (<i>Leave blank</i>)		2. REPORT DATE October 2002	3. REPORT TYPE AND DATES COVERED Technical Paper	
4. TITLE AND SUBTITLE Annular and Total Solar Eclipses of 2003			5. FUNDING NUMBERS 460	
6. AUTHOR(S) Fred Espenak and Jay Anderson				
7. PERFORMING ORGANIZATION NAME(S) AND ADDRESS (ES) Goddard Space Flight Center Greenbelt, Maryland 20771			8. PERFORMING ORGANIZATION REPORT NUMBER 2003-00184-0	
9. SPONSORING / MONITORING AGENCY NAME(S) AND ADDRESS (ES) National Aeronautics and Space Administration Washington, DC 20546-0001			10. SPONSORING / MONITORING AGENCY REPORT NUMBER 2002—TP—211618	
11. SUPPLEMENTARY NOTES J. Anderson, Environment Canada, Winnipeg, Manitoba, Canada.				
12a. DISTRIBUTION / AVAILABILITY STATEMENT Unclassified—Unlimited Subject Category: 89 Report available from the NASA Center for AeroSpace Information, 7121 Standard Drive, Hanover, MD 21076-1320. (301) 621-0390.			12b. DISTRIBUTION CODE	
13. ABSTRACT (<i>Maximum 200 words</i>) On 2003 May 31, an annular eclipse of the Sun will be visible from a large zone covering the North Atlantic. The path of the Moon's antumbral shadow begins in northern Scotland, crosses Iceland and central Greenland, and ends at sunrise in Baffin Bay (Canada). A partial eclipse will be seen within the much broader path of the Moon's penumbral shadow, which includes most of Europe, the Middle East, central and northern Asia, and northwestern North America. Six months later on 2003 November 23, a total eclipse of the Sun will be visible from a broad corridor that traverses portions of the Southern Hemisphere. The path of the Moon's umbral shadow begins in the Indian Ocean, crosses Antarctica, and ends at sunrise near the edge of the southern continent. A partial eclipse will be seen within the much larger path of the Moon's penumbral shadow, which includes Australia, New Zealand, Antarctica and southern South America. Detailed predictions for these two events are presented and include besselian elements, geographic coordinates of the path of umbral eclipse, physical ephemeris of the umbra, topocentric limb profile corrections, local circumstances for hundreds of cities, maps of the eclipse paths, weather prospects, the lunar limb profiles and the sky during totality. Information on safe eclipse viewing and additional web resources is included.				
14. SUBJECT TERMS Solar eclipse, celestial mechanics, ephemeris, Sun, Moon.			15. NUMBER OF PAGES 75	
			16. PRICE CODE	
17. SECURITY CLASSIFICATION OF REPORT Unclassified	18. SECURITY CLASSIFICATION OF THIS PAGE Unclassified	19. SECURITY CLASSIFICATION OF ABSTRACT Unclassified	20. LIMITATION OF ABSTRACT UL	

